

**UNIVERSIDADE FEDERAL DE SANTA MARIA
CENTRO DE CIÊNCIAS DA SAÚDE
PROGRAMA DE PÓS-GRADUAÇÃO EM CIÊNCIAS
FARMACÊUTICAS**

**NANOPARTÍCULAS DE QUITOSANA pH-SENSÍVEIS
CONTENDO DOXORRUBICINA:
DESENVOLVIMENTO E ESTUDO DA ATIVIDADE
ANTITUMORAL *IN VITRO***

DISSERTAÇÃO DE MESTRADO

Laís Engroff Scheeren

**Santa Maria, RS, Brasil
2015**

**NANOPARTÍCULAS DE QUITOSANA pH-SENSÍVEIS
CONTENDO DOXORRUBICINA: DESENVOLVIMENTO E
ESTUDO DA ATIVIDADE ANTITUMORAL *IN VITRO***

por

Laís Engroff Scheeren

Dissertação apresentada ao Curso de Mestrado do Programa de Pós-Graduação em Ciências Farmacêuticas, área de concentração em Controle de Qualidade e Avaliação Biofarmacêutica de Insumos e Medicamentos, da Universidade Federal de Santa Maria (UFSM, RS), como requisito parcial para obtenção do grau de **Mestre em Ciências Farmacêuticas**.

**Orientador (a): Prof. Dr^a. Clarice Madalena Bueno Rolim
Co-orientador (a): Dr^a. Daniele Rubert Nogueira**

**Santa Maria, RS, Brasil
2015**

Ficha catalográfica elaborada através do Programa de Geração Automática da Biblioteca Central da UFSM, com os dados fornecidos pelo(a) autor(a).

Scheeren, Laís Engroff

NANOPARTÍCULAS DE QUITOSANA pH-SENSÍVEIS CONTENDO DOXORRUBICINA: DESENVOLVIMENTO E ESTUDO DA ATIVIDADE ANTITUMORAL *IN VITRO*

Laís Engroff Scheeren.-2015. 170 p.; 30cm

Orientadora: Clarice Madalena Bueno Rolim

Coorientadora: Daniele Rubert Nogueira

Dissertação (mestrado) - Universidade Federal de Santa Maria, Centro de Ciências da Saúde, Programa de Pós- Graduação em Ciências Farmacêuticas, RS, 2015

1. Atividade antitumoral in vitro
 2. Doxorrubicina
 3. Tensoativo derivado de lisina
 4. Nanopartículas de quitosana pH-sensíveis
 5. Métodos analíticos
- I. Bueno Rolim, Clarice Madalena II. Rubert Nogueira, Daniele III. Título.

**Universidade Federal de Santa Maria
Centro de Ciências da Saúde
Programa de Pós-Graduação em Ciências Farmacêuticas**

A Comissão Examinadora, abaixo assinada,
aprova a Dissertação de Mestrado

**NANOPARTÍCULAS DE QUITOSANA pH-SENSÍVEIS CONTENDO
DOXORRUBICINA: DESENVOLVIMENTO E ESTUDO DA
ATIVIDADE ANTITUMORAL *IN VITRO***

elaborada por
Laís Engroff Scheeren

como requisito parcial para obtenção do grau de
Mestre em Ciências Farmacêuticas

COMISSÃO EXAMINADORA

Clarice Madalena Bueno Rolim, Dr^a (UFSM)
(Presidente/Orientador)

Maria Pilar Vinardell Martínez-Hidalgo, Dr^a (UB)

Scheila Rezende Schaffazick, Dr^a (UFSM)

Santa Maria, 01 de setembro de 2015.

Dedico este trabalho:

*À minha família, aos amigos, colegas e a todos que me acompanharam,
incentivando-me durante esta caminhada.*

AGRADECIMENTOS

Agradeço, primeiramente, à Deus pela minha vida, pela minha família, pela nossa saúde e pelas oportunidades que temos para que estejamos sempre em busca de algo maior, pela Sua presença nos dias felizes e também nos dias difíceis;

Aos meus pais, Lauri e Márcia, exemplos de caráter, dedicação e responsabilidade nos quais me espelho, que ao meu lado se esforçaram, vibraram e se emocionaram, desde a saída de casa até quando recebo este título. Pelo amor e carinho incondicionais;

Ao meu irmão Mauri e, de forma carinhosa, à minha irmã, Laura, que além de irmã, é grande amiga e incentivadora e que esteve sempre junto comigo, demonstrando carinho, amor, paciência e interesse pelas minhas atividades, por me esperar com um mate e lanche quando cheguei tarde em casa depois de horas no laboratório e mesmo pelas brincadeiras que fez quando passei dias em frente ao notebook;

À Professora Clarice, minha orientadora, por ter me concedido a oportunidade de entrar em seu grupo de pesquisa. Obrigada por ensinar valores como dedicação e responsabilidade, por sempre nos mostrar um jeito alegre de viver, pelo suporte e pela disponibilidade;

À Dani, minha co-orientadora, pelos ensinamentos, teóricos e práticos, pelo tempo despendido para esclarecer dúvidas e correções, por acreditar na minha capacidade para a realização deste trabalho e por estar sempre presente para a finalização deste;

À toda equipe do LabCQ, que me ensinou que o maior presente que a pesquisa pode nos dar é a união, a cumplicidade e o companheirismo, agradeço pela amizade e compreensão, pelo momentos alegres e pelos tristes também, por todas as ideias e conhecimentos divididos, pelos mates, cafés, sushis, festas e risadas;

Aos meus amigos e colegas do curso de Farmácia da UFSM, aos que estiveram ao meu lado comemorando as vitórias, oferecendo força, suporte e conselhos durante as situações menos felizes e compreendendo os momentos em que estive ausente;

Aos componentes da banca, pela disponibilidade em avaliar e contribuir para o meu trabalho;

Aos demais laboratórios desta universidade, que de alguma maneira colaboraram para a obtenção dos resultados que compõem este trabalho;

À Fundação de Amparo à Pesquisa do Estado do Rio Grande do Sul – FAPERGS pela concessão da bolsa de estudos;

À Universidade Federal de Santa Maria e ao Programa de Pós Graduação em Ciências Farmacêuticas, pela oportunidade de realizar este trabalho e engrandecer meu conhecimento;

A todos que, mesmo não citados, contribuíram de alguma maneira para a conclusão deste trabalho.

A todos vocês, minha gratidão!

RESUMO

Dissertação de Mestrado
Programa de Pós-Graduação em Ciências Farmacêuticas
Universidade Federal de Santa Maria

NANOPARTÍCULAS DE QUITOSANA pH-SENSÍVEIS CONTENDO DOXORRUBICINA: DESENVOLVIMENTO E ESTUDO DA ATIVIDADE ANTITUMORAL *IN VITRO*

AUTORA: LAÍS ENGROFF SCHEEREN
ORIENTADORA: PROF. Dr^a. CLARICE MADALENA BUENO ROLIM
CO-ORIENTADORA: Dr^a. DANIELE RUBERT NOGUEIRA

Local e data da defesa: Santa Maria, 01 de setembro de 2015.

O câncer é uma doença altamente complexa, sendo que os tratamentos mais comuns estão limitados à quimioterapia, radioterapia e cirurgia. No entanto, a ocorrência de efeitos adversos é frequente, devido à limitada capacidade do fármaco de atuar especificamente na célula cancerosa. O antibiótico antraciclínico doxorrubicina (DOX) é amplamente utilizado na terapia do câncer, pois é efetivo contra uma série de tumores como câncer de mama, sarcomas e linfomas. Apesar disto, seu principal efeito indesejado é a cardiotoxicidade. Com o propósito de solucionar este problema, a nanotecnologia aparece como uma alternativa para melhorar o tratamento antitumoral e prevenir a toxicidade em células normais. Além disso, adjuvantes bioativos com propriedades pH-dependentes são promissores no campo do desenvolvimento tecnológico de nanoestruturas como mediadores de uma maior eficiência de liberação de fármacos a nível intracelular e/ou do espaço extracelular do tecido tumoral ($pH_e \sim 6,6$). Estudos prévios demonstram o comportamento pH-sensível do tensoativo N^a,N^e -dioctanoil lisina com contra-íon sódio (77KS) em romper membranas celulares bem como a sua baixa toxicidade. Assim, nanopartículas (NPs) de quitosana pH-sensíveis incorporando o tensoativo 77KS foram desenvolvidas, pelo método de gelificação iônica, como sistema carreador da DOX, visando alcançar uma liberação específica do fármaco antitumoral em alvos como o microambiente do tumor e os compartimentos intracelulares. Por outro lado, também foram realizadas modificações nas NPs, como a inclusão de polietilenoglicol e poloxamer. A caracterização físico-química das NPs mostrou tamanho hidrodinâmico inferior a 227 nm, bem como valores positivos de potencial zeta e eficiência de encapsulação próxima de 65%. Os métodos analíticos validados mostraram-se adequados para a análise quantitativa do fármaco encapsulado. Os estudos de liberação *in vitro* demonstraram que a DOX foi liberada de forma acelerada em meio ácido, independente das modificações nas NPs. Ensaios de hemólise, utilizando o eritrócito como modelo de membrana endossomal, comprovaram o comportamento pH-sensível das NPs contendo 77KS. Além disso, as NPs desenvolvidas apresentaram maior citotoxicidade em células tumorais comparadas ao fármaco livre, especialmente quando os experimentos foram realizados em pH 6,6. Por outro lado, resultados que comprovam a baixa toxicidade das NPs foram obtidos em ensaios utilizando

linhagem celular não-tumoral. Portanto, pode-se considerar que as NPs poliméricas pH-sensíveis desenvolvidas neste trabalho são carreadores promissores para desencadear a liberação da DOX no microambiente do tumor e/ou no interior da célula cancerosa.

Palavras-chave: Atividade antitumoral *in vitro*. Doxorrubicina. Métodos analíticos. Nanopartículas de quitosana pH-sensíveis. Polietilenoglicol. Poloxamer. Tensoativo derivado de lisina.

ABSTRACT

Master's Degree Dissertation
Postgraduate Program in Pharmaceutical Sciences
Federal University of Santa Maria

pH-SENSITIVE DOXORUBICIN-LOADED-CHITOSAN NANOPARTICLES: DEVELOPMENT AND *IN VITRO* ANTITUMOR ACTIVITY STUDY

AUTHOR: LAÍS ENGROFF SCHEEREN
ADVISOR: PROF. Dr^a. CLARICE MADALENA BUENO ROLIM
CO-ADVISOR: Dr^a. DANIELE RUBERT NOGUEIRA

Presentation date: Santa Maria, September 01, 2015.

Cancer is a highly complex disease and the most common treatments are limited to chemotherapy, radiation and surgery. However, the occurrence of side effects is frequent, especially due to limited drug capability to act specifically on cancer cells. The anthracycline antibiotic doxorubicin (DOX) is widely used in cancer therapy because it is effective against several tumors, such as breast cancer, sarcomas and lymphomas. Nevertheless, its main side effect is cardiotoxicity. In order to overcome this problem, nanotechnology is an alternative to improve the antitumor treatment and to prevent the toxicity in normal cells. Furthermore, pH-responsive bioactive adjuvants are promising for the technological development of nanostructures, as they can mediate greater drug release to tumor microenvironment ($\text{pH}_e \sim 6.6$) and/or intracellular compartments. Previous studies have showed the pH-sensitive membrane-lytic behavior of the surfactant N^{α},N^{ϵ} -dioctanoyl lysine with an inorganic sodium counterion (77KS), as well as low toxicity. Thus, pH-sensitive chitosan-based nanoparticles (CS-NPs) incorporating the surfactant 77KS were developed by ionotropic gelation as DOX delivery system in an attempt to achieve a specific drug release on tumor tissue and intracellular compartments. Furthermore, modifications on NPs were performed, as inclusion of polyethylene glycol (PEG) and poloxamer. The physicochemical characterization of NPs showed mean hydrodynamic size lower than 227 nm, as well as positive zeta potential values and encapsulation efficiency around 65%. The validated analytical methods were suitable for the quantitative analysis of the entrapped drug. *In vitro* release studies displayed accelerated DOX release under acidic conditions, regardless the modifiers included. The hemolysis assay, with the erythrocyte as a model for the endosomal membrane, proved the pH-dependent membrane-lytic behavior of NPs with 77KS. Moreover, the designed NPs showed higher cytotoxicity in tumor cells than free drug, especially when the *in vitro* experiments were performed at pH 6.6. On the other hand, low cytotoxic effects were obtained in tests using a control non-tumor cell line. Therefore, it can be considered that the pH-responsive polymeric NPs developed in this work are promising carriers to trigger DOX release in the tumor microenvironment and/or inside the cancer cell.

Keywords: Analytical methods. Doxorubicin. *In vitro* antitumor activity. Lysine-based surfactant. pH-sensitive chitosan-based nanoparticles. Poloxamer. Polyethylene glycol.

LISTA DE ABREVIATURAS E SIGLAS

77K: N^a,N^e- dioctanoil lisina

77KS: N^a,N^e- dioctanoil lisina com contra-íon sódio

CLAE: Cromatografia a líquido de alta eficiência

CS: Quitosana

DAD: Detector de arranjo de diodos

DNA: Ácido desoxirribonucleico

DOX: Doxorrubicina

DPR: Desvio padrão relativo

EE%: Eficiência de encapsulação

EPR: *Enhanced permeability and retention*

FDA: *Food and Drug Administration*

FT-IR: Espectroscopia no infravermelho com transformada de Fourier

HeLa: Linhagem celular de câncer de cervical

MCF-7: Linhagem celular de adenocarcinoma de mama

MDR: *Multidrug resistance*

MTT: 3-(4,5-dimetil)-2,5 difenil brometo de tetrazolio

NPs: Nanopartículas

NRU: ensaio de captação do corante vital vermelho neutro

PDI: Índice de polidispersão

PEG: Polietileno glicol

Pgp: Glicoproteína-P

PZ: Potencial zeta

TPP: Tripolifosfato de sódio

UV-Vis: Ultravioleta-visível

LISTA DE ILUSTRAÇÕES

REVISÃO DA LITERATURA

FIGURA 1- Estrutura química do fármaco antitumoral doxorrubicina.....35

FIGURA 2- Estrutura química do polímero natural quitosana.....39

FIGURA 3- Estrutura química do 77KS (N^{α},N^{ϵ} - dioctanoil lisina com contra-íon sódio).....48

ARTIGO I

FIGURA 1- Results of the specificity tests: (A) Representative RP-LC chromatograms and (B) Absorption spectra obtained by UV-Vis spectrophotometric method. Trace (1) represents unloaded-NPs, (2) DOX reference solution (15 µg/mL) and (3) DOX-loaded CS-NPs (15 µg/mL).76

FIGURA 2- Pareto chart of standardized effects. Chart (A) corresponds to the main factors and their combinations for UV-Vis spectrophotometric method, and chart (B) for RP-LC method. The vertical line indicates the critical t -value for $\alpha = 0.05$77

FIGURA 3- *In vitro* cumulative release of DOX from CS-NPs in PBS pH 7.4 and 5.4. Results are expressed as the mean \pm standard error of three independent experiments. Statistical analyses were performed by ANOVA followed by Tukey´s multiple comparison test. *significant difference from PBS pH 7.4 ($p < 0.05$) and **high significant difference from PBS pH 7.4 ($p < 0.01$).78

FIGURA 4- Zero-order plot represents the degradation kinetics of DOX-loaded CS-NPs under photolytic conditions (UVC light) during the total exposure time.....79

ARTIGO II

FIGURA 1- Design of pH-responsive DOX-loaded CS-NPs to facilitate target drug release at the tumor site107

FIGURA 2- UV-Vis absorption spectra of the DOX extracted from NPs (A) and DOX aqueous solution (B)..... 108

FIGURE 3- pH-dependent *in vitro* cumulative DOX release from NPs in PBS buffer at pH 7.4, 6.6 and 5.4. (A) DOX-CS-NPs, (B) PEG-DOX-CS-NPs, (C) Polox-DOX-CS-NPs and (D) DOX-CS-NPs without 77KS. Results are expressed as the mean ± SE of three independent experiments. Statistical analyses were performed using ANOVA followed by Tukey's multiple comparison test. ^a Significant difference from PBS pH 7.4 ($p < 0.05$), ^b highly significant difference from PBS pH 7.4 ($p < 0.01$)..... 109

FIGURA 4- FT-IR spectra of pure DOX (A), CS raw material (B), DOX-CS-NPs (C) and PEG-DOX-CS-NPs (D). 110

FIGURA 5- *In vitro* antitumor activity of unloaded-CS-NPs, free DOX and DOX-loaded CS-NPs in HeLa cell line. 111

ARTIGO III

FIGURA 1- Schematic representation of a proposed mechanism for the cellular uptake and drug release of pH-responsive CS-NPs. (1) Internalization of NPs by endocytosis, (2) Under mildly acidic environments found in endosomes, the carboxylic group of 77KS would become protonated, which would enhance its hydrophobicity and cause the disruption of endosomal membranes, releasing thus the loaded drug into the cytoplasm, and (3) without a specific mechanism for endosomal escape, DOX-loaded CS-NPs would be trafficked to lysosomes, where degradation of the drug may occur..... 122

FIGURA 2- Characterization of unloaded and DOX-loaded CS-NPs in water and cell culture medium: (a) and (b) Hydrodynamic diameters, and (c) and (d) zeta potential values, of fresh prepared NP suspensions and of NPs suspending in cell culture medium, respectively. The measurements in cell culture medium were performed right after dispersion as well as after 24 hours of storage at 37° C. DOX-NP01, DOX-NP02 and DOX-NP03 represent DOX-CS-NPs, PEG-DOX-CS-NPs and Polox-DOX-CS-NPs, respectively. Unloaded-NPs represent the same formulations without the drug..... 124

FIGURA 3- pH-responsive membranolytic behavior of unloaded CS-NPs: (a) CS-NPs without 77KS, (b) CS-NPs with 77KS, (c) PEG-CS-NPs with 77KS and (d) Polox-CS-NPs with 77KS. NP-induced membrane-lysis is expressed as a function of pH, concentration and incubation time. Results are expressed as the mean \pm SE of three independent experiments. Statistical analyses were performed using ANOVA followed by Tukey's multiple comparison test. ^a Significantly different from pH 7.4 ($p < 0.05$), ^b from pH 6.6 ($p < 0.05$), ^c from pH 7.4 ($p < 0.005$) and ^d from pH 6.6 ($p < 0.005$).127

FIGURA 4- pH-responsive membranolytic behavior of free drug and DOX-loaded CS-NPs: (a) free DOX, (b) DOX-CS-NPs without 77KS, (c) DOX-CS-NPs with 77KS, (d) PEG-DOX-CS-NPs with 77KS and (e) Polox-DOX-CS-NPs with 77KS. NP-induced membrane-lysis is expressed as a function of pH, concentration and incubation time. Results are expressed as the mean \pm SE of three independent experiments. Statistical analyses were performed using ANOVA followed by Tukey's multiple comparison test. ^a Significantly different from pH 7.4 ($p < 0.05$), ^b from pH 6.6 ($p < 0.05$), ^c from pH 7.4 ($p < 0.005$) and ^d from pH 6.6 ($p < 0.005$).....128

FIGURA 5- Cytotoxicity of varying concentrations of CS-NPs and free drug after 24 h incubation: (a) unloaded-CS-NPs in 3T3, HeLa and MCF-7 cell lines; (b) free drug and DOX-loaded CS-NPs in 3T3 cells by MTT assay, (c) in HeLa cells by MTT assay, (d) in HeLa cells by NRU assay, (e) in MCF-7 cells by MTT assay, and (f) in MCF-7 cells by NRU assay. (g) and (h) expressed CS-NPs and free drug in HeLa and MCF-7 cells by MTT assay, respectively, after 48 h incubation. Data are expressed as the mean of three independent experiments \pm SE. Statistical analyses were performed using ANOVA followed by Tukey's or Dunnett's multiple comparison tests. ^a Significant ($p < 0.05$) and ^b highly significant ($p < 0.005$) difference from 3T3 cells. * $p < 0.05$ and ** $p < 0.005$ denote significant differences from free DOX. DOX-NP01, DOX-NP02 and DOX-NP03 represent DOX-CS-NPs, PEG-DOX-CS-NPs and Polox-DOX-CS-NPs, respectively.....130

FIGURA 6- *In vitro* cell viability by MTT assay in tumor cell lines following 24 h-treatment with free drug and DOX-loaded CS-NPs at pH_e 6.6, simulating the pH of the tumor microenvironment: (a) HeLa and (b) MCF-7 cells. Data are expressed as the mean of three independent experiments \pm SE. Statistical analyses were performed using

ANOVA followed by Tukey's multiple comparison tests. ^a Significant ($p < 0.05$) and ^b highly significant ($p < 0.005$) difference from cytotoxicity at pH 7.4 (data reported in Fig. 5c and e). DOX-NP01, DOX-NP02 and DOX-NP03 represent DOX-CS-NPs, PEG-DOX-CS-NPs and Polox-DOX-CS-NPs, respectively.....133

FIGURA 7- Percentage of hemolysis caused by free drug and DOX-loaded CS-NPs after 10 and 60 min of incubation with human erythrocytes: (a) free DOX, (b) DOX-CS-NPs, (c) PEG-DOX-CS-NPs and (d) Polox-DOX-CS-NPs. Each value represents the mean \pm SE of three experiments.....136

LISTA DE TABELAS

ARTIGO I

TABELA 1- Repeatability, intermediate precision and accuracy data of UV-Vis spectrophotometric and RP-LC methods for DOX in samples of chitosan-based NPs.....73

TABELA 2- Robustness assessment by full factorial design for UV-Vis spectrophotometric and RP-LC methods, with simultaneous variations of the factors.....74

TABELA 3- Comparison between the UV-Vis spectrophotometric and RP-LC methods applied for the analysis of DOX in samples of chitosan-based NPs.....75

ARTIGO II

TABELA 1- Characterization of unloaded and DOX-loaded CS-NPs with or without 77KS. The lyophilized NPs (L-NPs) were analyzed after redispersion in ultra-pure water.....105

TABELA 2- Observed rate constants, correlation coefficients, MSC and half-lives ($t_{1/2}$) obtained by mathematical modeling of DOX release from the different NPs when immersed in PBS buffer at pH 7.4, 6.6 and 5.4. Results are expressed as mean \pm standard deviation (SD) of three experiments.....106

ARTIGO III

TABELA 1- Antitumor activity of free drug and DOX-loaded CS-NPs expressed as IC₅₀ (μg/ml) and SI values.....131

SUMÁRIO

1. INTRODUÇÃO	25
2. OBJETIVOS	29
3. REVISÃO DA LITERATURA.....	33
4. ARTIGO CIENTÍFICO I: “A comparative study of RP-LC and UV-Vis spectrophotometry to assess doxorubicin from pH-sensitive nanoparticles”.....	53
5. ARTIGO CIENTÍFICO II: “PEGylated and poloxamer-modified chitosan nanoparticles incorporating a lysine-based surfactant for pH triggered doxorubicin release”	81
6. ARTIGO CIENTÍFICO III: “Chitosan nanoparticles functionalized with a pH-responsive surfactant improved the <i>in vitro</i> antineoplastic effects of doxorubicin”..	113
7. DISCUSSÃO GERAL	145
8. CONCLUSÕES.....	155
9. REFERÊNCIAS BIBLIOGRÁFICAS	159

INTRODUÇÃO

1. INTRODUÇÃO

O câncer é uma enfermidade altamente complexa e, segundo a Organização Mundial de Saúde (*World Health Organization*, WHO), o número de novos casos da doença, que, em 2012 eram 14 milhões, deve chegar a 22 milhões nas próximas duas décadas, sendo que o câncer de pulmão, fígado, estômago, colo retal e de mama são os responsáveis pela maioria das mortes a cada ano. Além disso, pode-se dizer que esta patologia está relacionada ao elevado índice de massa corporal, baixa ingestão de frutas e legumes, falta de atividade física, tabagismo e uso de álcool (WHO, 2014).

Antibióticos antraciclínicos estão entre os fármacos mais utilizados na terapia do câncer desde 1960, quando foram isolados pela primeira vez a partir bactéria *Streptomyces peucetius*. Dentre estes antibióticos destaca-se a doxorrubicina (DOX), que é efetiva contra uma série de tumores, principalmente câncer de mama, tumores sólidos infantis, sarcomas de tecidos moles e linfomas agressivos. Apesar disso, a DOX é capaz de provocar cardiotoxicidade, além de desenvolver resistência nas células tumorais, as quais superexpressam bombas de efluxo como a glicoproteína-P (KABANOV et al., 2002; MINOTTI et al., 2004).

Neste contexto, há uma grande necessidade de desenvolver tecnologias inovadoras que possam ajudar na obtenção de um tratamento mais eficiente e específico contra as células cancerosas. Atualmente considera-se a nanotecnologia como uma área do conhecimento farmacêutico com diversas aplicações na biologia do câncer, desde o diagnóstico precoce até o tratamento mais adequado. (SINGH; NEHRU, 2008; CAI et al., 2008; ALIOSMANOGLU; BARASAN, 2012). Nanopartículas (NPs) poliméricas que atuam como carreadores terapêuticos de fármacos antitumorais são preparadas, especialmente, a partir de polímeros biodegradáveis e biocompatíveis e têm sido amplamente investigadas para aplicação na medicina oncológica (WANG et al., 2012). Por apresentar estas características, a quitosana (CS, da sigla em inglês) é um polímero promissor para a preparação de sistemas de liberação de fármacos, com propriedades úteis no diagnóstico e na terapia do câncer (DASH et al., 2011; PRABAHARAN, 2015).

As NPs tendem a acumular-se na região tumoral via permeabilidade e retenção aumentadas (do inglês *Enhanced Permeability and Retention*, EPR) (WANG et al., 2012). Além disso, a inclusão de compostos bioativos, capazes de responder a estímulos físicos, químicos ou biológicos, vem sendo estudada como uma alternativa promissora para melhorar

a efetividade do sistema nanoestruturado (LIU et al., 2014). Considerando-se a terapia do câncer, destacam-se os sistemas de liberação de fármacos pH-sensíveis, uma vez que o microambiente do tumor apresenta pH levemente acidificado (pH entre 6,5 – 7,2) em relação ao pH dos tecidos normais (~ 7,4) (TIAN; BAE, 2012). Além disso, estes sistemas podem constituir-se como adjuvantes tecnológicos capazes de melhorar a eficiência de liberação de fármacos a partir das NPs a nível intracelular (AKAGI et al., 2010; NOGUEIRA et al., 2014). Neste contexto, destaca-se o tensoativo biocompatível derivado do aminoácido lisina, 77KS (N^{α},N^{ϵ} -dioctanoil lisina, com contra-íon sódio) (VIVES et al., 1999), que em estudos prévios demonstrou atividade lítica de membrana dependente do pH, bem como baixa citotoxicidade em ensaios *in vitro* utilizando linhagens celulares tumorais e não-tumorais (NOGUEIRA et al., 2011a; NOGUEIRA et al., 2011b). Frente a estas características, o tensoativo mencionado apresenta-se como um adjuvante bioativo promissor para aplicações na área farmacêutica, especialmente no que se refere ao desenvolvimento de formulações de base nanotecnológica para a liberação intracelular de fármacos.

Modelos *in vitro* baseados em cultivos celulares são metodologias atrativas para estudar a atividade e o perfil toxicológico de novas nanotecnologias, especialmente no que se refere a aspectos éticos e ao alto custo dos testes *in vivo* (SOHAEBUDDIN et al., 2010; TAVANO et al., 2013). Métodos *in vitro* são indispensáveis na fase inicial de desenvolvimento de novos produtos, uma vez que representam um compromisso sensato entre esforço e ganho de informação, permitindo a comparação direta entre vários nanomateriais em um curto espaço de tempo. Além disso, permitem identificar os mecanismos envolvidos em sua atividade tóxica e/ou terapêutica.

Considerando a necessidade de direcionar fármacos antitumorais especificamente ao espaço extracelular do tecido neoplásico e/ou ao interior da célula cancerosa, este trabalho teve como principal objetivo o desenvolvimento de um sistema carreador para a DOX baseado no polímero quitosana e contendo o tensoativo pH-sensível 77KS como adjuvante bioativo. Somado a isso, objetivou-se avaliar a atividade lítica de membrana pH-dependente das NPs, bem como sua atividade antitumoral *in vitro*, utilizando métodos baseados em modelos celulares. Todos os objetivos estabelecidos estão associados à busca de resultados significativos que possam contribuir diretamente para o desenvolvimento de formulações mais específicas e com menor incidência de efeitos adversos.

OBJETIVOS

2. OBJETIVOS

2.1 Objetivo Geral

Preparar e caracterizar nanopartículas de quitosana pH-sensíveis contendo DOX como potenciais carreadores para o tratamento do câncer, bem como estudar sua potencial atividade antitumoral utilizando métodos *in vitro* baseados em modelos celulares.

2.2 Objetivos Específicos

- Desenvolver NPs contendo DOX a partir do polímero natural CS incorporando o tensoativo 77KS como adjuvante bioativo pH-sensível;
- Realizar modificações estruturais nas NPs como a inclusão de PEG e poloxamer 188;
- Caracterizar as NPs quanto a sua eficiência de encapsulação, pH, diâmetro médio de partículas, índice de polidispersão, potencial zeta e teor do fármaco;
- Desenvolver e validar método analítico por cromatografia a líquido de alta eficiência;
- Desenvolver e validar método simples e rápido por espectrofotometria no UV-Vis;
- Avaliar o perfil de liberação *in vitro* do fármaco a partir das NPs em meios com diferentes valores de pH;
- Avaliar a estabilidade e a fotoestabilidade das NPs;
- Determinar a atividade pH-dependente das NPs, utilizando o eritrócito como modelo de membrana endossomal;
- Avaliar a hemocompatibilidade das NPs empregando o ensaio de hemólise;
- Estudar a atividade antitumoral das NPs contendo DOX de forma comparativa ao fármaco não-encapsulado, utilizando modelos *in vitro* baseados em linhagens celulares tumorais e não-tumorais e diferentes ensaios de viabilidade celular.

REVISÃO DA LITERATURA

3. REVISÃO DA LITERATURA

3.1 Câncer

O câncer é caracterizado como centenas de doenças distintas (ANDERSON, 2001), que passam por um processo de progressão celular de normal para uma condição pré-neoplásica e, finalmente, para a forma maligna, invasiva e com características celulares alteradas (KRIZMAN et al., 1999).

O tratamento clássico do câncer envolve terapias como a cirurgia, radioterapia, quimioterapia e, mais recentemente, a imunoterapia e a terapia fotodinâmica (RAMAKRISHNAN; GABRILOVICH, 2013). A quimioterapia é o tratamento a base de fármacos citotóxicos e sua eficácia é limitada pela alta toxicidade em tecidos normais e baixa seletividade por células cancerosas (JAIN; JAIN, 2008). Sendo assim, as terapias tradicionais resultam em efeitos colaterais graves causados pela perda da função das células normais, afetando diretamente a qualidade de vida do paciente durante o tratamento (PEPPAS; BLANCHETTE, 2012). Neste contexto, a pesquisa com ênfase no desenvolvimento de tratamentos mais seletivos para esta doença tem sido considerada muito relevante.

A região tumoral possui características particulares que variam de acordo com o diâmetro e a localização dentro do tumor. Um tumor sólido divide-se em três regiões: região necrótica avascular, semi-necrótica e região com alguns vasos e arteríolas. A vascularização do tumor é, geralmente, diferenciada em relação à distribuição, comprimento, diâmetro e densidade dos vasos, esta última diminuindo da periferia para o centro do tumor. Essa vasculatura heterogênea contribui para a distribuição irregular e insatisfatória do fármaco dentro de tumores sólidos (LI et al., 2012). Além disso, a região tumoral apresenta morfologia desorganizada, com endotélio descontínuo e poroso, membrana basal interrompida ou inexistente e falta de drenagem linfática (GABIZON et al, 2012).

Estudos focados em formas de direcionar o fármaco ao tumor vêm sendo conduzidos a fim de melhorar a eficácia do tratamento antitumoral e reduzir sua toxicidade inespecífica. Esses objetivos podem ser alcançados através da encapsulação do fármaco em sistemas nanoestruturados, modificando a biodistribuição destes (vetorização passiva) ou pelo uso de ligantes celulares específicos, como anticorpos, proteínas e peptídeos (vetorização ativa). Outra alternativa estudada é o direcionamento destes sistemas nanoestruturados ao pH ácido

característico do microambiente tumoral e compartimentos intracelulares (LEE et al., 2008; LI et al., 2012).

3.2 Doxorrubicina

Antibióticos antraciclínicos são altamente efetivos e amplamente utilizados como agentes citotóxicos no tratamento do câncer (SAWYER et al., 2010). Alcançam esse resultado através de diferentes mecanismos de ação, tais como: inibição da topoisomerase II, inibição da síntese de DNA, formação de radicais livres, ligação cruzada com o DNA, separação da fita de DNA, efeitos sobre a membrana e indução à apoptose (GEWIRTZ, 1999). Antraciclinas têm sido utilizadas como agentes antitumorais desde 1960 (BARENHOLZ, 2012) e, a partir de então, muitas outras têm sido descobertas e sintetizadas a fim de superar o alto efeito tóxico e a resistência a múltiplos fármacos (do inglês *Multidrug Resistance*, MDR) que essas substâncias apresentam (ZAGOTTO et al., 2001).

A doxorrubicina (DOX) é uma antraciclina e, assim como os demais antibióticos desta classe, é isolada a partir da bactéria *Streptomyces peucetius* (var. *caesius*) (BARENHOLZ, 2012). Também chamada de adriamicina, a DOX possui um amplo espectro de ação, sendo efetiva contra sarcomas, linfomas, tumores infantis e câncer de mama. Apresenta-se na forma de cloridrato de doxorrubicina e cloridrato de doxorrubicina lipossomal peguilado. Sua aplicação é intravenosa exclusivamente e pode ser feita através de infusão contínua ou dose em *bolus*, sendo que o regime de tratamento pode variar de 4 até 10 ciclos, de acordo com o caso e, preferencialmente, com intervalo de 21 dias entre as administrações (VEJPONGSA; YEH, 2014).

Os antibióticos antraciclínicos apresentam como base de sua estrutura química uma porção aglicona (composto por um anel tetracíclico com grupo quinona-hidroquinona nos anéis C e B, um substituinte metóxi no anel D e uma curta cadeia lateral ligada ao anel A) e uma porção açúcar chamada daunosamina, a qual está unida por ligação glicosídica no anel A. A estrutura química da DOX (figura 1) diferencia-se das demais antraciclinas pelo final da curta cadeia lateral, que termina em um álcool primário (ARCAMONE et al., 1969; MINOTTI et al., 2004). DOX é um pó cristalino vermelho alaranjado, higroscópico, solúvel em água e levemente solúvel em metanol. Apresenta pKa igual a 8,2 (TAVANO et al., 2014).

Apesar do amplo espectro de ação e extenso uso como agente quimioterápico, a DOX apresenta efeitos adversos graves, uma vez que sua atividade citotóxica pode ser

desencadeada pelos diferentes mecanismos citados anteriormente. A geração de radicais livres está fortemente relacionada com o efeito cardiotóxico das antraciclinas, pois estes interferem na função mitocondrial (GEWIRTZ, 1999). Degeneração e atrofia são mudanças histológicas observadas em células musculares cardíacas de pacientes com morte relacionadas ao coração.

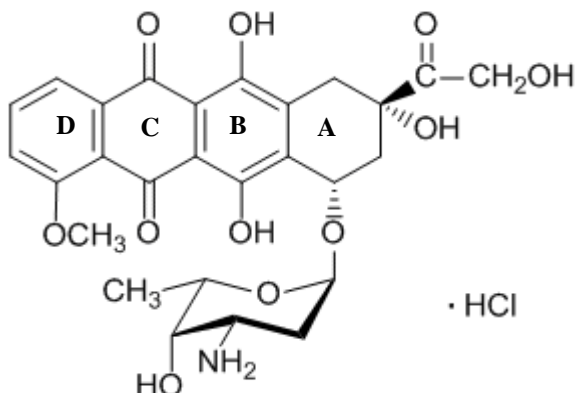


Figura 1. Estrutura química do fármaco antitumoral doxorrubicina.

Além disso, alterações degenerativas (inchamento e lise da membrana) podem ser vistas a nível mitocondrial (AUBEL-SADRON; LONDOS-GAGLIARDI, 1984).

Muitos trabalhos têm demonstrado o efeito cardiotóxico da DOX (SINGAL et al., 1997; TAKEMURA; FUJIWARA, 2007; OCTAVIA et al., 2012). Jain (2000) sugere que esse efeito se deve a uma combinação da produção de radicais livres pelos metabólitos deste fármaco e a sensibilidade dos mamíferos aos efeitos citotóxicos do estresse oxidativo. Octavia e colaboradores (2012) relatam que efeitos cardiotóxicos em decorrência do tratamento antineoplásico com DOX podem ser adiados por 10 a 15 anos após o término da quimioterapia. A cardiotoxicidade é caracterizada por mudanças no eletrocardiograma, pericardite e cardiomiopatia. A cardiotoxicidade pode ocorrer mesmo em doses baixas, já que depende da suscetibilidade individual. Por outro lado, a cardiomiopatia está relacionada com a dose.

A efetividade do tratamento do câncer é limitada pelo desenvolvimento de resistência por parte das células tumorais contra os agentes terapêuticos. As células cancerosas apresentam alterações na membrana, as quais levam a um aumento do transporte do fármaco para fora da célula (efluxo) e, portanto, à resistência (AUBEL-SADRON; LONDOS-GAGLIARDI, 1984). Células com resistência a múltiplos fármacos superexpressam transportadores da família cassette de ligação ATP (transportadores ABC), tais como a bomba

de efluxo glicoproteína-P (Pgp). Acredita-se que a DOX é reconhecida pela Pgp, caracterizando, assim, o principal mecanismo de resistência deste fármaco (KABANOV et al., 2002).

3.3 Métodos analíticos aplicados à quantificação de doxorrubicina

Metodologia analítica para caracterização e quantificação de cloridrato de doxorrubicina está descrita nas Farmacopeias Britânica, Americana e Europeia (BRITISH PHARMACOPOEIA, 2007; EUROPEAN PHARMACOPOEIA, 2008; USP, 2014). Além disso, a Farmacopeia Britânica e USP também apresentam metodologia para análise de DOX solução para injeção.

De maneira geral, metodologias analíticas estão disponíveis para quantificação de DOX, seus metabólitos e outras antraciclinas em amostras biológicas com aplicação em estudos de farmacocinética. Estes métodos baseiam-se em eletroforese capilar com detecção UV e fluorescência (GAVENDA et al., 2001; LU et al., 2009) e cromatografia a líquido de alta eficiência (CLAE) com os mesmos detectores (ZHOU; CHOWBAY, 2002; URVA et al., 2009), além de detector de massas (ARNOLD et al., 2004). Além disso, método por CLAE foi desenvolvido para quantificar DOX em tecidos oculares de coelhos após administração intravitreal de dose simples de microesferas de poli-β-hidroxibutirato contendo o fármaco (HU et al., 2007). Alhareth e colaboradores (2012) desenvolveram método por CLAE para quantificar DOX em amostras biológicas de ratos tratados com NPs de poli (cianoacrilato de alquila) contendo o fármaco antitumoral. Os métodos utilizaram detector UV e fluorimétrico e fases móveis de pH 4,0 e 2,5, respectivamente. Ambos foram aplicados a estudos de farmacocinética.

Método relativamente simples foi validado por Zhao e colaboradores (1999) para quantificação de DOX liberada em meio pH 7,4 a partir de implantes a base de gelatina. Utilizou-se coluna de fase reversa Luna C₁₈ (50 x 1 mm; 5µm) e detector de fluorescência. A fase móvel foi constituída por água, acetonitrila e ácido acético (80:19:1 v/v/v), sendo o pH aparente 3,0, que seria o pH apropriado para manutenção da estabilidade da DOX e da coluna cromatográfica. Segundo os autores, o método validado mostrou-se exato, simples e sensível.

Zagotto e colaboradores (2001), através de uma revisão bibliográfica, descreveram métodos de separação e quantificação de uma série de antraciclinas. Em relação à DOX, metodologias por eletroforese capilar, cromatografia a líquido de alta eficiência e

espectrofotometria UV-Vis são detalhadas. Os métodos objetivam monitorar as concentrações dos fármacos e seus metabólitos em fluidos biológicos e tecidos, como uma forma de garantir a eficácia do tratamento e evitar a exposição do paciente a uma sobredose que possa ocasionar efeitos adversos significativos.

Método analítico para quantificar simultaneamente DOX e vincristina em preparações farmacêuticas utilizadas no tratamento de mieloma múltiplo refratário foi desenvolvido e validado por Rodrigues e colaboradores (2009), que utilizaram cromatografia a líquido de fase reversa (coluna Waters Spherisorb C₁₈) e detector UV (230 nm). A fase móvel foi constituída por acetonitrila 90% e tampão fosfato de potássio 50 mM pH 3,2 (32:68 v/v), a qual foi eluída em fluxo isocrático de 1,5 mL/min. O método provou ser específico, exato e preciso de acordo com os padrões ICH.

De acordo com nosso melhor conhecimento, poucos métodos para direta quantificação da DOX em NPs foram validados. Para o cálculo de EE% e quantificação do fármaco em estudos de liberação *in vitro* muitos autores utilizam métodos por espectrofotometria UV-Vis em comprimentos de onda na região de 480 nm, (KANG et al., 2003; ZHAO et al., 2011; LV et al., 2014; UNSOY et al., 2014). No entanto, estes autores não apresentam maiores detalhes sobre a adequabilidade do método e parâmetros de validação.

3.4 Nanopartículas poliméricas

As NPs poliméricas possuem tamanho inferior a 1 μm e englobam dois tipos diferentes de estruturas, nanocápsulas e nanoesferas, as quais se diferem de acordo com a organização estrutural e composição. Nanocápsulas possuem núcleo oleoso ou aquoso envolto por um polímero e o fármaco pode encontrar-se dissolvido no núcleo e/ou adsorvido à parede. As nanoesferas, por sua vez, não possuem um núcleo diferenciado, mas sim, são formadas por uma matriz homogênea, ao longo da qual o fármaco se encontra retido e/ou adsorvido (COUVREUR et al., 2002; SCHAFFAZICK et al., 2003).

O tamanho nanométrico das partículas facilita sua aproximação com a região tumoral, devido à ocorrência de um fenômeno de vetorização passiva conhecido como efeito de permeabilidade e retenção aumentada (efeito EPR, da sigla em inglês). O tumor é uma região caracterizada pela elevada permeabilidade vascular própria do processo de angiogênese tumoral. Além disso, apresenta carência de drenagem linfática, o que acaba permitindo a retenção da partícula. Permanecendo neste local por tempo prolongado, as NPs liberam o

fármaco gradualmente, aumentando o tempo de exposição do tumor ao efeito farmacológico do fármaco antitumoral (GABIZON et al., 2012).

Sistemas carreadores de base nanotecnológica apresentam-se como alternativa para superar a resistência das células contra fármacos antitumorais através do encapsulamento destes (KABANOV et al., 2002; KIEVIT et al., 2012). Além disso, o direcionamento do fármaco encapsulado ao tecido tumoral pela adição de modificadores que respondem a estímulos físicos, químicos ou biológicos surge como uma grande promessa para melhorar a efetividade do tratamento antitumoral e prevenir a toxicidade em tecidos normais (YE et al., 2014; LIU et al., 2014).

Recentes desenvolvimentos em nanotecnologia continuam demonstrando NPs poliméricas como potenciais carreadores de fármacos antitumorais (AYDIN; PULAT, 2012; LIU et al, 2012; PANDEY et al., 2015). Além da biocompatibilidade e biodegradabilidade da matriz polimérica, estas NPs possuem características físico-químicas e propriedades biológicas favoráveis devido ao seu tamanho reduzido, o que as torna capazes de ultrapassar barreiras do tecido e cruzar células (WILCZEWSKA et al., 2012). Demais vantagens do uso de NPs são a possibilidade de manipular sua superfície para alcançar vetorização passiva ou ativa e poder controlar a velocidade e o local de liberação do fármaco (MOHANRAJ; CHEN, 2006).

A liberação do fármaco a partir da NP e a subsequente biodegradação do polímero são importantes para o sucesso no desenvolvimento de uma formulação. Os polímeros sintéticos biodegradáveis mais descritos na literatura são poli(ácido lático) (PLA), poli(ácido lático-co-ácido glicólico) (PLGA) e poli(ϵ -caprolactona) (PCL). Em relação aos polímeros naturais biodegradáveis, tem-se a quitosana (CS, da sigla em inglês), gelatina e albumina (KUMARI et al., 2010; WILCZEWSKA et al., 2012).

3.5 Quitosana

A CS é um polímero catiônico natural, obtido a partir do processo de desacetilação da quitina, que por sua vez, provém da carapaça de crustáceos, além de espécies de moluscos, insetos e fungos. O processo de desacetilação da quitina ocorre em condições básicas (hidróxido de sódio 40%) a 120°C por 1 a 3 horas e resulta na remoção dos grupos acetil da cadeia da molécula, formando um grupo amino (-NH₂) e duas hidroxilas livres (figura 2). A

produção de CS por essa fonte é considerada barata e fácil (KUMAR, 2000; GEORGE; ABRAHAM, 2006; ABDEL-FATTAH et al., 2007).

O grau de desacetilação da CS comercializada varia entre 70 e 95% e a massa molar média pode variar entre 10 e 1000 kDa (GEORGE; ABRAHAM, 2006). Essas duas características influenciam diretamente no tamanho e na agregação das partículas formadas (TIYABOONCHAI, 2003; NOGUEIRA et al., 2015).

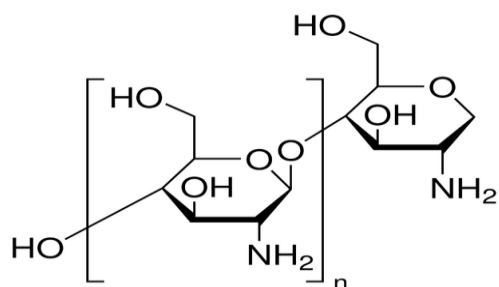


Figura 2. Estrutura química do polímero natural quitosana.

A CS é o segundo polímero natural mais abundante, antecedido apenas pela celulose (GEORGE; ABRAHAM, 2006). Apresenta característica básica, é solúvel em ácido diluído tal como ácido acético e ácido fórmico (KUMAR, 2000). O ácido acético é comumente utilizado na solubilização da CS na concentração de 1,0 mol/L ou 1% (v/v), já que esta se dissolve com facilidade em baixo pH pela protonação do grupo amino (RINAUDO et al., 1999; RINAUDO, 2006). Alguns autores têm trabalhado com este polímero solubilizado em ácido acético na concentração de 0,05 a 5% (v/v) (NGAH et al., 2005; RAMPINO et al., 2013).

Devido às características de biocompatibilidade, biodegradabilidade, não-toxicidade, baixo custo, propriedade mucoadesiva e aprovação pelo *Food and Drug Administration* (FDA), a aplicação da CS nas áreas farmacêutica (em sistemas de liberação controlada) e alimentícia tem aumentado significativamente nos últimos anos (TIYABOONCHAI, 2003; NAGPAL et al., 2010). Outras aplicações deste polímero são na área da cosmetologia, oftalmologia, fotografia, agricultura, captação de íons metálicos e engenharia de tecidos (KUMAR, 2000; AGNIHOTRI et al., 2004; RINAUDO, 2006).

Existem muitas técnicas para preparação de NPs de CS, dentre as quais se destacam a microemulsão, emulsificação difusão de solvente, gelificação iônica e formação de complexos

de polieletrólitos, sendo que os mais amplamente utilizados são os dois últimos, os quais são métodos vantajosos no sentido de que não empregam solventes orgânicos, são simples e não precisam de alta força de cisalhamento (TIYABOONCHAI, 2003; AGNIHOTRI et al., 2004).

Calvo e colaboradores (1997) descreveram pela primeira vez o método de gelificação iônica para preparação de NPs a partir do polímero natural CS e do polianion tripolifosfato de sódio (TPP). Trata-se de uma técnica branda, extremamente simples, rápida e livre de solventes orgânicos. O método envolve a mistura de duas fases aquosas sob agitação magnética à temperatura ambiente. Uma das fases refere-se ao polímero solubilizado em ácido acético, com presença ou não de um agente estabilizador, e a outra, ao polianion TPP solubilizado em água. Ao final, uma suspensão opalescente é observada, confirmando a formação espontânea das NPs devido à ligação eletrostática entre as cargas negativas do TPP e positiva da CS.

Diversos trabalhos que avaliam a razão CS/TPP (m/m) estão descritos na literatura. Esta proporção pode ser manipulada de acordo com o tamanho de partícula desejado, configurando, assim, um estudo essencial no desenvolvimento das NPs (AYDIN; PULAT, 2012, RAMPINO et al., 2013; NOGUEIRA et al., 2015). Gan e colaboradores (2007) demonstraram, ainda, que a menor razão polímero/poliânion (m/m) favorece o encapsulamento e aumenta a liberação do fármaco. Em geral, a liberação do fármaco a partir da NP depende da solubilização do fármaco, sua dessorção da superfície, difusão a partir da matriz polimérica, degradação da matriz e da combinação dos processos de erosão e difusão (MOHANRAJ; CHEN, 2006; GAN; WANG, 2007).

A DOX vem sendo associada a diferentes tipos de sistemas de liberação de fármaco baseados no polímero natural CS para a terapia do câncer. Tan e colaboradores (2009) apresentam estudos onde DOX foi encapsulada em NPs, microesferas, micelas e filmes de CS. Os autores ressaltam que é difícil definir qual é o método mais efetivo para encapsular a DOX. Além disso, cada sistema apresenta vantagens e desvantagens e que, portanto, a melhor escolha depende, principalmente, do alvo pretendido.

Com o objetivo de aumentar a quantidade de DOX encapsulada em NPs de CS pelo método de gelificação iônica, Janes e colaboradores (2001) incorporaram o polianion dextran no protocolo de preparação, o qual seria capaz de reduzir a repulsão das cargas positivas da CS e da DOX. Para isso, a DOX foi, primeiramente, incubada com dextran por 20 – 30 segundos e após, adicionada ao polímero. Por último, o TPP foi adicionado, sob agitação magnética. Resultados considerados positivos pelos autores foram encontrados para a eficiência de encapsulação (EE%). As NPs contendo dextran apresentaram EE% de 21,9%,

enquanto somente 9,1% do fármaco foi encapsulado nas NPs sem o poliânon. No estudo de liberação *in vitro* em pH 4,0, essas NPs apresentaram efeito *burst* de 17% em 2 horas seguido de liberação adicional de 4,5% em 48 horas. Por microscopia confocal, os autores comprovaram a internalização celular das NPs.

Mitra e colaboradores (2001) utilizaram o método de microemulsão para preparar NPs de CS contendo DOX conjugada ao dextran (dextran-DOX), com o objetivo de melhorar a eficácia terapêutica e reduzir os efeitos colaterais do fármaco. A EE% alcançada foi entre 60 e 65% e o diâmetro médio de partícula foi de 100 nm, o que reitera a possibilidade da liberação do fármaco no tumor sólido, bem como sua permeabilidade e acumulação seletiva no local (efeito EPR). A eficácia terapêutica foi testada *in vivo* e mostrou que NPs CS-dextran-DOX tiveram efeitos mais expressivos na redução do volume do tumor, além de maior percentual de animais sobreviventes no grupo tratado com essas NPs (50%) quando comparado com o grupo dextran-DOX conjugada (25%), afirmando que a encapsulação exerce significativo efeito sobre a regressão do tumor.

CS foi hidrofobicamente modificada com ácido oleico para sintetizar a óleo-quitosana (OCH) com o objetivo de melhorar a encapsulação de fármacos hidrofóbicos em NPs auto-organizadas (*self-assembled*). As NPs OCH e DOX-OCH apresentaram diâmetro médio de 255,3 nm e 315,2 nm, respectivamente. A EE% foi de 52,6% e o perfil de liberação *in vitro* foi investigado em pH 3,8 e 7,4, o qual indicou que 100% e 65% do fármaco foi liberado em 6 horas, respectivamente. Estudo de hemólise mostrou efeito prejudicial à membrana do eritrócito muito baixo (menor que 3,1%). Quatro diferentes linhagens de células tumorais humanas foram usadas no estudo de citotoxicidade (A549, Bel-7402, HeLa e SGC-7901) e, para todas, a taxa de inibição das células tumorais aumentou proporcionalmente à concentração de DOX e à extensão do tempo de tratamento (ZHANG et al., 2007).

A biodistribuição de nanoagregados de isotiocianato de fluoresceína-glicol-quitosana (FTC-GC) por microscopia de fluorescência foi estudada por Son e colaboradores (2003) para predizer a biodistribuição de DOX encapsulada em nanoagregados de glicol-quitosana-DOX conjugada (DOX/GC-DOX). Maior biodistribuição foi encontrada nos rins, fígado e tumor, sendo que, para o último, o efeito aumentou do 1º para o 8º dia e isso pode ser explicado pela acumulação do nanoagregado na região do tumor (devido ao efeito EPR) e baixa acumulação em outros tecidos. DOX/GC-DOX supriu o tamanho do tumor induzido em ratos, confirmando a liberação do fármaco nesta região.

Rampino e colaboradores (2013) aplicaram o método de gelificação iônica para preparar NPs de CS-TPP e estudaram sua estabilidade, modificações do tamanho e

biocompatibilidade. Os autores definiram a proporção 5:1 (m/m) de CS:TPP como sendo a ideal para a obtenção de nanocarreadores de fármacos com características físico-químicas adequadas. CS de muito baixo peso molecular (32 kDa) formou NPs menores e apresentou evolução linear de diâmetro em função do tempo de estocagem. A liofilização das NPs foi estudada, testando diferentes crioprotetores, sendo que os melhores resultados foram obtidos com a trealose. Finalmente, a segurança da NP foi testada utilizando ensaio *in vivo* em membrana corioalantoide e confirmou a não-toxicidade tanto do polímero CS quanto da NP.

Ramasamy e colaboradores (2013) estudaram o efeito de três polianions no processo de preparação de NPs de CS pelo método de gelificação iônica ou coacervação: TPP, ácido hialurônico (HA) e sulfato de dextran (DS). DOX foi usada como fármaco modelo para encapsulação. Características físico-químicas e biológicas das NPs de CS-DOX com os diferentes polianions foram estudadas, sendo que menor tamanho médio de partícula foi encontrado para NPs CS-TPP/DOX (123,8 nm) e EE% maior que 50% foi obtida para os três sistemas. Estudos de citotoxicidade foram realizados em células MCF-7 e A549 através do ensaio de viabilidade celular MTT (3-(4,5-dimetil)-2,5 difenil brometo de tetrazolio). As NPs CS-HA/DOX mostraram atividade citotóxica significativamente maior, provavelmente devido à captação celular aumentada mediada pelo receptor CD44. Por outro lado, NPs CS-TPP/DOX e CS-DS/DOX exibiram melhor estabilidade física em plasma e liberação mais lenta e sustentada em pH fisiológico.

3.6 Polietilenoglicol e poloxamer

Após administração endovenosa, as NPs podem ser rapidamente retiradas da circulação sistêmica por células do sistema fagocitário mononuclear, passando a se acumular, principalmente, no baço e no fígado. Para aumentar o tempo das NPs na circulação sanguínea e, consequentemente, o seu acúmulo no local específico de ação, em um tumor sólido, por exemplo, as NPs podem ter sua estrutura modificada através do revestimento com polietilenoglicol (PEG) ou polissorbato 80 (HANS; LOWMAN, 2002; MOHANRAJ; CHEN, 2006).

NPs furtivas (*stealth*) são, frequentemente, caracterizadas como NPs revestidas com PEG. A peguilização contribui para a estabilização do sistema e proteção contra a opsonização resultando em diminuição na velocidade de depuração e aumento no tempo de circulação das NPs na corrente sanguínea (GABIZON et al., 2013). Além disso, a adição de PEG de

diferentes dimensões à superfície da NP forma uma camada hidrofílica que reduz a interação da partícula com os componentes sanguíneos, reduzindo a tendência natural à agregação (CARUTHERS et al., 2007).

Desde 1989, quando o termo *stealth* foi registrado, o Caelyx® (Schering-Plough), doxorubicina lipossomal peguilada para injeção, começou a ser estudado. Foi desenvolvido com o intuito de aumentar o tempo de circulação do fármaco e reduzir sua captação pelo sistema retículo endotelial (RES). Doxil® (Alza Pharmaceuticals, EUA) foi o primeiro nanofármaco aprovado pelo FDA, em 1995. Em fevereiro de 2013, o Lipodox, fabricado pela Sun Pharma, foi o primeiro genérico aprovado (RANSON et al., 2001; BARENHOLZ, 2012; FDA, 2013).

Kim e colaboradores (1995) descreveram a interação entre PEG e quitina como ocorrendo através de ligação cruzada entre os grupamentos hidroxil e amino, respectivamente. De outra maneira, Najafabadi e colaboradores (2014) preparam CS peguilada pela conjugação do PEG aos grupos OH da CS, já que os grupos amino foram protegidos por dodecilsulfato de sódio. Pela adição de TPP à CS peguilada, os autores encapsularam o fármaco ibuprofeno. As NPs de CS peguilada promoveram liberação do fármaco de maneira controlada em comparação com a NP de CS apenas.

Existem, ainda, outros estudos que associam a DOX a diferentes sistemas peguilados. NPs peguiladas de ácido hialurônico foram desenvolvidas para direcionamento da DOX ao tumor (HAN et al., 2013). Além disso, NPs superparamagnéticas de óxido de ferro (SPIONs) revestidas com PEG foram propostas como carreadores da DOX (GAUTIER et al., 2012). Allard-Vannier e colaboradores (2012) compararam a atividade *in vivo* da DOX lipossomal peguilada (Caelyx, Schering-Plough) e DOX dendrímero peguilada e constataram a similaridade nos resultados, bem como baixa captação dos sistemas pelos tecidos não alvo.

Park e colaboradores (2009) utilizaram o método de emulsão simples para preparar NPs peguiladas a partir do polímero PLGA contendo DOX. As NPs apresentaram EE% de 47% e 130 nm de diâmetro médio. Através do estudo de biodistribuição, verificou-se que as NPs peguiladas permaneceram por mais tempo na circulação, confirmando o potencial clínico desse sistema. Além disso, notou-se uma redução da cardiotoxicidade ao mesmo tempo em que a atividade contra células tumorais foi mantida, sendo útil, portanto, para vetorização passiva em tumores sólidos. Por fim, as NPs mostraram-se capazes de superar a resistência a múltiplos fármacos.

Termsarasab e colaboradores (2014) preparam NPs de CS modificada contendo PEG para aumentar o tempo de circulação da DOX. Como resultado, os autores obtiveram NPs

com maior tamanho médio de partícula e menor valor de potencial zeta. Essas características resultam do caráter hidrofílico e não-iônico do PEG, que forma uma camada externa na NP (MOHANRAJ; CHEN, 2006). Ainda neste trabalho, os autores realizaram estudos de citotoxicidade em linhagem de célula tumoral e os resultados sugeriram que este nanocarreador pode ser utilizado com segurança. Além disso, foi realizado estudo de farmacocinética em ratos, com resultados que indicam que as NPs desenvolvidas exibiram baixa depuração e, portanto, maior tempo de circulação no sangue.

Poloxamer (ou Pluronic®, BASF Corporation) é um copolímero linear não-iônico, composto por uma cadeia hidrofóbica central (polióxipropileno) e duas cadeias hidrofílicas laterais (polióxidoetileno). Esta estrutura confere caráter anfifílico ao copolímero. Além disso, ele possui a habilidade de reparar danos em membranas celulares por aumentar a densidade de empacotamentos lipídicos (MOLOUGHNEY; WEISLEDER, 2013). Do mesmo modo, a capacidade do poloxamer em sensibilizar células MDR mostra sua grande utilidade como modificador biológico em NPs desenvolvidas como carreadores de fármacos antitumorais (CHO et al., 2011). Tal propriedade é alcançada através de diferentes e complexos mecanismos, inclusive pela inibição de transportadores de efluxo como a Pgp (BATRAKOVA; KABANOV, 2008). Como adjuvante em formulações farmacêuticas em geral, o poloxamer exibe propriedades estabilizantes e capazes de aumentar a solubilidade do fármaco, o que o faz extremamente útil na área farmacêutica (HOSSEINZADEH et al., 2012).

DOX com poloxamer representa uma nova e promissora estratégia para superar a resistência que as células cancerosas apresentam. A interação entre o poloxamer e a mitocôndria leva à inibição da respiração celular e, portanto, significante redução nos níveis de ATP. Estudos de atividade antitumoral mostraram que esta combinação aumenta o efeito antitumoral da DOX em células MDR e não-MDR. Além disso, evidenciou-se que o poloxamer promove apoptose em células resistentes (BATRAKOVA et al., 2010).

3.7 Sistemas nanoparticulados pH-sensíveis para liberação de DOX

A vasculatura na região tumoral é, frequentemente, mal desenvolvida e insuficiente para nutrir adequadamente a rápida divisão celular. A falta de oxigênio e nutrientes desencadeia uma alteração no metabolismo da célula cancerosa como adaptação a essa deficiência. A produção de ácido lático e de íons H⁺ e, dessa forma, a redução do pH da região tumoral (pH_e ~ 6,6), são consequências das condições anaeróbias. A diminuição do pH

pode, ainda, levar à menor captação de fármacos de caráter básico como a DOX (TIAN; BAE, 2012). Por outro lado, compartimentos intracelulares como endossomas e lisossomas apresentam pH ainda mais acidificado (pH 5 - 6) (BAE et al., 2005). Em conjunto, estas características fisiológicas conferem um grande diferencial aos tratamentos antitumorais baseados em carreadores pH-sensíveis de base nanotecnológica. Uma mudança de pH provoca a protonação/deprotonação do composto bioativo com propriedades pH-dependentes, diminuindo assim a estabilidade do nanosistema e desencadeando a liberação do fármaco encapsulado (TIAN; BAE, 2012). Segundo Liu e colaboradores (2014), os sistemas pH-sensíveis vêm sendo amplamente empregados para liberação de fármacos como uma tentativa para melhorar a terapia do câncer, justamente devido a esse gradiente encontrado entre os pHs do tumor e dos tecidos sadios.

Visando aumentar a especificidade das NPs, compostos bioativos com propriedade pH-dependente são fonte de constante estudo no campo do desenvolvimento tecnológico destes carreadores. Devido à capacidade de mudar sua conformação e atividade quando em condições de ácidas, esses compostos podem apresentar maior eficiência para a liberação de fármacos a nível intracelular e/ou a nível do espaço extracelular do tecido tumoral (LEE et al., 2007; NOGUEIRA et al., 2013).

Nesse cenário, Du e colaboradores (2011) preparam NPs pH-sensíveis para melhorar a liberação do fármaco na região tumoral. O anidro de ácido 2, 3-dimetilmaleico (DMMA) foi o responsável pela atividade pH-dependente. Para demonstrar a liberação da DOX, as NP foram incubadas em pH 7,4, 6,8 e 5,0 resultando em 22,60%, 25,56% e mais de 75% de DOX liberada em 184 h, respectivamente, indicando que a NP pode reduzir a liberação precoce do fármaco na circulação, melhorando-a a nível intracelular. Para ilustrar a eficiente internalização celular das NPs pelas células tumorais, sua biodistribuição foi avaliada através de microscopia confocal.

Termsarasab e colaboradores (2013) sintetizaram quitosana oligossacarídeo-ácido araquidônico (CSOAA) e a utilizaram para o desenvolvimento de NPs contendo DOX pelo método de evaporação de solvente. As características físico-químicas das NPs foram satisfatórias, com eficiência de encapsulação de 53%. Liberação sustentada e pH-dependente da DOX foi observada, já que ocorreu de forma expressiva em pH 5,5 em comparação com pH 6,8 e 7,4, indicando que a NP pode ser acumulada e liberar grande quantidade de fármaco no tecido tumoral, com menos DOX livre em regiões não-alvo. Além disso, o sistema não apresentou toxicidade severa na linhagem celular utilizada e inibiu o crescimento tumoral induzido no estudo *in vivo*.

Jin e colaboradores (2012) preparam e estudaram NPs pH-sensíveis contendo DOX a partir da quitosana carboximetilada. A carboximetilação é, neste caso, a responsável pela sensibilidade ao pH. Potencial zeta negativo sugere que o grupo carboximetil foi distribuído na superfície devido a sua natureza hidrofílica. A auto-organização e deformação (para liberação da DOX) das NPs mostrou-se induzida pelo pH ácido. Assim, o perfil de liberação *in vitro* foi sustentado, sendo acelerado em pH ácido (5,0). As NPs contendo DOX suprimiram o crescimento das células MCF-7 e MCF-7/Adr (versão resistente à adriamicina ou DOX) de maneira dose e tempo dependente, provando que o sistema é eficiente contra células resistentes.

Unsoy e colaboradores (2014) sintetizaram NPs magnéticas revestidas com CS para liberação pH-dependente da DOX. A CS possui, além das propriedades biológicas já citadas, propriedades que lhe conferem algum comportamento pH-sensível. Espera-se que NPs de CS pH-sensíveis sejam efetivas para liberação de fármacos no microambiente do tumor já que a velocidade de liberação é acelerada em baixos valores de pH (AYDIN; PULAT, 2012).

Ainda, DOX tem sido associada a outros sistemas de liberação de fármaco pH-sensíveis como microgéis, preparados a partir de oligo (polietilenoglicol) fumarato e metacrilato de sódio (DADSETAN et al., 2013), DOX em pro-fármaco de folato-soro fetal bovino (DU et al., 2013), complexos iônicos de poli (β -L-ácido málico) (LANZ-LANDÁZURI et al., 2014), micelas auto-organizadas de ácido hialurônico g-poli (L-histidina) (QIU et al., 2014) e polieletrólitos de ácido hialurônico (WANG et al., 2015). Estes trabalhos demonstram a liberação pH-dependente da DOX a partir dos respectivos sistemas nanoestruturados, além de sua aplicação em estudos de citotoxicidade. No entanto, destaca-se como principal desvantagem das formulações descritas a complexidade dos métodos de preparação, que envolvem diversas etapas. Apenas Qiu e colaboradores (2014) expõem resultados em relação à hemocompatibilidade do sistema, mas nenhum dos trabalhos citados estudou em detalhes a atividade lítica de membrana dependente do pH utilizando um modelo de membrana endossomal.

3.8 Tensoativos derivados do aminoácido lisina

Recentes estudos têm demonstrado a propriedade pH-sensível de uma família de tensoativos derivados do aminoácido lisina (N^{α},N^{ϵ} - dioctanoil lisina, 77K). Utilizando-se o ensaio de hemólise e o eritrócito como modelo de membrana endossomal, os autores

evidenciaram a capacidade destes compostos em romper a bicamada lipídica de maneira pH-dependente (NOGUEIRA et al., 2011a).

Esses tensoativos são preparados por simples neutralização do ácido intermediário 77K com a base do contra-íon correspondente. A estrutura química é composta por duas cadeias hidrofóbicas de oito carbonos (condensadas aos grupos α -amino e ϵ -amino da lisina) e pela cabeça aniônica da lisina com o correspondente contra-íon. A pureza dos compostos é 98%. Os contra-íons utilizados para preparação dos derivados foram potássio (77KP), lítio (77KL), sódio (77KS), lisina (77KK) e tris (hidróximetil) aminometano (77KT) (VIVES et al., 1999).

O perfil citotóxico dos tensoativos foi estudado por Nogueira e colaboradores (2011b), onde duas linhagens tumorais (HeLa e MCF-7) e quatro não-tumorais (3T3, 3T6, HaCaT e NCTC 2544) foram utilizadas e a viabilidade celular foi determinada através dos ensaios MTT e NRU (3-(4,5-dimetil)-2,5 difenil brometo de tetrazolio e ensaio de captação do corante vital vermelho neutro, respectivamente). O trabalho ressalta a importância de um estudo completo, baseado na combinação de diferentes linhagens celulares e diferentes ensaios de viabilidade para aumentar e melhorar as informações sobre os possíveis efeitos tóxicos de compostos bioativos (tensoativos) antes de aplicá-los em formulações farmacêuticas, uma vez que estão entre os excipientes farmacêuticos mais utilizados. Características particulares para cada tipo celular levam a diferentes mecanismos de defesa e graus de sensibilidade. Cabe ressaltar que o ensaio MTT sugere toxicidade a nível mitocondrial e de caráter metabólico, isto é, estágios anteriores aos que podem ser detectados pelo ensaio NRU (estágios finais, a nível de integridade das membranas celulares, especialmente a lisossomal).

No contexto do estudo da atividade e do perfil toxicológico de novas nanotecnologias, destaca-se a crescente utilização de modelos *in vitro* baseados em cultivos celulares (SOHAEBUDDIN et al., 2010; TAVANO et al., 2013; NOGUEIRA et al., 2014). Justifica-se o emprego desse tipo de metodologia, especialmente nas fases iniciais de desenvolvimento de uma nova formulação, pelo fato de que os testes de toxicidade em animais são extremamente caros e devem ser reduzidos por razões éticas inegáveis (HARTUNG, 2010). Além disso, os métodos *in vitro* também apresentam vantagens como a possibilidade de demonstração dos efeitos primários em células alvo, assim como identificação dos mecanismos envolvidos na atividade tóxica e/ou terapêutica na ausência de fatores fisiológicos e compensatórios que confundem a interpretação dos estudos utilizando modelos animais (HUANG et al., 2010).

A aplicabilidade do tensoativo 77KL (N^{α},N^{ϵ} - dioctanoil lisina com contra-íon lítio) como composto bioativo capaz de desencadear a liberação do fármaco antitumoral metotrexato no pH ácido da região tumoral foi demonstrada quando este foi incorporado a NPs de CS. As propriedades pH-sensíveis das NPs contendo o tensoativo foram confirmadas através de estudos de liberação *in vitro* do fármaco encapsulado e por sua capacidade de romper membranas biológicas em meio levemente acidificado. Ainda, as NPs contendo 77KL apresentaram atividade citotóxica aumentada contra linhagens celulares tumorais (NOGUEIRA et al., 2013).

O tensoativo aniônico 77KS (figura 3) possui peso molecular 421,5 g/mol e concentração micellar crítica (CMC) de 3×10^3 µg/ml (SANCHEZ et al., 2007) e, em estudos anteriores, demonstrou atividade pH-dependente em estudos de hemólise, com valores de concentração capaz de induzir 50% de hemólise (CH_{50}) menores quando realizados em pH 5,4. A atividade hemolítica apresentou-se fortemente dependente da concentração. De maneira geral, os tensoativos promovem o rompimento das membranas através da parcial solubilização dos lipídios e proteínas e por osmose, modificando a permeabilidade da membrana (NOGUEIRA et al., 2011a).

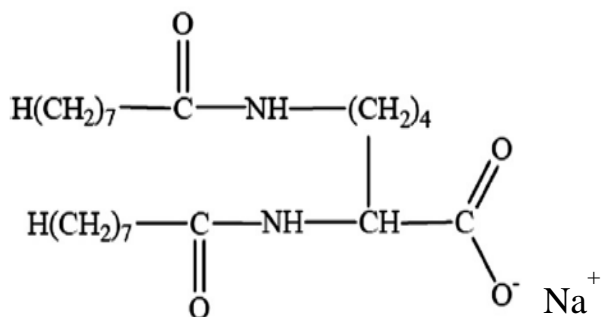


Figura 3. Estrutura química do 77KS (N^{α},N^{ϵ} - dioctanoil lisina com contra-íon sódio).

Mais recentemente, nosso grupo comparou a capacidade hemolítica de NPs brancas de CS preparadas pelo método de gelificação iônica incorporando 77KL ou 77KS como composto bioativo. A atividade lítica de membranas mostrou-se aumentada pela presença dos tensoativos nas NPs, independentemente do contra-íon (lítio ou sódio). Além disso, a hemólise foi dependente da concentração de tensoativo, do tempo de contato entre as NPs e os eritrócitos e ocorreu de maneira mais significativa quando em pH 6,6 e 5,4, o que configura a propriedade pH-sensível destes tensoativos. O aumento na taxa de hemólise induzida pelas

NPs incorporando os tensoativos pH-dependentes pode ser explicada pela protonação destes composto quando em pH ácido, o que torna a molécula não-iônica. Dessa forma, a hidrofobicidade do tensoativo é aumentada, facilitando sua ligação com as membranas e, consequentemente, o rompimento destas. (NOGUEIRA et al., 2015).

Neste mesmo estudo, a comparação entre o perfil citotóxico *in vitro* destes tensoativos em modelo celular (3T3) foi realizada. Tanto o 77KL quanto o 77KS exibiram baixa toxicidade celular através dos ensaios de viabilidade MTT e NRU. Pelo método NRU, as concentrações de tensoativo testadas não apresentaram citotoxicidade. Por outro lado, através do MTT, alguma citotoxicidade foi determinada para a concentração mais alta testada, onde as NPs incorporando o 77KS apresentaram baixa citotoxicidade (86,70% das células viáveis), enquanto a NP contendo o 77KL apresentou citotoxicidade levemente aumentada (81,22% das células viáveis). De um modo geral, os resultados apresentados acima indicam que esses sistemas nanoparticulados constituem-se carreadores promissores para a liberação de fármacos na região ácida do tumor e também a nível intracelular (NOGUEIRA et al., 2015).

ARTIGOS CIENTÍFICOS

4. ARTIGO CIENTÍFICO I:

“A comparative study of RP-LC and UV-Vis spectrophotometry to assess doxorubicin from pH-sensitive nanoparticles”

O presente manuscrito está disposto no formato de submissão ao periódico *Journal of Chromatographic Science* (Fator de impacto 1,363. WebQualis B2).

APRESENTAÇÃO EM PORTUGUÊS

Estudo comparativo de métodos analíticos por cromatografia a líquido em fase reversa e espectrofotometria UV-Vis para quantificar doxorrubicina em nanopartículas pH-sensíveis

Estão disponíveis na literatura alguns métodos por CLAE para quantificação da DOX em diferentes matrizes (plasma e tecidos), os quais utilizam diferentes tipos de detectores (fluorescência, massas e UV). No entanto, em relação à DOX associada a NPs, há apenas um método descrito para sua quantificação em plasma e tecidos após administração de uma dose de NPs de poli cianoacrilato de alquila (PACA). Portanto, o presente trabalho foi baseado na carência de métodos analíticos validados por CLAE disponíveis para quantificação da DOX em NPs de quitosana e, principalmente, devido à utilização por outros autores somente de análises por espectrofotometria UV-Vis para quantificação do fármaco em estudos de liberação e cálculo da eficiência de encapsulação. Destaca-se que estes trabalhos não exibem detalhes sobre a validação do método utilizado. Dessa forma, procedeu-se ao desenvolvimento e validação de método específico e sensível por CLAE e, concomitantemente, de um método rápido e simples por espectrofotometria UV-Vis para determinação da DOX em matrizes poliméricas. Utilizou-se cromatógrafo 1260 Agilent Technologies, provido de software EZChrom, injetor automático, bomba quaternária e detector UV-Vis e espectrofotômetro Shimadzu UV-1800, respectivamente. Para verificar o índice de pureza de pico durante a avaliação da especificidade do método por CLAE, utilizou-se cromatógrafo Shimadzu com detector de arranjo de diodos (DAD). Os métodos foram validados de acordo com o ICH para os parâmetros especificidade, linearidade, precisão, exatidão e robustez. As CS-NPs utilizadas como amostras foram preparadas segundo o método de gelificação iônica que consiste, basicamente, na mistura de duas fases aquosas, uma catiônica (CS e DOX) e outra aniônica (TPP e 77KS). Nesse caso, o método padrão compreendeu algumas modificações como a inclusão do tensoativo aniônico derivado do amino ácido lisina com contra íon sódio, 77KS, que, conforme relatado em estudos anteriores, apresenta propriedade pH-sensível. O tensoativo em questão foi sintetizado pelo CSIC (*Consejo Superior de Investigaciones Científicas, Barcelona, Espanha*) e gentilmente doado ao nosso grupo de pesquisa. Os métodos desenvolvidos mostraram-se específicos, lineares, precisos, exatos e robustos, bem como, adequados para as aplicações pretendidas e expostas no decorrer do estudo.

A comparative study of RP-LC and UV-Vis spectrophotometry to assess doxorubicin from pH-sensitive nanoparticles

ABSTRACT

Analytical methods by reversed-phase liquid chromatography (RP-LC) and UV-Vis spectrophotometry were developed and validated to determine doxorubicin in pH-sensitive chitosan nanoparticles (NPs). Chromatographic separation was performed on a RP-C₁₈ column, with UV detection at 254 nm and mobile phase compounded by 90% (v/v) acetonitrile in water and water pH 3.0 (33:67, v/v). UV-Vis spectrophotometric method had the wavelength set at 480 nm, and water pH 3.0 was used as diluent. Calibration curves were linear from 1 to 30 µg/mL ($r > 0.9995$) and the specificity was proven by checking the absence of any interference from NP components. The values of accuracy and precision were within acceptable limits, and robustness studies were performed by a two-level full factorial design. The validated methods were further tested to assess doxorubicin content in six different batches of pH-sensitive chitosan NPs, and the comparative analyses showed non-significant differences ($p > 0.05$). Likewise, the RP-LC method was successfully applied to determine the drug encapsulation efficiency, and to measure doxorubicin during *in vitro* release assays and degradation kinetic studies under UVC radiation. Both methods fulfilled all validation parameters, and proven to be suitable for the characterization of doxorubicin-loaded pH-sensitive chitosan NPs, without interference from NP matrix.

Keywords: doxorubicin; chitosan nanoparticles; reversed phase-liquid chromatography; UV-Vis spectrophotometry; validation

Introduction

Doxorubicin (DOX) belongs to the anthracycline antibiotic group and is among the drugs more extensively used in cancer chemotherapy, including leukemia, non-Hodgkin lymphomas, breast cancer, Hodgkin's disease and sarcomas (1,2). The antineoplastic effect is achieved through different mechanisms of action as DNA intercalation and alkylation, generation of reactive oxygen species, interference with RNA and DNA polymerase and inhibition of topoisomerase II (3). However, DOX can induce tumor cell resistance and cause important side effects, such as myelosuppression and cumulative dose-related cardiotoxicity, which, in turn, can lead to irreversible cardiomyopathy and congestive heart failure (4).

In this context, nanotechnology and nanoscience approaches have been gaining growing importance in the pharmaceutical industry regarding their potential application in diagnosis and treatment of different pathologies. Besides to their small size, the functionalized nanoparticulate systems may enhance the drug delivery to specific cells and locations, decreasing, thus, the traditional side effects (5). Herein, appear the polymeric nanoparticles (NPs) with pH-responsive behavior, which achieve the tumor acidic environment by i.e., incorporation of a pH-sensitive surfactant into the nanostructure matrix (6).

Chitosan (CS) is a biocompatible and non-toxic cationic natural polymer (7). Calvo et al. (8) firstly described the procedure to prepare CS-NPs by ionotropic gelation, in which the polymer CS interacts with a polyanion (i.e. tripolyphosphate, TPP). DOX-loaded CS-NPs have been synthesized by different methods of preparation in order to enhance the cytotoxic effects of this drug specifically against tumor cells (9-11).

Several methods by liquid chromatography (LC) are reported in the literature for DOX quantification in different matrixes and with many analytical purposes, such as pharmacokinetic studies (12-14) and researches regarding the drug determination in plasma and tissues (15,16) or in pharmaceutical preparations for chemotherapeutic association (17). Additionally, UV-Vis spectrophotometric methods have been described to quantify DOX in pure form or in pharmaceutical formulations (18).

Likewise, LC methods have been described for DOX determination in human plasma (19) and rat plasma (20) after drug administration as PEGylated liposomal delivery system. Similarly, Alhareeth et al. (21) developed a LC method with fluorometric detection to assess DOX and its metabolites in plasma and tissues of rat treated with poly(alkylcyanoacrylate) (PACA) NPs. Regarding the applicability of analytical methods to assess DOX encapsulation efficiency into NPs and to measure the *in vitro* drug release from these delivery systems, most

researchers have been using spectrophotometry (11,22,23), probably to its simplicity and low cost. However, validation data of these methods were not reported and detailed.

Therefore, the aim of this study was to develop and validate a specific and effective RP-LC method and a simple and affordable method based on UV-Vis spectrophotometry to quantify DOX in pH-sensitive chitosan nanoparticles. The relevance and applicability of both methods for the determination of DOX content into NPs was evidenced. Furthermore, the RP-LC method was also successfully applied to fully characterize these nanocarriers, i.e. by assessing the drug encapsulation efficiency and *in vitro* release profile, and by studying the DOX photolytic degradation kinetics when encapsulated into NPs.

Experimental

Chemical and reagents

Doxorubicin (DOX, state purity 98.32%) was purchased from Zibo Ocean International Trade (Zibo, Shangdong, P.R., China). Chitosan (CS) of low molecular weight (deacetylation degree, 75-85%; viscosity, 20-300 cP according to the manufacturer's data sheet) and pentasodium tripolyphosphate (TPP) were obtained from Sigma-Aldrich (St. Louis, MO, USA). HPLC grade acetonitrile and glacial acetic acid were purchased from Tedia (Fairfield, USA). All chemicals used were of pharmaceutical or special analytical grade. For all analyses, ultrapure water was purified using a Mega RO/UP - Mega Purity system.

The anionic amino acid-based surfactant derived from N^a,N^e-dioctanoyl lysine and with an inorganic sodium counterion (77KS) was synthesized as previously described (24). It has a molecular weight of 421.5 g/mol, a critical micellar concentration (CMC) of 3 x 10³ µg/mL and its chemical structure is formed by two alkyl chains, each one with eight carbon atoms (25).

Instrumentation and analytical conditions

The chromatographic analysis was performed on a LC 1260 Agilent Technologies system (Agilent Technologies, Santa Clara, CA, USA) equipped with a 1260 Quat Pump VL quaternary pump, a 1260 ALS automatic injector and a 1260 VWD VL detector. Data collection, analysis and reporting were performed with EZChrom software program (version A.01.05). The analyses of DOX were carried out on a reversed-phase Waters (Milford, MA, USA) XBridgeTM C₁₈ column (250 mm x 4.6 mm I.D., with a 5 µm particle size and pore size

of 110 Å), with mobile phase consisted of 90% (v/v) acetonitrile (ACN) in water-water pH 3.0, acidified with glacial acetic acid (33:67, v/v). Prior to use, each eluent was filtered through a 0.45 µm pore size membrane filter (Millipore, Milford, MA, USA) and sonicated. The mobile phase was pumped isocratically at a flow rate of 1.0 mL/min, with a sample injection volume of 20 µl and a detection wavelength set at 254 nm. The total run time was 9 minutes and all experiments were performed at room temperature. Each day of analysis, the column was equilibrated for at least 30 min with the mobile phase flowing through the system.

The evaluation of the peak purity during the specificity test was performed on a Shimadzu LC system (Shimadzu, Kyoto, Japan) equipped with a SPD-M20A photodiode array (PDA) detector and LC Solution software program (version 1.24 SP1).

The UV-Vis spectrophotometric experiments were performed on a double-beam UV-Vis spectrophotometer (Shimadzu, Japan) model UV-1800, with a fixed slit width (2 nm) and a 10 mm quartz cell was used to obtain spectrum and absorbance measurements. The wavelength was 480 nm and the diluent used was water pH 3.0, acidified with glacial acetic acid.

Preparation of reference solution and nanoparticle samples

The DOX reference stock solution was prepared in ultrapure water to give a final concentration of 2 mg/mL. The stock solution was stored protected from light at 2-8 °C, and further dilutions were made fresh daily with mobile phase, for the LC analysis, or with water pH 3.0, for the UV-Vis spectrophotometric measurements, to obtain working solutions containing 1, 5, 10, 15, 20 and 30 µg/mL. Finally, the samples for LC analysis were filtered through a 0.45 µm membrane filter (Sartorius Stedim Biotech, Germany) before injection into the chromatographic system.

The nanoparticles were prepared following the procedure described by Calvo et al. (8), which is based on the ionotropic complexation of CS with TPP anions. Some modifications were included to the standard procedure, such as the incorporation of the biocompatible and pH-sensitive amino acid-based surfactant 77KS as a bioactive adjuvant (26). CS (0.1% w/v) was prepared dissolving the weighed mass in an aqueous acetic acid solution (1%, v/v). The pH of the CS final solution was adjusted to 5.5 with 1 M sodium hydroxide (27). A premixed TPP and 77 KS solution was prepared in ultrapure water (at 0.2% and 0.05%, w/v, respectively, with a TPP:77KS ratio equal to 2:0.5, w/w)

DOX-loaded CS-NPs (DOX-CS-NPs) were prepared as follows: to a CS (0.1% w/v), DOX was added to provide a concentration of 0.01% (w/v) of the antitumor drug (with a CS:DOX ratio equal 5:0.5, w/w). Thereafter, DOX-loaded NPs were formed spontaneously when the premixed TPP:77KS solution was added to the above mixture. This process was carried out under mild conditions without involving high temperatures or organic solvents, only using constant magnetic stirring (1000 rpm) during 30 minutes (10 min stirring CS + DOX, and further 20 min stirring after addition of TPP:77KS solution). Dark conditions were maintained to prevent any possible photodegradation. Unloaded CS-NPs were prepared according to the procedure previously detailed, omitting the drug.

During the validation procedures, nanoparticle suspensions used for the evaluation of all parameters were freshly prepared. In order to extract the drug from the NP matrix, an aliquot of NP suspension was firstly mixed with methanol (1:1, v/v) and then sonicated for 15 min, which allow the release of the entire encapsulated drug from the nanostructure. The resulting solution was further diluted in mobile phase or water pH 3.0, for the LC and UV-Vis spectrophotometric analyses, respectively, to a concentration of 15 µg/mL. The samples for LC experiments were finally filtered through a 0.45 µm membrane and injected in the HPLC system. The unloaded CS-NPs were also extracted following the same procedure in order to verify the occurrence of some interference of the NP components in the analytical conditions.

Validation of the RP-LC and UV-Vis spectrophotometric methods

The methods were validated for the requirements specificity, linearity, precision, accuracy, range and robustness, following the International Conference on Harmonisation (28) guideline.

Specificity was evaluated by comparing the chromatograms obtained for unloaded NPs and DOX-CS-NPs. In order to assess the exact measurement of the drug into the NPs, without interferences due to constituents that may be present, both formulations were treated in the same manner and injected into the LC system. Likewise, DOX standard solution was injected at a concentration of 15 µg/mL, as well was DOX-CS-NPs. Then, the purity of DOX peak was determined using a PDA detector. For the UV-Vis spectrophotometric method, the absorption spectra were compared in order to guarantee that there was no interference in the DOX absorbance region.

The linearity was determined by constructing three independent analytical curves, each one with six concentrations of DOX, in the range of 1-30 µg/mL (1, 5, 10, 15, 20 and 30 µg/mL), prepared in mobile phase or water pH 3.0 for the RP-LC or UV-Vis

spectrophotometric methods, respectively. Triplicate analyses of each sample were made to verify the repeatability of the responses. The peak areas of the chromatograms or the absorptions values were plotted versus drug concentration to obtain the analytical curve. The results were subjected to regression analysis by a least-squares method to calculate calibration equation and correlation coefficient.

Repeatability and intermediate precision were considered to verify the precision of the methods. Repeatability was examined by analyzing six samples of DOX-CS-NPs at the same concentration (15 µg/mL). All of them were prepared in a short period of time and under the same experimental conditions. The intermediate precision was assessed by carrying out the analysis on three different days (inter-days) and also by different operators performing the analysis in the same laboratory (inter-analysts). Precision was expressed as relative standard deviation (RSD) and the results must be less than 2.0%.

Accuracy was evaluated by the standard addition method where samples of known concentrations of DOX-CS-NPs (10 µg/mL) were spiked with three different concentrations of standard solution (2, 5 and 8 µg/mL, i.e., three different levels: lower, medium, and upper concentration), giving sample solutions with final concentrations of 12, 15 and 18 µg/mL, equivalent to 80, 100 and 120% of the nominal analytical concentration, respectively. The accuracy was calculated at each concentration level as the percentage of drug recovered from the sample (recovery %), which was calculated from differences between the responses obtained for spiked and unspiked solutions.

The robustness of an analytical method refers its capacity to be reproduced in different laboratories or under different, but deliberate, analytical procedure and circumstances without affect the results (29). Therefore, the robustness was determined by analyzing DOX-CS-NPs samples (15 µg/mL) under a variety of conditions with small variations of the method parameters. For the LC method, the robustness was determined by making small and deliberate changes in the factors flow rate, injection volume, aqueous phase pH and percentage of organic solvent in the mobile phase, while for the UV-Vis spectrophotometric method, changes were made in the wavelength, diluent pH and extraction time of the drug from the NPs. A two-level full factorial design (number of analyses equal to $2^k + n$, where k is the number of factors and n is the number of central points) was applied. Thus, for RP-LC method, 20 experimental runs were performed including 4 at the nominal conditions, and for the UV-Vis spectrophotometric method, 11 experiments were performed, being 3 at the nominal conditions (30,31).

The system suitability test was carried out for the RP-LC method to evaluate the reproducibility of the system for the analyses to be performed, using six replicates injections of reference solution containing 15 µg/mL of DOX. The parameters peak area, retention time, theoretical plates (N), tailing factor (peak symmetry) and capacity factor (k') were measured.

Applicability of the validated analytical methods

Analysis of DOX content into the formulations

For the quantitative analyses, an aliquot of the nanoparticles suspension was diluted in methanol (1:1, v/v) and sonicated for 15 minutes to extract the drug. Then, the obtained solution was diluted with mobile phase or water pH 3.0 to reach up a final concentration of 15 µg/mL and analyzed by LC and UV-Vis spectrophotometric methods, respectively. For the LC analyses, the samples were filtered through a 0.45 µm membrane filter to remove insoluble fractions before measurement. The total content of drug was calculated against a reference solution at same concentration. The results obtained by the two methods were statistically compared by Student's t test and ANOVA in order to verify the similarity of the experimental values and, thus, to determine the equivalence of both methods for the assessment of DOX in chitosan-based NPs.

Drug encapsulation efficiency

The encapsulation efficiency (EE%) was estimated as being the difference between total concentration of DOX in the NP suspension and free DOX concentration present in ultrafiltrate. For this, free drug was separated by ultrafiltration/centrifugation technique (Sigma 2-16P Centrifuge, Sigma, Germany) using Amicon Ultra-0.5 Centrifugal Filters (10,000 Da MWCO, Millipore) at 10,000 rpm for 20 minutes. EE% was calculated by using the RP-LC method.

In vitro DOX release study

In vitro release studies from pH-sensitive DOX-loaded CS-NPs were performed using the dialysis technique. An aliquot of NPs was placed in a dialysis bag (Sigma-Aldrich, 14,000 MWCO), which was then immersed in 50 mL of phosphate-buffered saline (PBS, pH 5.4 and 7.4) and maintained at $37 \pm 1^\circ\text{C}$ under continuous magnetic stirring (100 rpm) for 24 hours. At specific time intervals, 2 mL of medium was withdrawn and then replaced with 2 mL of fresh buffer to maintain constant volume and sink conditions. DOX content in the aliquots

collected was determined according to the previously validated RP-LC method. However, in order to assess the influence of the medium used, the method was co-validated for linearity and range using the release medium (PBS pH 5.4 or 7.4) as diluent. In addition, the concentration range assessed was extended toward a lower limit of quantification to allow a more reliable determination of DOX content.

Degradation under photolytic conditions

Photodegradation was induced by exposing the samples (DOX-CS-NP), into transparent capped cuvettes (Brand®, UV-Cuvettes micro) to UVC ($\lambda = 254$ nm) radiation in a mirrored chamber for 8 hours. Every hour, samples were collected from the chamber. The drug was extracted from the NPs as previously described and analyzed by LC to determine the DOX content. The drug content was calculated by comparison with samples not irradiated. DOX-CS-NPs that were subjected to the same procedure, but protected from light, serve to refute the hypothesis of thermal degradation and were used as control.

The photolytic degradation kinetics of the DOX-loaded NPs was calculated by the graphic method, through which it was possible to determine the degradation constant (k -value). Zero order, first order and second order graphics were delineated by plotting the drug concentration, \ln of drug concentration or the inverse of drug concentration *versus* time, respectively. The graph with the best fit was considered to establish the kinetic order, considering the correlation coefficient. Finally, the half-life ($t_{1/2}$) and the t_{90} value (time for 10% degradation) were determined from k -value (32,33).

Statistical analysis

Statistical analyses were performed using one-way analysis of variance (ANOVA) and/or Student's *t*-test to determine the differences between the datasets, followed by Tukey's post-hoc test for multiple comparisons using SPSS® software (SPSS Inc., Chicago, IL, USA). $p < 0.05$ was considered significant. The statistical analyses of robustness were performed by using Minitab® v.17 software (Minitab Inc., State College, PA, USA).

Results

Validation of the methods

The specificity of the methods for DOX quantification was achieved successfully in the presence of the matrix components. The chromatograms and absorption spectra (Figure 1)

showed that no signal at 254 nm and 480 nm, respectively, was detected when unloaded NPs were evaluated. Peak purity test showed that the DOX peak was free from any co-eluting peak (impurities and/or excipients), with values of peak purity index higher than 0.9999.

Linearity data were obtained after construction of three calibration curves. The linear regression equations obtained by the least-square method and the values of the correlation coefficient ($y = 895307.86x + 101138.40$, $r = 0.9996$, for RP-LC; and $y = 0.02051x + 0.00788$, $r = 0.9998$, for UV-Vis spectrophotometry; where x is concentration and y is the peak absolute area or absorbance) indicated the linearity of the analytical curves for both methods. Moreover, the validity of the assays was verified by ANOVA. This revealed that the regression equations were linear ($F_{\text{calculated}} = 4,751.46 > F_{\text{critical}} = 4.75$, $p < 0.05$, for the LC method; and $F_{\text{calculated}} = 26,385.62 > F_{\text{critical}} = 4.75$, $p < 0.05$, for the UV-Vis spectrophotometric method) with no linearity deviation ($F_{\text{calculated}} = 0.99 < F_{\text{critical}} = 3.26$; $p > 0.05$, for the LC method; and $F_{\text{calculated}} = 2.25 < F_{\text{critical}} = 3.26$; $p > 0.05$, for the UV-Vis spectrophotometric method).

The precision of the methods, evaluated as the repeatability, was checked by preparing six different batches of DOX-CS-NPs, which were extracted, diluted until 15 µg/mL and analyzed by both analytical methods. The test was performed on the same day and under the same experimental conditions, and the RSD of the assay was calculated as 1.10% and 0.97% for RP-LC and UV-Vis spectrophotometric methods, respectively. Likewise, the intermediate precision was verified by analyzing three samples of the DOX-loaded NPs on three different days (inter-day) and by three different analysts (inter-analyst) in the same laboratory. The results are given in Table I and the obtained RSD values are lower than the acceptance criterion of 2.0%. In addition, the results of repeatability ($p = 0.6644$), inter-day ($p = 0.3801$) and inter-analyst ($p = 0.1854$) were submitted to statistical Student's *t*-test ($p = 0.05$), which revealed no significant difference between the validated methods. Likewise, method accuracy was evaluated by means of the percentage recoveries of the known amounts of DOX standard solution added to NP samples. Good recoveries (98–102%) were obtained and are demonstrate in Table I.

Robustness was assessed by a 2^4 and 2^3 full factorial design for RP-LC and UV-Vis spectrophotometric methods, respectively, where simultaneous variations of the factors could be studied for the DOX assay. The analysis of DOX reference and sample solutions at 15 µg/mL were performed in each condition and, thereafter, the quantitative responses were calculated. All experiments were performed in randomized order to minimize the effects of

uncontrolled factors that may induce responses. The experimental domain of the selected variables is reported in Table II.

The pareto chart (Figure 2) shows that a single factor or their combinations presented no significant influence on the analytical performance. Moreover, the results of the experimental range of variables evaluated were within the acceptable deviation (RSD < 2.0%), which demonstrated that there were no significant changes in the chromatographic pattern and/or on assay data when the modifications were made in the experimental conditions, thus showing the methods to be robust under the conditions tested.

Finally, acceptable values of tailing factor (TF) and capacity factor (k') were found in system suitability test: 1.47 and 1.40, respectively. Moreover, the RSD values calculated for the peak area, retention time, TF and k' were lower than 0.73%, 0.28%, 1.57% and 1.05%, respectively. The number of theoretical plates was about 8992.83, with RSD < 1.48%.

Applicability of the validated analytical method

The determination of drug content in NP sample solutions by validated methods showed acceptable results (Table III). RSD values were lower than 2.0% from triplicate analysis of each sample. Besides, the experimental values of the two methods were compared statistically by the Student's *t*-test and by ANOVA, showing non-significant differences (calculated value < critical value; $p > 0.05$).

The amount of drug that was really entrapped into the NPs was determined by the RP-LC method, which proved to be effective and precise for these analyses. A good percentage of encapsulation was achieved (about 66.50%, with RSD lower than 2.70% for $n = 3$).

The chromatographic method was also applied to *in vitro* release studies of DOX from the NPs as a function of pH. First of all, analytical curves were constructed, in the concentration range of 0.25 to 30 $\mu\text{g}/\text{mL}$, using PBS pH 5.4 and 7.4 as diluents. Linear regression equations were obtained by the least-square method and the values of the correlation coefficient ($y = 721070.44x - 183476.77$; $r = 0.9994$, for PBS pH 5.4; and $y = 721998.57x - 33552.04$; $r = 0.9995$, for PBS pH 7.4; where x is concentration and y is the peak absolute area) indicated the linearity of both curves independently of the pH. Figure 3 illustrates the cumulative amount of DOX released from the NPs at both acidic and physiological pH. The amounts of drug released at pH 5.4 was significantly higher ($p < 0.05$) than that observed at pH 7.4 in almost all schedule times.

Finally, the LC method was successfully applied to assess the degradation profile of DOX entrapped in the NPs under UVC radiation. After 8 h exposure, almost 50% of the drug

was degraded. However, only reduction of peak area was noted, without the appearance of any additional peaks. The DOX peak purity index was determined by the PDA detector, providing great value (0.9999). It was observed that the DOX-CS-NP degradation profile followed the zero order kinetics, as the corresponding graphic provided the best correlation coefficient ($r = 0.9978$) by plotting the drug concentration as a function of time (Figure 4). The photodegradation rate constant (k) was determined by the graphic equation and the value obtained was $0.8797 \text{ } \mu\text{g mL}^{-1}\text{ min}^{-1}$. The calculated $t_{1/2}$ was 8.53 h, very close to the experimental value (~54% of degradation occurs in 8 h). When DOX-CS-NPs were protected from light, more than 98% of DOX remained intact after 8 h of irradiation. Moreover, the t_{90} value was estimated as 1.71 h under the same experimental conditions.

Discussion

Nanomaterial-based products usually contain a complex matrix, including polymers and surfactants. In this way, the current analytical methodology for the usual pharmaceutical formulations may not be appropriate for the analysis proposed. For this reason, the development and validation of specific analytical methods, without any interference of NP excipients, is necessary since the validation procedures warrant that the method is suitable for the application intended (34). Thus, in this work, two analytical methods were validated with the purpose to provide simple and reliable tools to quantify the antitumor drug DOX in pH-sensitive polymeric NPs.

The chromatographic and spectrophotometric conditions were adjusted in order to provide efficient and simple routine analysis, with reducing run time and low cost of analysis. To achieve the best performance of the chromatographic method, tests concerning the ideal composition of the mobile phase and the optimum pH were performed with the objective to provide selectivity and best peak shape. ACN was chosen as organic phase since it resulted in short analysis time, with improved peak symmetry (about 1.47). Concerning the aqueous phase, potassium phosphate buffer pH 3.2 was tested initially and showed good results. Thereafter, water pH 3.0, acidified with glacial acetic acid, was also evaluated and proved to be more suitable than the buffer. Moreover, water pH 3.0 was chosen due its easy preparation and also because it satisfies the stability characteristics of the drug (35). Likewise, avoiding the use of buffers, may aid to increase the column durability. Finally, the proportion 33:67 (v/v) of 90% ACN in water-water pH 3.0 was selected due to the fast elution of the analyte (retention time of 6.02 min), which was achieved without any interference from NP matrix. In

addition, this condition allowed low consumption of organic solvent and provided acceptable chromatographic parameters. The best detection wavelength was defined by using a PDA detector in accordance to the given DOX absorption spectrum, and was set as 254 nm.

A UV-Vis spectrophotometric method was also developed in view of its simplicity and low cost for the routine analysis (36). To choose the wavelength that allows the better quantification of DOX, scans were carried out between 200 and 700 nm. The established wavelength was not the one that corresponds to the maximum absorption. Indeed, the wavelength of 480 nm was the better option (23,37,38), once the drug is colored, and also because the components of the matrix definitively exhibited no absorbance at this UV range. As reported previously, DOX is stable in acidic pH (35) and soluble in water (39). Therefore, the ideal diluent for the samples was defined as water pH 3.0, acidified with glacial acetic acid.

Both analytical methods appeared to be specific for DOX determination in the presence of NP constituents. Therefore, it can be regarded that both RP-LC and UV-Vis spectrophotometric methods are specific, i.e., without any interference or overlaps of the NP components with the DOX signal. Finally, standard and sample solutions were analyzed concerning to the peak purity using a PDA detector and the absence of any interference in the LC method performance was confirmed.

The data for the analytical curves constructed suggest good linearity for both methods over a concentration range of 1-30 µg/mL, with great correlation coefficient values. Furthermore, the results achieved for precision and accuracy were within the acceptable range and, thus, the methods were deemed to be precise and accurate.

Literature revealed some design methodologies to assess robustness during analytical method validation, such as full factorial design and fractional factorial design, and highlight their significance for the evaluation of which sources of variations must be more tightly controlled during the method application, and which factors affect negatively the quality of pharmaceutical analyses (40). To evaluate the robustness of the RP-LC and UV-Vis spectrophotometric methods developed, we made a full factorial design, where each parameter examined represents a main variable and the combinations between two, three or four (the last for RP-LC method exclusively) main variables correspond to second, third or fourth order interactions, respectively (30). Regarding the RP-LC method, the main variables were injection volume, proportion of ACN 90%, flow rate and pH of aqueous phase. Here, second, third and fourth order interactions were studied. For the UV-Vis spectrophotometric method, the robustness was determined by analyzing samples after small changes in one, two,

or all of the following factors: detection wavelength, pH of the diluent and DOX extraction time from the NPs. Therefore, second and third order interactions were evaluated. The pareto chart supports the understanding of the results from the robustness studies. In the Figure 2, the bars represent the influence that each main variable or the combinations among these variables had on the response obtained. For both methods, a single factor or their combinations showed no significant influence on the analytical performance, since the bars did not cross the vertical line (critical t -value for $\alpha = 0.05$).

The system suitability test was carried out to evaluate the adequability and reproducibility of the LC system for the analyses to be performed. Altogether, the experimental results showed that the parameters tested were within the acceptable range (RSD < 2.0%), indicating that the system is suitable for the analysis intended.

The proposed methods were successfully applied for the determination of DOX content into six different batches of DOX-loaded CS-NPs, using the conditions optimized and validated for each methodology.

The RP-LC method was also used to assess DOX EE%, since the determination of the amount of drug that is really entrapped into the nanocarrier it is of great importance during NP development and quality control studies. Although many authors opted for spectrophotometric methods to determine DOX EE% into NPs (11,22,23), here we used the proposed RP-LC method for this purpose. It is worth pointing out that the LC method allows analysis of samples with smaller volumes than the spectrophotometric method, which is particularly important for the quantitative analysis of drug content into the small amount of ultrafiltrate obtained from the Amicon dispersive.

Furthermore, liquid chromatographic systems usually have a greater ability to quantify lower drug concentrations in diluted samples. This feature is particularly advantageous in release studies, where very small amount of drug can be present in the medium (41,42). Analytical curves constructed with PBS pH 5.4 and 7.4 proved that the use of such diluents did not modify the chromatographic performance and/or altered the quantification power of the validated LC method. Therefore, it was successfully applied to quantify DOX during the release studies. The drug was released faster at pH 5.4 than at physiological conditions, which, thus, demonstrated the pH-dependent properties of the formulation.

As the last application, the LC method was used to assess the degradation profile of the encapsulated DOX under UVC radiation. The method proved to be appropriate and effective for this purpose and the results of peak purity index indicated that it might have a stability-indicating capability, which evidently has to be confirmed by other forced

degradation studies. The graphics of zero, first and second order were constructed for modeling the DOX kinetics degradation. Once the drug showed zero-order degradation profile, it means that the reaction rate is independent of DOX concentration and of temperature, but is dependent of the incident radiation.

Conclusions

The validation studies showed that the RP-LC and UV-Vis spectrophotometric methods are specific, linear, precise and accurate. A full factorial design was effectively applied to evaluate robustness with many advantages over the traditional one-variable-at-time approaches. The applicability of both methods was successfully demonstrated for the assessment of DOX content in pH-sensitive chitosan-based NPs, with no interference of the polymers and surfactant present in the formulation. Moreover, the RP-LC method was proved to be suitable to assess DOX encapsulation efficiency, as well as to determine the *in vitro* DOX release and the photodegradation kinetics of the encapsulated drug. Altogether, the results demonstrated that the validated methods are appropriate tools to quantify DOX in complex matrices of nanotechnology-based polymeric formulations. Finally, it is worth mentioning that the availability of reliable analytical methodologies can contribute to improve the quality and to assure the therapeutic efficacy of novel pharmaceutical nanoformulations that have been developed.

Acknowledgments

This research was supported by Projects 447548/2014-0 and 401069/2014-1 of the *Conselho Nacional de Desenvolvimento Científico e Tecnológico* (CNPq - Brazil), 2293-2551/14-0 of *Fundação de Amparo à Pesquisa do Estado do Rio Grande do Sul* (FAPERGS - Brazil) and MAT2012-38047-C02-01 of the *Ministerio de Economía y Competitividad* (Spain). Laís E. Scheeren and Daniele R. Nogueira thank FAPERGS and PNPD-CAPES (Brazil) for the Masters' and Postdoctoral fellowships, respectively.

References

1. Aubel-Sadron, G. and Londos-Gagliardi, D.; Daunorubicin and doxorubicin, anthracycline antibiotics, a physicochemical and biological review; *Biochimie*, (1984); 66: 333-352.
2. Keizer, H.G., Pinedo, H.M., Schuurhuis, G.J. and Joenje, H.; Doxorubicin (adriamycin): a critical review of free radical-dependent mechanisms of cytotoxicity; *Pharmacology & Therapeutics*, (1990); 47: 219-231.
3. Gewirtz, D.A.A.; Critical evaluation of the mechanisms of action proposed for the antitumor effects of the anthracycline antibiotics adriamycin and daunorubicin; *Biochemical Pharmacology*, (1999); 57: 727-741
4. Hortobágyi, G.N.; Anthracyclines in the treatment of cancer; *Drugs*, (1997); 54: 1-7.
5. Moghimi, S.M., Hunter, A.C. and Murray, J.C.; Nanomedicine: current status and future prospects; *The FASEB Journal*, (2005); 19: 311-330.
6. Nogueira, D.R., Tavano, L., Mitjans, M., Pérez, L., Infante, M.R. and Vinardell, M. P.; In vitro antitumor activity of methotrexate via pH-sensitive chitosan nanoparticles; *Biomaterials*, (2013); 34: 2758-2772.
7. Kean, T. and Thanou, M.; Biodegradation, biodistribution and toxicity of chitosan; *Advanced Drug Delivery Reviews*, (2010); 62: 3-11.
8. Calvo, P., Remuñán-López, C., Vila-Jato, J.L. and Alonso, M.J.; Novel hydrophilic chitosan-polyethylene oxide nanoparticles as protein carriers; *Journal of Applied Polymer Science*, (1997); 63: 125-132.
9. Janes, K.A., Fresneau, M.P., Marazuela, A., Fabra, A. and Alonso, M.J.; Chitosan nanoparticles as delivery systems for doxorubicin; *Journal Controlled Release*, (2001); 73: 255-267.
10. Termsarasab, U., Yoon, I., Park, J., Moon, H.T., Cho, H. and Kim, D.; Polyethylene glycol-modified arachidyl chitosan-based nanoparticles for prolonged blood circulation of doxorubicin; *International Journal of Pharmaceutics*, (2014); 464: 127-134.
11. Unsoy, G., Khodadust, R., Yalcin, S., Mutlu, P. and Gunduz, U.; Synthesis of Doxorubicin loaded magnetic chitosan nanoparticles for pH responsive targeted drug delivery; *European Journal of Pharmaceutical Sciences*, (2014); 62: 243-250.
12. Urva, S.R., Shin, B.S., Yang, V.C. and Balthasar, J.P.; Sensitive high performance liquid chromatographic assay for assessment of doxorubicin pharmacokinetics in mouse plasma and tissues; *Journal of Chromatography B*, (2009); 887: 837-841.
13. Hu, T., Leb, Q., Wu, Z. and Wu, W.; Determination of doxorubicin in rabbit ocular tissues and pharmacokinetics after intravitreal injection of a single dose of doxorubicin-loaded poly-

β -hydroxybutyrate microspheres; *Journal of Pharmaceutical and Biomedical Analysis*, (2007); 43: 263-269.

14. Ahmad, M., Usman, M., Madni, A., Zubair, M., Qamar-uz-Zaman, Qureshi, M.S., Munir, A., Ahmad, M. and Mahmood, A.; A fast and simple HPLC-UV method for simultaneous determination of three anti-cancer agents in plasma of breast cancer patients and its application to clinical pharmacokinetics; *African Journal of Pharmacy and Pharmacology*, (2011); 5: 915-922.
15. Zhou, Q. and Chowbay, B.; Determination of doxorubicin and its metabolites in rat serum and bile by LC: application to preclinical pharmacokinetic studies; *Journal of Pharmaceutical and Biomedical Analysis*, (2002); 30: 1063-1074.
16. Gilbert, C.M., McGearya, R.P., Filippich, L.J., Norris, R.L.G. and Charles, B.G.; Simultaneous liquid chromatographic determination of doxorubicin and its major metabolite doxorubicinol in parrot plasma; *Journal of Chromatography B*, (2005); 826: 273-276.
17. Rodrigues, A.S., Lopes, A.R., Leão, A., Couceiro, A., Ribeiro, A.B.S., Ramos, F., Silveira, M.I.N. and Oliveira, C.R.; Development of an analytical methodology for simultaneous determination of vincristine and doxorubicin in pharmaceutical preparations for oncology by HPLC-UV; *Journal of Chromatographic Science*, (2009); 47: 387-391.
18. Sastry, C.S. and Rao, J.S.L.; Determination of doxorubicin hydrochloride by visible spectrophotometry; *Talanta*, (1996); 43: 1827-1835.
19. Chin, D.L., Lum, B.L. and Sikic, B.I.; Rapid determination of PEGylated liposomal doxorubicin and its major metabolite in human plasma by ultraviolet-visible high-performance liquid chromatography; *Journal of Chromatography B*, (2002); 779: 259-269.
20. Liu, Y., Yang, Y., Liu, X. and Jiang, T.; Quantification of pegylated liposomal doxorubicin and doxorubicinol in rat plasma by liquid chromatography/electrospray tandem mass spectroscopy: Application to preclinical pharmacokinetic studies; *Talanta*, (2008); 74: 887-895.
21. Alhareth, K., Vauthier, C., Gueutin, C., Ponchel, G. and Moussac, F.; HPLC quantification of doxorubicin in plasma and tissues of rats treated with doxorubicin loaded poly(alkylcyanoacrylate) nanoparticles; *Journal of Chromatography B*, (2012); 887-888 128-132.
22. Mussi, S.V., Silva, R.C., Oliveira, M.C., Lucci, C.M., Azevedo, R.B. and Ferreira, L.A.M.; New approach to improve encapsulation and antitumor activity of doxorubicin loaded in solid lipid nanoparticles; *European Journal of Pharmaceutical Sciences*, (2013); 48: 282-290.

23. Lv, S., Tang, Z., Li, M., Lin, J., Song, W., Liu, H., Huang, Y., Zhang, Y. and Chen, X.; Co-delivery of doxorubicin and paclitaxel by PEG-polypeptide nanovehicle for the treatment of non-small cell lung cancer; *Biomaterials*, (2014); 35: 6118-6129.
24. Vives, M.A., Infante, M.R., Gracia, E., Selve, C., Maugras, M. and Vinardell, M.P.; Erythrocyte hemolysis and shape changes induced by new lysine-derivate surfactants; *Chemico-Biological Interactions*, (1999); 118: 1-18.
25. Sánchez, L., Mitjans, M., Infante, M.R., Garcia, M.T., Manresa, M.A. and Vinardell, M.P.; The biological properties of lysine-derived surfactants; *Amino Acids*, (2007); 32: 133-136.
26. Nogueira, D.R., Mitjans, M., Infante, M.R. and Vinardell, M.P.; The role of counterions in the membrane-disruptive properties of pH-sensitive lysine-based surfactants; *Acta Biomaterialia*, (2011); 7: 2846-2856.
27. Gan, Q., Wang, T., Cochrane, C. and McCarron, P.; Modulation of surface charge, particle size and morphological properties of chitosan-TPP nanoparticles intended for gene delivery; *Colloids and Surfaces B Biointerfaces*, (2005); 44: 65-73.
28. ICH Q2(R1). Validation of Analytical Procedures: text and methodology. International conference on harmonization of technical requirements for the registration of pharmaceutical for human use; 2005.
29. Heyden, Y.V., Nijhuis, A., Smeyers-Verbeke, J., Vandeginste, B.G.M. and Massart, D.L.; Guidance for robustness: ruggedness tests in method validation; *Journal of Pharmaceutical and Biomedical Analysis*, (2001); 24: 723-753.
30. Teófilo, R.F. and Ferreira, M.M.C.; Quimiometria II: planilhas eletrônicas para cálculos de planejamentos experimentais, um tutorial; *Química Nova*, (2006); 29: 338-350.
31. Kahsay, G., Song, H., Eerdekkens, F., Tiea, Y., Hendriks, D., Van Schepdael, A., Cabooter, D. and Adams, E.; Development and validation of LC methods for the separation of misoprostol related substances and diastereoisomers; *Journal of Pharmaceutical and Biomedical Analysis*, (2015); 111: 91-99.
32. Ourique, A.F., Pohlmann, A.R., Guterres, S.S. and Beck, R.C.R.; Tretinoin-loaded nanocapsules: Preparation, physicochemical characterization, and photostability study; *International Journal of Pharmaceutics*, (2008); 352: 1-4.
33. Almeida, J.S., Lima, F., Da Ros, S., Bulhões, L.O.S., Carvalho, L.M. and Beck, R.C.R.; Nanostructured systems containing rutin: In vitro antioxidant activity and photostability studies; *Nanoscale Research Letters*, (2010); 5: 1603-1610.
34. Silva-Buzanello, R.A., Ferro, A.C., Bona, E., Cardozo-Filho, L., Araújo, P.H.H., Leimann, F.V. and Gonçalves, O.H.; Validation of an Ultraviolet-visible (UV-Vis) technique

for the quantitative determination of curcumin in poly(L-lactic acid) nanoparticles; *Food Chemistry*, (2015); 172: 99-104.

35. Zhao, P. and Dash, A.K.; A simple HPLC method using a microbore column for the analysis of doxorubicin; *Journal of Pharmaceutical and Biomedical Analysis*, (1999); 20: 543-548.
36. Weich, A., Oliveira, D.C., Melo, J., Goebel, K. and Rolim, C.M.B.; Validation of UV spectrophotometric and HPLC methods for quantitative determination of atenolol in pharmaceutical preparations; *Latin American Journal of Pharmacy*, (2007); 26: 765-770.
37. Kang, S.I., Na, K. and Bae, Y.H.; Physicochemical characteristics and doxorubicin-release behaviors of pH/temperature-sensitive polymeric nanoparticles; *Colloids and Surfaces A Physicochemical and Engineering Aspects*, (2003); 231: 103-112.
38. Zhao, Y., Sun, C., Lu, C., Dai, D., Lv, H., Wub, Y., Wan, C., Chen, L., Lin, M. and Li, X.; Characterization and anti-tumor activity of chemical conjugation of doxorubicin in polymeric micelles (DOX-P) in vitro; *Cancer Letters*, (2011); 311: 187-194.
39. British Pharmacopoeia 2014; The Stationery Office: London, 2014.
40. Ganorkar, S.B., Dhumal, D.M. and Shirkhedkar, A.A.; Development and validation of simple RP-HPLC-PDA analytical protocol for zileuton assisted with design of experiments for robustness determination; *Arabian Journal of Chemistry*, In press.
41. Branquinho, R.T., Mosqueira, V.C.F., Kano, E.K., Souza, J., Dorim, D.D.R., Saúde-Guimarães, D.A. and Lana, M.; HPLC-DAD and UV-Spectrophotometry for the determination of lycnopholide in nanocapsule dosage form: validation and application to release kinetic study; *Journal of Chromatographic Science*, (2014); 52: 19-26.
42. Oliveira, A.R., Caland, L.B., Oliveira, E.G., Egito, E.S.T., Pedrosa, M.F.F. and Júnior, A.A.S.; HPLC-DAD and UV-Vis spectrophotometric methods for methotrexate assay in different biodegradable microparticles; *Journal of the Brazilian Chemical Society*, (2015); 26: 649-659.

Table I. Repeatability[†], intermediate precision[§] and accuracy data of UV-Vis spectrophotometric and RP-LC methods for DOX in samples of chitosan-based NPs

UV-Vis spectrophotometry		RP-LC		
	Recovery ± SD (%)	RSD [*] (%)	Recovery ± SD (%)	RSD [*] (%)
Precision				
Intra-day (n = 6)	103.59 ± 1.000	0.97	103.31 ± 1.144	1.10
Inter-day				
Day 1 (n = 3)	102.74 ± 0.003	0.27	102.53 ± 0.010	0.96
Day 2 (n = 3)	101.62 ± 0.009	0.84	100.11 ± 0.016	1.64
Day 3 (n = 3)	104.21 ± 0.009	0.82	102.63 ± 0.004	0.43
Mean (n = 9)	102.85 ± 0.013	1.26	101.76 ± 0.014	1.40
Between-analysts				
Analyst 1 (n = 3)	102.24 ± 0.003	0.27	100.11 ± 0.016	1.64
Analyst 2 (n = 3)	100.86 ± 0.004	0.37	100.66 ± 0.012	1.16
Analyst 3 (n = 3)	101.59 ± 0.003	0.31	101.35 ± 0.009	0.86
Mean (n = 9)	101.56 ± 0.007	0.68	100.71 ± 0.006	0.62
Accuracy				
12 µg/mL	98.17 ± 0,162	0.27	100.89 ± 0,136	0.05
15 µg/mL	99.83 ± 0,087	1.19	98.11 ± 0,092	0.02
18 µg/mL	98.82 ± 0,029	0.15	98.25 ± 0,075	0.14

[†] intra-day[§] inter-day and between-analysts

*RSD = relative standard deviation

Table II. Robustness assessment by full factorial design for UV-Vis spectrophotometric and RP-LC methods, with simultaneous variations of the factors

Experiments	UV-Vis spectrophotometry			Assay (%)
	Wavelength (nm)	pH aqueous phase	Extraction time (min)	
1	475	2.7	18	104.01
2	475	3.3	12	104.99
3	485	2.7	12	104.78
4	485	2.7	18	103.05
5*	480	3.0	15	102.65
6	475	3.3	18	102.57
7	475	2.7	12	101.28
8	485	3.3	18	103.56
9*	480	3.0	15	100.97
10*	480	3.0	15	103.90
11	485	3.3	12	102.85
Mean				103.14
RSD (%)				1.28
RP-LC				
	Injection volume (μL)	% ACN 90%	Flow rate (mL/min)	pH aqueous phase
1	30	36	1.1	2.7
2	30	36	0.9	2.7
3	10	36	0.9	2.7
4	10	36	1.1	3.3
5	30	30	1.1	2.7
6*	20	33	1.0	3.0
7	10	30	0.9	2.7
8	30	36	1.1	3.3
9	30	30	0.9	3.3
10	30	30	0.9	2.7
11	10	36	0.9	3.3
12	10	30	0.9	3.3
13	30	36	0.9	3.3
14*	20	33	1.0	3.0
15	10	30	1.1	3.3
16	10	30	1.1	2.7
17	10	36	1.1	2.7
18*	20	33	1.0	3.0
19	30	30	1.1	3.3
20*	20	33	1.0	3.0
Mean				101.90
RSD (%)				1.24

*optimized conditions points

Table III. Comparison between the UV-Vis spectrophotometric and RP-LC methods applied for the analysis of DOX in samples of chitosan-based NPs

UV-Vis spectrophotometry			RP-LC	
Sample	Recovery (%)	RSD* (%)	Recovery (%)	RSD* (%)
1	105.98	0.69	104.64	0.04
2	103.72	0.23	105.15	0.10
3	108.75	0.67	106.00	0.34
4	108.93	0.02	103.82	0.02
5	106.67	1.38	106.03	0.15
6	104.94	0.23	104.82	0.03
Mean	106.50	1.10	105.08	1.09
<i>Statistical analysis</i>		Critical value [§]	Calculated value	
Student's <i>t</i> -test		2.36	0.16	
ANOVA		4.96	2.43	

* RSD = relative standard deviation ($n = 3$)

[§] significance level $p = 0.05$

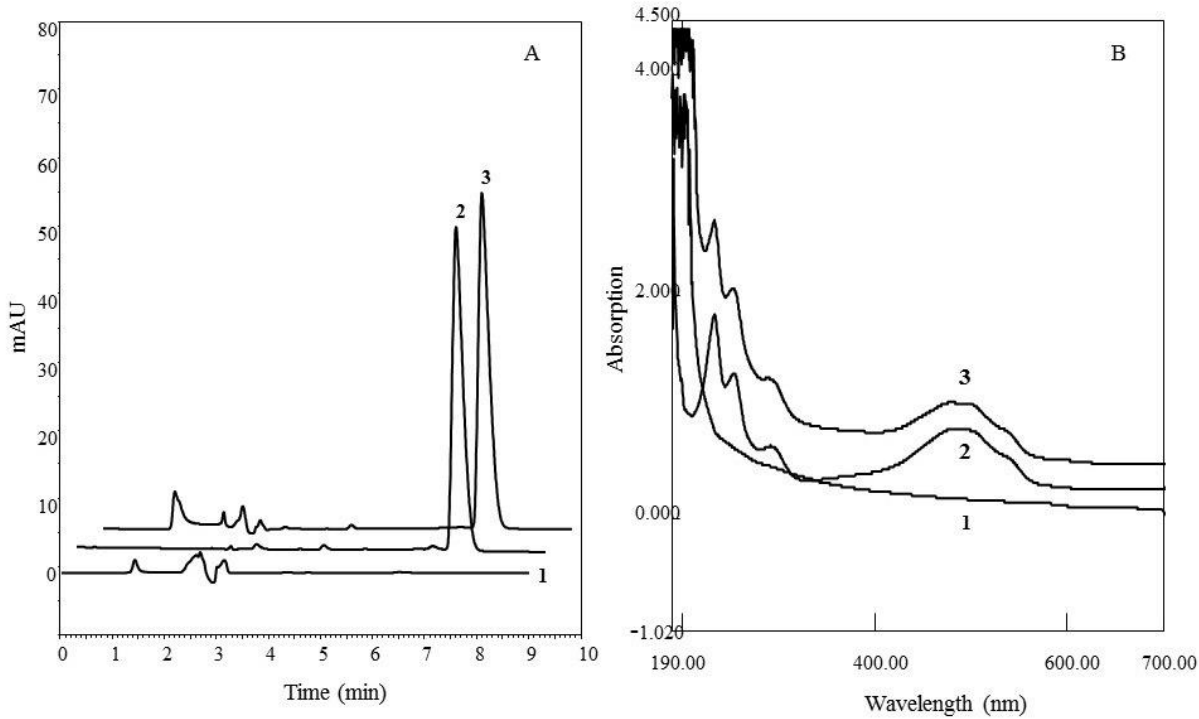


Figure 1. Results of the specificity tests: (A) Representative RP-LC chromatograms and (B) Absorption spectra obtained by UV-Vis spectrophotometric method. Trace (1) represents unloaded-NPs, (2) DOX reference solution (15 $\mu\text{g}/\text{mL}$) and (3) DOX-loaded CS-NPs (15 $\mu\text{g}/\text{mL}$).

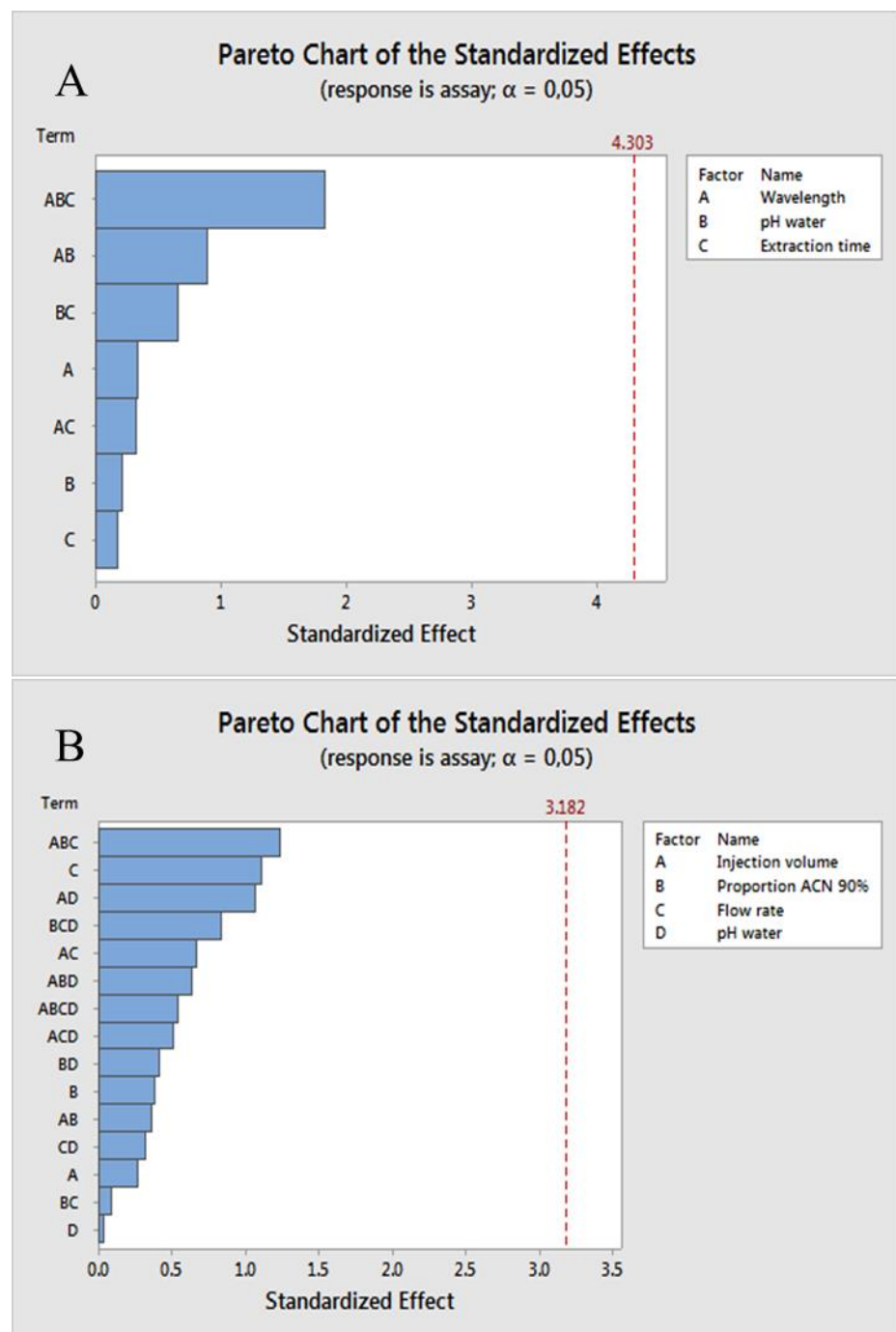


Figure 2. Pareto chart of standardized effects. Chart (A) corresponds to the main factors and their combinations for UV-Vis spectrophotometric method, and chart (B) for RP-LC method. The vertical line indicates the critical t -value for $\alpha = 0.05$.

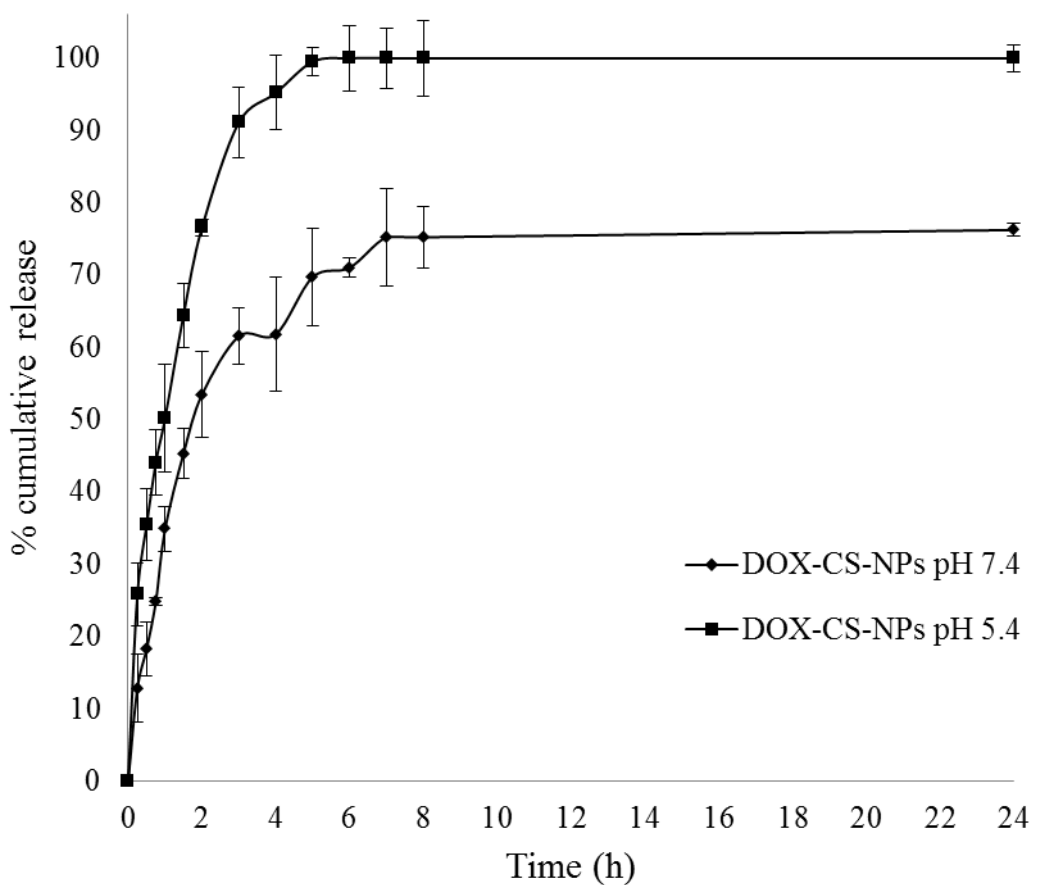


Figure 3. *In vitro* cumulative release of DOX from CS-NPs in PBS pH 7.4 and 5.4. Results are expressed as the mean \pm standard error of three independent experiments. Statistical analyses were performed by ANOVA followed by Tukey's multiple comparison test. *significant difference from PBS pH 7.4 ($p < 0.05$) and **high significant difference from PBS pH 7.4 ($p < 0.01$).

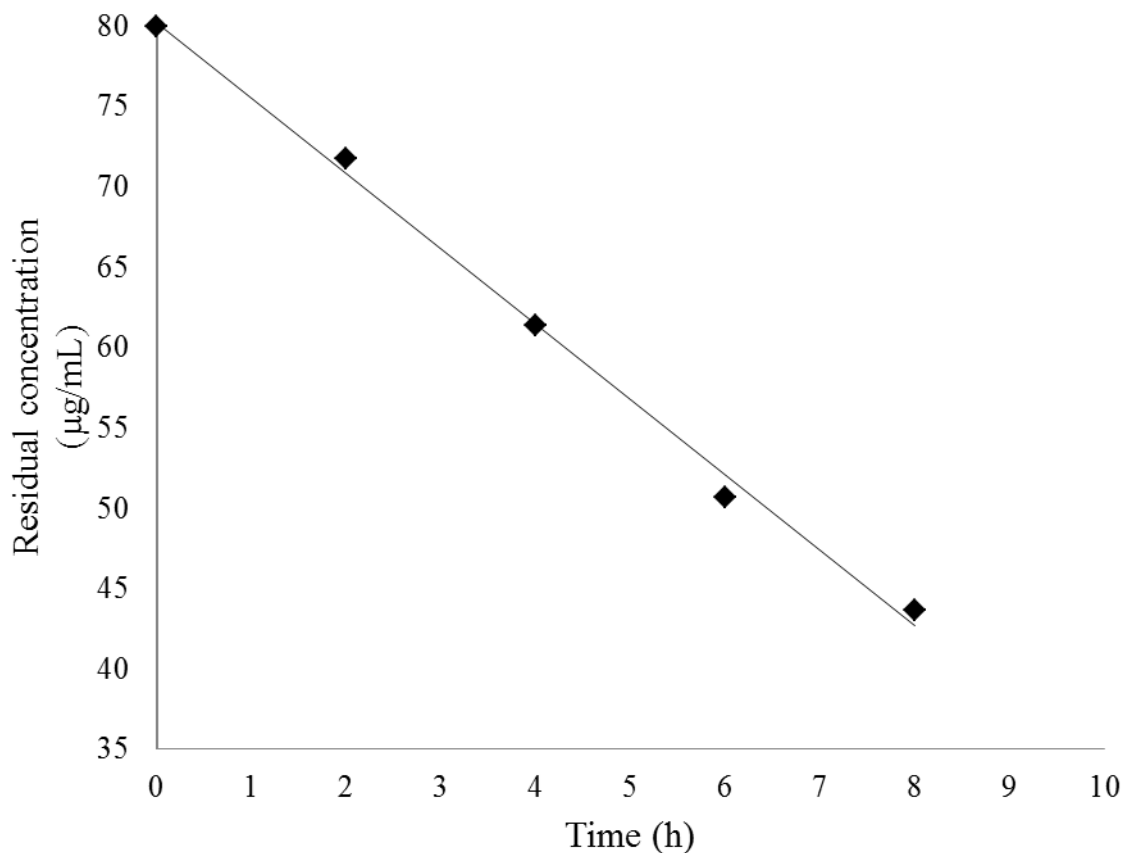


Figure 4. Zero-order plot represents the degradation kinetics of DOX-loaded CS-NPs under photolytic conditions (UVC light) during the total exposure time.

5. ARTIGO CIENTÍFICO II:

“PEGylated and poloxamer-modified chitosan nanoparticles incorporating a lysine-based surfactant for pH triggered doxorubicin release”

O presente manuscrito está disposto no formato de submissão ao periódico *Colloids and Surfaces B: Biointerfaces* (Fator de impacto 4,152. WebQualis A2).

APRESENTAÇÃO EM PORTUGUÊS

Nanopartículas de quitosana modificadas com PEG ou poloxamer e contendo um tensoativo derivado de lisina para desencadear a liberação pH-dependente de doxorrubicina

A doxorrubicina é um antibiótico antraciclínico com ampla utilização na terapia antitumoral. No entanto, seu uso pode promover a ocorrência de efeitos adversos graves como a cardiototoxicidade e desenvolvimento de resistência pelas células tumorais. Esses quadros devem-se à baixa capacidade do fármaco em atuar especificamente na célula cancerosa, atingindo, assim, tecidos normais, e devido à superexpressão de bombas de efluxo pelas células do tecido tumoral. Dessa forma, foram desenvolvidas nanopartículas de quitosana (CS-NPs) incorporando o tensoativo pH-sensível 77KS ($\text{N}^{\alpha},\text{N}^{\epsilon}$ - dioctanoil lisina com contrião sódio), pelo método de gelificação iônica, visando ao direcionamento das NPs à região ácida do tumor. O 77KS foi sintetizado e doado a nosso grupo de pesquisa pelo CSIC (*Consejo Superior de Investigaciones Científicas, Barcelona, Espanha*) e sua incorporação às NPs foi baseada em estudos prévios, que demonstraram a capacidade do 77KS em romper membranas celulares de forma pH-dependente, podendo ser capaz, portanto, de promover a liberação do fármaco encapsulado no interior da célula tumoral. A liberação seria desencadeada de acordo com o pH da região onde se encontram as NPs, ocorrendo de forma acelerada em pHs acidificados que simulam o microambiente tumoral ($\text{pH}_e \sim 6,6$) e os compartimentos intracelulares ($\text{pH } 6,5 - 5,5$), devido à mudança nas cargas dos componentes da matriz, com consequente desestabilização da estrutura das NPs e liberação da DOX. Além disso, foram realizadas modificações nas NPs como a inclusão de PEG ou poloxamer. O PEG apresenta a característica de aumentar o tempo de permanência das NPs na corrente sanguínea, que, dessa forma, poderiam alcançar o sítio de ação específico. O poloxamer é um tensoativo com propriedade de sensibilizar células resistentes, principalmente pela inibição da bomba de efluxo glicoproteína-P. As NPs apresentaram características físico-químicas adequadas, com tamanhos médios dentro da faixa nanométrica, índice de polidispersão menor que 0,24 e eficiência de encapsulação satisfatória. Os resultados encontrados nos estudos de liberação demonstraram a acelerada liberação da DOX encapsulada em meios acidificados (6,6 e 5,4) em comparação ao pH dos tecidos normais, sugerindo, portanto, que as NPs incorporando o tensoativo 77KS são potenciais carreadores para alcançar a região tumoral e desencadear a liberação da DOX nos pHs do microambiente do tumor e compartimentos intracelulares.

PEGylated and poloxamer-modified chitosan nanoparticles incorporating a lysine-based surfactant for pH triggered doxorubicin release

ABSTRACT

The growing demand for efficient chemotherapy in many cancers requires novel approaches in target-delivery technologies. Nanomaterials with pH-responsive behavior appear to have potential ability to selectively release the encapsulated molecules by sensing the acidic tumor microenvironment or the low pH found in endosomes. Likewise, polyethylene glycol (PEG)- and poloxamer-modified nanocarriers have been gaining attention regarding their potential to improve the effectiveness of cancer therapy. In this context, DOX-loaded pH-responsive nanoparticles (NPs) modified with PEG or poloxamer were prepared and the effects of these modifiers were evaluated on the overall characteristics of these nanostructures. Chitosan and tripolyphosphate were selected to form NPs by the interaction of oppositely charged compounds. A pH-sensitive lysine-based amphiphile (77KS) was used as a bioactive adjuvant. The strong dependence of 77KS ionization with pH makes this compound an interesting candidate to be used for the design of pH-sensitive devices. The physicochemical characterization of all NPs has been performed, and it was shown that the presence of 77KS clearly promotes a pH-triggered DOX release. Accelerated and continuous release patterns of DOX from CS-NPs under acidic conditions were observed regardless of the presence of PEG or poloxamer. Moreover, photodegradation studies have indicated that the lyophilization of NPs improved DOX stability under UVA radiation. Finally, cytotoxicity experiments have shown the ability of DOX-loaded CS-NPs to kill HeLa tumor cells. Hence, the overall results suggest that these pH-responsive CS-NPs are highly potent delivery systems to target tumor and intracellular environments, rendering them promising DOX carrier systems for cancer therapy.

Keywords: chitosan nanoparticles; doxorubicin; *in vitro* release; *in vitro* cytotoxicity; lysine-based surfactant; pH-sensitivity

1. Introduction

Doxorubicin (DOX) is an anthracycline antibiotic commonly used as a chemotherapeutic agent [1]. Due to its broad-spectrum of antitumor activity, it has been incorporated into several nano-sized materials, including pH-responsive microgels [2], temperature-responsive micelles [3], liposomes [4] and polymeric nanoparticles (NPs) [5,6]. DOX antineoplastic effects can occur by different mechanisms, such as free radical generation, which is well associated with the cardiotoxicity of anthracyclines [7]. Drug delivery systems have been gaining attention in recent years as a promising approach to improve cancer treatment and prevent toxicity in healthy tissues. It is noteworthy that by adding different modifiers, these systems can be designed for cancer cell-specific targeting as well as for biological, chemical, or physical stimulus response [8,9].

Considering that endosomal pH (\sim 6.5 to 5.5) [10] and the tumor extracellular pH ($pH_e \sim$ 6.6) are notably lower than those of normal tissue ($pH \sim$ 7.4) [11], pH-sensitive devices have been widely researched as drug delivery strategies for cancerous diseases [9]. In this context, our group has paid special attention to a bioactive amino acid-based surfactant derived from N^{α},N^{ϵ} -dioctanoyl lysine with an inorganic sodium counterion (77KS), which in previous studies shown pH-responsive properties and low cytotoxicity [12-14]. Therefore, here we selected 77KS as an adjuvant with potential ability to promote the pH-triggered DOX release in the tumor microenvironment and endosomal compartments (Fig. 1).

Chitosan (CS) is a nontoxic, biocompatible and biodegradable polymer that has been emerging as one of the most promising delivery vehicles for cancer chemotherapy [15]. Chitosan has been widely used for the development of DOX-loaded NPs by simple and mild preparation techniques [5,16-18]. CS-NPs modified by polyethylene glycol (PEG) are explored due to the ability of this hydrophilic polymer to prolong the circulation time of nanocarriers in the blood stream. This mechanism allows NP accumulation in the tumor region via enhanced permeability and retention (EPR) effect, which, in turn, increases tumor exposure to the encapsulated drug [19-22]. Likewise, Pluronic block copolymers (or non-proprietary name “poloxamer”) have been studied as biological response modifiers. They are amphiphilic synthetic polymers with tumor-sensitizing activity in multidrug resistant (MDR) cells, which is especially attributed to the inhibition of P-glycoprotein [23]. For this reason, it has been reported that the association of DOX to poloxamer-based formulations potentiates the drug activity against non-MDR and, especially, MDR tumor cells [24-26].

Therefore, the aim of the present study was to prepare PEGylated and poloxamer-modified CS-NPs incorporating a lysine-based surfactant as a pH-responsive bioactive

adjuvant. The NPs were well characterized and the mathematical modeling of pH-triggered DOX release profiles was discussed. NP suspensions and lyophilized samples were analyzed regarding their stability at low temperature and under UVA radiation. Finally, in order to gain preliminary insights into the role of the modifiers on the antitumor activity of NPs, the cytotoxicity of free and entrapped drug was assessed by an *in vitro* cell-based assay.

2. Materials and methods

2.1. Materials

Chitosan (CS) of low molecular weight (deacetylation degree, 75-85%; viscosity, 20-300 cP according to the data sheet of the manufacturer), pentasodium tripolyphosphate (TPP), polyethylene glycol methyl ether (mPEG, $M_n = 5,000$), poloxamer 188 solution (10%, w/v) and 2,5-diphenyl-3,-(4,5-dimethyl-2-thiazolyl) and tetrazolium bromide (MTT) were purchased from Sigma-Aldrich (St. Louis, MO, USA). Reagents for cell culture were from Vitrocell (Campinas, SP, Brazil). Doxorubicin (DOX, state purity 98.32%) was obtained from Zibo Ocean International Trade (Zibo, Shangdong, P.R., China). Acetonitrile and glacial acetic acid were purchased from Tedia (Fairfield, USA). All other solvents and reagents were of analytical grade.

2.2. Surfactant included in the nanoparticles

An anionic amino acid-based surfactant derived from $N^{\alpha},N^{\varepsilon}$ -dioctanoyl lysine and with an inorganic sodium counterion (77KS) was included in the NP formulation. The surfactant chemical structure is formed by two alkyl chains (each with eight carbon atoms) bound to the amino acid lysine. It has a molecular weight of 421.5 g/mol and a critical micellar concentration (CMC) of $3 \times 10^3 \mu\text{g/ml}$ [27,28]. This surfactant was synthesized as described elsewhere [29].

2.3. Preparation of nanoparticles

CS-NPs were spontaneously formed by ionotropic gelation process, according to the methodology first described by Calvo et al. [30]. DOX stock solution was prepared in ultrapure water in order to give a final concentration of 2.0 mg/ml. Chitosan at 1.0 mg/ml was dissolved in a 1.0% (v/v) acetic acid aqueous solution under magnetic stirring for 2 h, and pH was adjusted to 5.5 with 1 M NaOH [31]. A mixed solution of the cross-linker TPP and the surfactant 77KS was prepared in ultra-pure water at 2.0 mg/ml and 0.5 mg/ml, respectively.

Initially, DOX stock solution was added to 5 ml of CS solution (CS:DOX ratio 5:0.5, w/w) and maintained under magnetic stirring (1000 rpm) for 10 min. Then, 1 ml of a premixed TPP:77KS solution (ratio equal 2:0.5, w/w) was added drop-wise into the CS:DOX solution. NPs (DOX-CS-NPs) were formed spontaneously and the gelation process was carried out under constant magnetic stirring for 20 min at room temperature.

In order to obtain PEGylated DOX-CS-NPs (PEG-DOX-CS-NPs), a mixed solution of CS and PEG (at 1 mg/ml and 10 mg/ml, respectively) was prepared in 1.0% (v/v) acetic acid. To 5 ml of this solution, DOX stock solution was added and stirred for 10 min (CS:PEG:DOX ratio 5:50:0.5, w/w/w). Afterwards, 1 ml of TPP:77KS (2:0.5, w/w) was added drop-wise and stirred for 20 min.

Poloxamer-modified DOX-CS-NPs (Polox-DOX-CS-NPs) were obtained by adding 0.5% (w/v) of poloxamer to 5 ml of a 1 mg/ml CS solution. Next, DOX stock solution was added to give a final ratio of CS:Poloxamer:DOX 5:25:0.5 (w/w/w). Finally, 1 ml of TPP:77KS (2:0.5, w/w) was added drop-wise under vigorous magnetic stirring for 20 min.

Unloaded NPs were prepared similarly for each formulation, thus omitting the drug. All procedures involving DOX were conducted in a low incidence of light. The resulting DOX-loaded NPs were purified by dialysis for 1 h in distilled water (dialysis bag - Sigma-Aldrich, 14,000 MWCO), in order to remove the non-encapsulated drug and non-incorporated constituents.

2.4. Characterization of nanoparticles

The mean hydrodynamic diameter and the polydispersity index (PDI) of the NPs were determined by dynamic light scattering (DLS) using a Malvern Zetasizer ZS (Malvern Instruments, Malvern, UK), without any dilution of the samples. The zeta potential (ZP) values of the NPs were assessed by determining electrophoretic mobility using the same equipment after dilution of the formulations in 10 mM NaCl aqueous solution (1:10 volume per volume). Each measurement was performed using at least three sets of ten runs at 25°C. The pH measurements were verified directly in the NP suspensions, using a calibrated potentiometer (UB-10; Denver Instrument, Bohemia, NY, USA), at room temperature. Finally, the spectral properties of the drug were assessed before its encapsulation and also after extraction from the NP structure. This assay was performed in order to verify the stability of DOX after entrapment into the NP matrix. Experiments were performed on a double-beam UV-Vis spectrophotometer (Shimadzu, Japan) model UV-1800, with a fixed slit

width (2 nm) and a 10 mm quartz cell was used to obtain spectrum and absorbance measurements. The diluent optimized was water pH 3.0, acidified with glacial acetic acid.

2.5. Drug encapsulation efficiency

The quantitative analyses were performed by a reversed-phase liquid chromatography (RP-LC) method that was previously validated according to international guidelines and proved to be specific, linear, precise, accurate and robust (unpublished data). Chromatographic analyses were carried out on a LC 1260 Agilent Technologies system (Agilent Technologies, Santa Clara, CA, USA), using a Waters XBridgeTM C₁₈ column (250 mm x 4.6 mm I.D., 5µm), with a mobile phase consisting of 90% (v/v) acetonitrile in water and water pH 3.0, acidified with glacial acetic acid (33:67, v/v) and UV detection set at 254 nm. Data analysis was performed with EZChrom software program (version A.01.05). Total drug content was achieved by dilution of the NP suspensions in methanol (1:1, v/v) followed by sonication for 15 min, which allowed total drug extraction from the NP matrix. The resulting solution was diluted to the suitable concentration and analyzed by RP-LC. The drug association efficiency was determined by ultrafiltration/centrifugation technique using Amicon Ultra-0.5 Centrifugal Filters (10,000 Da MWCO, Millipore). An amount of the non-purified NP suspension was placed into this device and submitted to 10,000 rpm for 20 min in a Sigma 2-16P Centrifuge (Sigma, Germany). The encapsulation efficiency (EE%) was calculated as the difference between total and free DOX concentrations determined in the NP suspension (total drug content) and in the ultrafiltrate, respectively, using the mentioned analytical method.

*2.6. pH-dependent *in vitro* DOX release*

In vitro release assessments of DOX from the different CS-NPs were performed using the dialysis method. An aliquot of the NPs (1 ml) was placed into a dialysis bag (Sigma-Aldrich, 14,000 MWCO), which was immersed in 50 ml of phosphate buffered saline (PBS) at 37°C and kept under gentle magnetic stirring (100 rpm) for 24 h. This process was carried out, separately, in PBS at pH 7.4, 6.6 and 5.4. At specific time intervals, an aliquot of 2 ml of the external medium was withdrawn and filtered through a 0.45-µm membrane. Thereafter, equal volume of fresh buffer was added to maintain the sink conditions and constant volume. The release of the free drug was also investigated in the same way. The released amount of DOX in each scheduled time was estimated by the RP-LC method described in the previous section (*section 2.5*), using analytical curves obtained with the release medium (PBS at pH 7.4, 6.6 or

5.4) as diluents. The cumulative release percentage (CR%) of DOX was determined from the following equation (Eq. (1)):

$$CR\% = (M_t/M_i) 100 \quad (1)$$

where M_t and M_i are the amount of drug released at the time t and the initial amount of drug encapsulated in the NPs, respectively. The *in vitro* release studies were carried out in triplicate.

For understanding the pH-sensitivity behavior of NPs, swelling studies were performed by soaking lyophilized NPs into PBS pH 7.4, 6.6 and 5.4 at room temperature and under gentle shake. Hydrodynamic diameter was measured after 3 h incubation.

2.7. Mathematical modeling of drug release profiles

Monoexponential (Eq. (2)) and biexponential (Eq. (3)) mathematical models as well as the Korsmeyer-Peppas model (Eq. (4)) were used to analyze DOX *in vitro* release profile (MicroMath® Scientist version 2.01, USA). The model that best fit the drug release profile was selected according to the model selection criteria (MSC), correlation coefficient (r), and graphical adjustment. The release kinetic rate constants are k (for monoexponential), k_1 and k_2 (for biexponential). C_0 , a and b are the initial concentration for mono- and biexponential models, respectively [32,33]. Finally, the DOX release mechanism was investigated by fitting 60% of the initial amount of drug released from CS-NPs to the Korsmeyer-Peppas model. In its corresponding equation, n is the exponent that characterizes the release mechanism and a is a constant comprising the structural and geometric characteristics of the carrier [34-36].

$$C = C_0 e^{-kt} \quad (2)$$

$$C = a e^{-k_1 t} + b e^{-k_2 t} \quad (3)$$

$$f t = a t^n \quad (4)$$

2.8. Lyophilization of nanoparticles

NP suspensions DOX-CS-NPs, PEG-DOX-CS-NPs and Polox-DOX-CS-NPs were subjected to the lyophilization process to obtain dried formulations (L-DOX-CS-NPs, L-PEG-DOX-CS-NPs and L-Polox-DOX-CS-NPs, respectively). To avoid possible particle aggregation,

glycerol (10%, w/v), mannitol (1%, w/v) and lactose (1, 5 and 10%, w/v) were tested for their cryoprotectant efficiency. Cryoprotectants were dissolved in the entire volume of NPs under magnetic stirring for 20 min. Then, these mixtures were frozen at -20°C for 48 h. The water was removed from frozen NPs by sublimation under vacuum for 48 h using a bench top lyophilizer (Liotorp L101, Liobras, São Carlos, Brazil). As required, lyophilized products were redispersed with ultra-pure water by magnetic stirring for 10 min. The macroscopic appearance, physicochemical properties and EE% were evaluated.

2.9. Fourier Transform Infrared Spectroscopy (FT-IR) analysis

In order to investigate the interactions between the drug and NP matrix, FT-IR spectra of pure DOX, CS raw material and dried NPs were recorded using compressed KBr disk method with a FT-IR spectrophotometer (Bruker Tensor 27, Bruker Optik, Ettlingen, Germany). Spectral acquisition was carried out from 4000 to 400 cm^{-1} range.

2.10. Stability studies of nanoparticles

NP suspensions (DOX-CS-NPs, PEG-DOX-CS-NPs and Polox-DOX-CS-NPs) and the lyophilized formulations (L-DOX-CS-NPs and L-PEG-DOX-CS-NPs) were studied for their stability in low temperature (2 – 8°C). Experiments were conducted over 8 weeks. Lyophilized samples were first placed inside a desiccator containing silica and then exposed to low temperature whilst protected from light. Analyses were carried out on the first day of the study, and subsequently after 2, 4 and 8 weeks. In each time point, all samples were evaluated for particle size, PDI, ZP and drug content (total drug amount (%)) in regard to freshly prepared formulations).

Additionally, photostability studies were carried out to assess whether suspensions and/or lyophilized formulations were able to protect the drug after exposure to UVA radiation. An aliquot of DOX solution or DOX-loaded NPs was put separately into transparent capped cuvettes (Brand®, UV-Cuvettes micro) and placed into a mirrored chamber with approximately 1,350 W h/m^2 incident UVA radiation [37]. On the other hand, an amount of the lyophilized formulations were weighed and well distributed in Petri dishes. The drug concentration was measured in different schedule times (0, 2, 8, 24 and 48 h) by the validated RP-LC method. Zero, first and second order graphics were delineated and the one with the best fit was considered to establish the kinetic order.

2.11. Cytotoxicity assays

The *in vitro* antitumor activity of unloaded-CS-NPs, DOX-loaded CS-NPs and free DOX was determined against HeLa cell line (human epithelial cervical cancer), which was cultured in DMEM medium (4.5 g/l glucose) supplemented with 10% (v/v) FBS, at 37°C in a 5% CO₂ atmosphere. HeLa cells were seeded into 96-well cell culture plates at a density of 7.5 x 10⁴ cells/ml. Cells were incubated for 24 h under 5% CO₂ at 37°C and afterwards, the medium was replaced with 100 µl of fresh medium containing the treatments. Free DOX as well as DOX-loaded CS-NPs were assayed at 1 and 10 µg/ml DOX concentration, while unloaded CS-NPs were assessed at 50 and 200 µg/ml. Following 24 h incubation, the medium was removed and 100 µl of MTT in PBS (5 mg/ml) diluted 1:10 in medium without FBS was added to the cells and incubated for 3 h. Finally, the MTT containing medium was removed and 100 µl of DMSO was added to each well in order to dissolve the purple formazan product. After shaking, the absorbance of the resulting solution was measured using a SpectraMax M2 (Molecular Devices, Sunnyvale, CA, USA) microplate reader at 550 nm. Cell viability was calculated as the percentage of tetrazolium salt reduced by viable cells in each sample. The untreated cell control (cells with medium only) was taken as 100% viability.

2.12. Statistical analyses

Results are expressed as mean ± standard error (SE) or mean ± standard deviation (SD) of three independent experiments, and statistical analyses were performed using one-way analysis of variance (ANOVA) to determine the differences between the datasets, followed by Tukey's post-hoc test for multiple comparisons, using SPSS® software (SPSS Inc., Chicago, IL, USA). *p* < 0.05 and *p* < 0.01 indicated significant and highly significant differences, respectively.

3. Results and discussion

In this study, NPs encapsulating DOX were prepared by combination of the standard ionotropic gelation method [30] and the inclusion of procedures deliberated by our research group. Therefore, novel pH-responsive CS-NPs were obtained using a mild and solvent-free process for efficient drug loading [38]. CS is widely regarded as being a non-toxic and biologically compatible polymer, with great medical potential [39]. Once dissolved in acetic acid aqueous solution, the amino groups of CS are protonated (NH₃⁺) and available to interact with the negatively charged TPP (P₃O₁₀⁵⁻) to spontaneously form the NPs [40,41]. With the aim to find the suitable CS:TPP ratio (w/w), different TPP concentrations were tested since

the size and PDI of NPs depended on the amount of TPP in the formulation. The first condition tested was CS:TPP (5:1, w/w), but the ratio CS:TPP (5:2, w/w) was chosen since it presented the smallest size and PDI value. This behavior can be attributed to the greater interaction of CS positive charges with increasing amount of negative charges of the polyanion TPP [42]. These results are in agreement with the study reported by Gan et al. [43], in which a linear decrease of size with decreasing CS to TPP weight ratio was observed. Furthermore, it is worth pointing out that by increasing the amount of negative charges into the formulation matrix, the free positive charges of CS were reduced. This lower protonation diminishes the repulsion between CS and DOX (also positively charged), which, in turn, increases the drug encapsulation efficiency.

The surfactant 77KS was selected as a bioactive adjuvant in the NP formulation based on previous studies, which showed its pH-sensitive activity along with improved kinetics in the endosomal pH range and low cytotoxic potential [12,13]. Moreover, it was already demonstrated that the inclusion of another amphiphile from the same family (77KL, with lithium counterion) in the composition of polymeric NPs improved their *in vitro* antitumor activity and also gave them a pH-responsive behavior [44]. The surfactant 77KS was included into the NPs at a concentration below its CMC, indicating that it is present in the formulations in the monomer form. Different concentrations of the surfactant were tested, ranging from CS:TPP:77KS 5:2:0.1 to 5:2:1 (w/w/w), with 0.1 increase amount of 77KS each time. By having the concentration ratio of 77KS higher than 5:2:0.5, a flocculation of the NPs took place. In contrast, concentrations between 0.1 and 0.5 provided satisfactory results. Therefore, the ratio 5:2:0.5 (w/w/w) of CS:TPP:77KS was chosen and maintained for all formulations.

The process to prepare the NPs was optimized to be simple and fast. Firstly, positive charges (DOX and CS) were mixed [5,17] and, a premixed solution of the negatively charged compounds (TPP and 77KS) was added drop-wise, leading to spontaneous formation of the colloidal system. It is known that the polyanion TPP has multiple charged functional groups, which makes it able to interact with both DOX and CS, resulting in shielding and electrostatic interactions [17]. The pH of CS solution was set at 5.5, in which about 90% of the amino groups of CS ($pK_a = 6.5$) are protonated [45]. Likewise, DOX ($pK_a = 8.2$) possess an amino sugar moiety also protonated at this pH [46], which allowed competitive binding of DOX to the negatively charged cross-linking agent (TPP) while forming the NPs.

The PEGylation of nanomaterials was shown not only to diminish clearance of the loaded drug, but also to provide enhanced tumor targeting ability due to the prolongation of plasma circulation time [47]. PEGylated DOX-CS-NPs were prepared from CS and PEG joint

solubilization prior to gelation process, where a CS/PEG network is formed by cross-linking between hydroxyl groups of PEG and amino groups of CS [48]. Likewise, it is known that block copolymers, such as the poloxamers, are biological response modifiers with potential ability to modulate drug resistance in MDR cancer cells. Therefore, here poloxamer-modified DOX-CS-NPs were prepared upon the addition of TPP:77KS into CS:Poloxamer:DOX solution [49]. Different concentrations of poloxamer were tested (0.2%, 0.5% and 1%, w/v), and the intermediate one (0.5%) was chose with acceptable physicochemical characteristics. It was previously reported that micelles containing block copolymers at 0.25 and 2% (w/v), in which DOX is also non-covalently incorporated, exhibited greater efficacy than free DOX in *in vitro* and *in vivo* tumor models [50].

3.1. Characterization and EE% of nanoparticles

Following the preparation procedure, the stability of the drug after its encapsulation was assessed through the spectral analysis, as shown in Fig. 2. The UV-Vis spectrum of the drug extracted from NPs was similar to that obtained for DOX in free solution, which proved the integrity of DOX molecule after its entrapment into the NP matrix. Moreover, as summarized in Table 1, DOX-loaded and unloaded NPs were characterized for particle size, PDI, ZP and pH. The average particle size analysis is a common characterization method, which allows the understanding of their dispersion and aggregation, as well as helping to predict their possible biodistribution. The size of unloaded NPs was in the range of 170 to 211 nm. Increasing diameters were noticed when DOX was added, indicating the retention of the drug. Likewise, the mean diameter of PEGylated NPs increased with respect to unmodified NPs, which is a good indicator of PEG incorporation into the NP structure [22]. Here, it can be stated that PEG was incorporated into the colloidal gel system via hydrogen bonding between the oxygen atom of PEG and amino groups of CS. This interaction is weak, which makes the structure of the PEGylated NPs looser and, consequently, increases their mean diameter [20]. Conversely, poloxamer-modified NPs presented smaller mean diameter than those PEG-modified NPs. This is due to the stabilizer power of poloxamer, fact that leads to a rigid arrangement of particles with less water uptake [49]. Additionally, all CS-based NPs formed systems with narrow size distribution with PDI values lower than 0.24. The ZP values of the NPs in the range of 21 to 25 mV indicate a positively charged surface owing to the cationic amino groups of CS. Likewise, when DOX was present, the electric charge remained positive and no considerable changes were noted.

DOX-loaded NPs displayed high EE% and the mean values obtained for all formulations were constantly around 65%. These results are in agreement with those found elsewhere [22,51], and allow us to state that the drug was entrapped into the polymeric network regardless of modifications made in NPs. Indeed, different amounts of drug loading were tested and discussed based on EE% capacity. By increasing DOX concentration from 80 to 154 µg/ml, the DOX EE% decreased from $66.50\% \pm 2.68$ to $51.09\% \pm 2.88$. Similar results were found elsewhere [17,18,52], pointing out that a larger amount of drug does not mean any increase in encapsulation efficiency. As a limited number of functional groups is available for electrostatic interactions with the drug in the NP matrix, the increase in the amount of drug added to the formulation could have resulted in a decrease in drug entrapment efficiency. Finally, it is worthy mentioning that NPs without 77KS showed the highest mean EE% value. This behavior could be attributed to the assembling of a consistent CS/TPP network with greater amount of TPP molecules and, thus, of remaining negative charges that allow DOX association. When 77KS (with only one negatively charged group) binds to CS, no free negative charge remains available to interact with DOX, therefore leading to diminished EE%. However, it is important to highlight that when 77KS was incorporated, we achieved higher EE% values than previous studies that reported DOX EE% values in the order of 47% for PLGA NPs and 20% for CS-based NPs [5,53].

3.2. In vitro DOX release

Taking advantage of the acidic pH_e (6.5 – 7.2) found in the tumor environment compared to the normal tissues [11,54], pH-sensitive NPs have been developed to achieve accelerated drug release at the tumor site. In this context, the *in vitro* drug release profiles of DOX-CS-NPs, PEG-DOX-CS-NPs and Polox-DOX-CS-NPs were studied in PBS buffer mediums at pH 7.4, 6.6 and 5.4 at $37 \pm 2^\circ\text{C}$ (Fig. 3).

When 77KS was first studied, it demonstrated pH-dependent membrane-lytic activity on hemolysis assay, with significant increase at pH 5.4; although with no pharmaceutical applications up to this time [13]. Here, this surfactant was incorporated into DOX-loaded CS-based NPs and, as can be seen in Fig. 3A, it was clearly demonstrated the pH-dependent release pattern of these nanostructures. In acidic environment, the release rate was accelerated; with 97 and 100% of DOX released at pH 6.6 and 5.4 after 6 h, respectively, while only 71% of drug release was reached at pH 7.4. The cumulative release amount of DOX at pH 6.6 and 5.4 was in general significantly faster ($p < 0.05$) than at pH 7.4. A control

experiment using free DOX was also carried out under similar conditions and almost total drug release was reached after 6 h.

The release of PEG-DOX-CS-NPs was also studied at different pH values, wherein at acidic conditions the release was noticeably accelerated with 100% of the DOX available in both pH 6.6 and 5.4 mediums after only 4 h (Fig. 3B). These results demonstrate that PEG did not inhibit drug release at acidic conditions, which is particularly important in order to maintain the improved drug delivery in the tumor microenvironment and intracellular compartments. Unexpectedly, DOX release from PEGylated NPs was not delayed at physiological pH in comparison with those NPs without PEG (~75 and 76% DOX released at 24 h, respectively). This behavior appears to be attributed to the formation of a semi-interpenetrating network between CS and PEG [48] and not to the assembly of a PEG shell around the NPs.

Among the three formulations, Polox-DOX-CS-NPs was the one that presented faster release rate: release amount of DOX reached 100% after 3 h, 5 h and 8 h at pH 5.4, 6.6 and 7.4, respectively (Fig. 3C). This behavior may be explained by the hydrophilic pattern of poloxamer that consequently forms a porous structure in the surface of the DOX-CS-NPs [55]. Poloxamers are reported to be pore-forming agents and drug-releasing enhancers [56], which corroborated our results. At this point there is no significant difference among the release rates at each pH ($p > 0.05$), which may be justified by the faster release achieved at physiological conditions.

The release mechanisms from CS-based NPs have been reported to be desorption of the drug from the surface, diffusion of the drug through pores, and degradation of the polymeric matrix [43]. In the swelling experiments, a considerable increase of particle size was noticed with a decrease of the buffer pH from 7.4 and 6.6 to 5.4 (178.9 nm, 173.6 nm and 309.7 nm, respectively). At lower pH value, the protonation of the amino groups of CS is promoted, leading to an increase of electric density and repulsion force between cross-linked CS chains [57]. This mechanism allows the medium to penetrate into the nanoparticulate system, consequently increasing the mean hydrodynamic size [58]. This pH-sensitive swelling behavior, in turn, could be one of the mechanisms underlying the faster diffusion of DOX from NPs, especially in acidic environments with pH as low as 5.4. On the other hand, the lack of swelling at pH 6.6 is probably attributed to the diminishing CS protonation in this condition, suggesting that the repulsion forces are not enough to induce NP swelling and, thus, other mechanisms are involved in the accelerated drug release.

It is worth mentioning that besides the swelling mechanism of CS, DOX may have an improved solubility and, TPP, a reduced ionization in acidic environments [17,57]. This later condition may result in NP network destabilization and thus faster drug delivery, which could be the basis for the pH-responsive drug release observed for the NPs without 77KS (Fig. 3D). However, noteworthy is that even when CS-based NPs showed pH-sensitivity, this behavior was not as significant as it was when CS-NPs incorporated 77KS. Therefore, 77KS acts synergistically with CS to give to the NPs the pH-responsive behavior. The ionization of 77KS is expected to be reduced in an acidic environment [13], which in turn would also contribute for the destabilization of the NP structure due to the reduced amount of available anionic charges that interact electrostatically with CS. This process would facilitate the drug release as the pH decreases to 6.6 and 5.4. Moreover, the incorporation of 77KS, with different hydrophobicity from CS, appears to contribute to perturb covalent crosslink between CS chains and, thus, to facilitate drug release [59].

The increased release at pH 6.6 and 5.4 shows that drug delivery appears to be triggered at tumor extracellular pH_e, as well as at the acidic environment of endosomes. Moreover, the low DOX release at normal physiological conditions may reduce the side effects that can occur during cancer treatment. Altogether, these results support the idea that these nanocarriers are a potential design to be used as a pH-sensitive system to improve the drug availability on tumor microenvironment and intracellular compartments.

3.3. Mathematical modeling

The data obtained from *in vitro* release studies were used to calculate values of release constants and release exponents with the aim to help understanding the mathematics of release profiles (Table 2). According to the values of the correlation coefficients (*r*) and MSC, the data for all NPs suspensions at pH 7.4 fit better to the biexponential equation (*r* > 0.99). At this condition, the DOX release showed an initial burst release (*k*₁), continued by a steady-state release (*k*₂). These two phases can be explained by the initial drug release from NP surface (drug adsorbed or entrapped in surface layer), followed by buffer penetration into NPs and drug diffusion through the swollen rubbery matrix [58]. Moreover, according to the results for *a* and *b* parameters, approximately 68% of the drug was in Polox-DOX-CS-NPs and only 31% was superficially adsorbed on this nanostructure. Conversely, PEG-DOX-CS-NPs and DOX-CS-NPs had about 25% encapsulated and 75% adsorbed on NP surface. When the mathematical modeling was performed for pH 6.6 and 5.4, a good fit was observed using

the monoexponential model, with constant rates (k) in the following ranking order: PEG-DOX-CS-NPs > Polox-DOX-CS-NPs > DOX-CS-NPs.

In the Korsmeyer-Peppas model, high correlation coefficient was obtained ($r > 0.99$ for NPs and $r > 0.98$ for free DOX). The values of release exponent (n) between 0.43 and 0.85 for DOX-CS-NPs (release medium at pH 7.4, 6.6 and 5.4, with $n = 0.6836$, 0.4608 and 0.5235, respectively) indicate a non-Fickian-type release mechanism, i.e., the phenomena responsible for the DOX release are drug diffusion process from the NPs coupled to relaxation of the polymeric chains [60]. A non-Fickian model also was found for PEG-DOX-CS-NPs at pH 7.4 ($n = 0.5010$) and Polox-DOX-CS-NPs at pH 7.4 and pH 5.4 ($n = 0.4836$ and 0.6638, respectively). The same mechanism transport was identified for the release of rivastigmine from CS-based nanoparticles for brain targeting [61]. When the release data of PEG-DOX-CS-NPs at pH 6.6 and 5.4 mediums were analyzed, $n < 0.43$ was obtained and, therefore, the release mechanism was Fickian, suggesting that the release is a consequential effect of only DOX amount diffused from the nanostructure. The same occurred for Polox-DOX-CS-NPs at pH 6.6. Fickian release mechanism was also presented to an anticancer drug loaded into CS-NPs [57]. Finally, $n = 0.2276$ was obtained for non-encapsulated DOX, indicating that its release profile is diffusion-controlled. Altogether, our results demonstrated the remarkable contribution of the relaxational process of the polymeric matrix for DOX release at pH 7.4, which may justify the slower drug release under physiological conditions.

3.4. Lyophilization of nanoparticles

Nanoparticulate systems for drug delivery have been subjected to lyophilization in order to overcome their instabilities [62]. Herein, NP suspensions were lyophilized by freeze drying with lactose, mannitol or glycerol as cryoprotectants, which are important adjuvants with the ability to protect NP suspensions from the stresses generated during the lyophilization process, i.e. freezing and desiccation [63]. When mannitol and glycerol were tested as protectants, the obtained result was not satisfactory since the redispersion procedure showed a strong tendency to form aggregates. For the sake of choosing between 1, 5 and 10% lactose, the major criteria evaluated were the yield, drug content and redispersibility index (ratio between the size after lyophilization and before lyophilization). Satisfactory values were achieved for 10% lactose (~92%, ~93% and 1.10, respectively). Moreover, only 10% lactose was able to produce a clear suspension, without any visible precipitates (Table 1). Sugars are suitable protective agents, acting by hydrogen bonding and maintaining the solute in a pseudo

hydrated state during the dehydration step, which thus protect the NP structure from damage in dehydration and rehydration process [64].

3.5. FT-IR analysis

FT-IR analyses were performed in order to support the CS:TPP cross-link as proof of NP formation, as well as to confirm the grafting of PEG on the surface of NPs (Fig. 4). Fig. 4B represents the FT-IR spectrum of CS. The characteristic absorption peak at 3384 cm^{-1} , representing the presence of OH- groups, indicates that CS is partially deacetylated. [65]. Pure DOX spectrum (Fig. 4A) shows peaks at 2933 (C-H), 1730 (C-O), 1617 and 1582 (N-H), 1413 (C-C) and 1072 cm^{-1} (C-O). In DOX-CS-NPs spectrum (Fig. 4C), these peaks are also presented as shifted to 2900 (C-H), 1642 and 1572 (N-H), 1415(C-C) and 1031 cm^{-1} (C-O). Thus, these results indicate that DOX was loaded into CS-NPs [18]. Another peak that can be observed in DOX-CS-NPs spectrum (Fig. 4C) is at 1202 cm^{-1} , corresponding to P=O stretching of the TPP [65]. Absorption peaks associated to PEG can be seen at 784 and 897 cm^{-1} , suggesting that PEG grafting was successfully achieved in PEG-DOX-CS-NPs (Fig. 4D) [21].

3.6. Stability studies of nanoparticles

NP suspensions and NPs after lyophilization were submitted to stability studies for a storage period of 8 weeks at $2 - 8^\circ\text{C}$. Particle size, PDI, ZP and drug content were evaluated in each scheduled time. After two weeks storage, all samples presented a tendency to aggregate. The parameters evaluated that prove this fact are particle size ($> 600\text{ nm}$) and PDI (> 0.3), suggesting an increase in the number of larger particles and a decrease in the narrow size distribution of the suspension. These results were not unexpected, as it was previously reported that CS microparticles showed reduced ZP and enhanced particle size after 28 days storage [66]. Factors to explain the size evolution during time storage are swelling, particle aggregation and interaction of free polymer chains with the particle network [64]. On the other hand, NP suspensions presented no considerable variations for drug content, which remained around 99% during storage time. However, the lyophilized NPs displayed a slight decrease in the drug content after 1-month storage. Altogether, the results obtained in these preliminary studies indicated that further studies must be conducted in this field in order to improve the stability of the design formulations.

With the aim to study the ability of the nanosystems to protect the encapsulated drug from photodegradation, DOX water solution, as well as DOX-CS-NPs and PEG-DOX-CS-NPs in both suspension and lyophilized states were exposed to UVA radiation. DOX water solution followed a first kinetic order ($r = 0.9857$), with half-live ($t_{1/2}$) = 9.15 h. Likewise, the degradation profiles of DOX into DOX-CS-NPs and PEG-DOX-CS-NPs were according to a first ($r = 0.9374$) and second kinetic order ($r = 0.9818$), with $t_{1/2} = 4.17$ h and 5.57 h, respectively. These findings of $t_{1/2}$, therefore, revealed that the nanostructured systems were not able to protect DOX from the UVA radiation during the entire study period. In contrast, the lyophilized samples L-DOX-CS-NPs and L-PEG-DOX-CS-NPs followed a second kinetic degradation order ($r = 0.9975$ and 0.9950, respectively) and presented encouraging results about $t_{1/2}$. L-DOX-CS-NPs and L-PEG-DOX-CS-NPs demonstrated $t_{1/2}$ values 15- and 7.5-fold greater (62.5 h and 41.67 h) compared to their suspension forms, respectively, suggesting an improvement on photostability of dry solid forms.

3.7. Cytotoxicity assays

In vitro assays are very attractive due to ethical aspects and for being a rapid and effective pathway to assess toxicological responses of new nanotechnologies before going to *in vivo* studies. Therefore, here we performed a preliminary study on the potential antitumor activity of the pH-responsive DOX-loaded NPs using an *in vitro* cell model. The cytotoxic responses of unloaded CS-NPs, DOX-loaded CS-NPs and free DOX were evaluated against HeLa tumor cells using MTT viability assay. A dose-dependent effect for all formulations tested can be seen in Fig. 5. The results obtained with DOX-loaded NPs were compared to those with free DOX in order to ensure that the drug encapsulation improves or at least maintains the cytotoxic effects of DOX. The *in vitro* antitumor activity of modified and unmodified DOX-loaded NPs was generally higher than that of free DOX at both tested concentrations. Finally, the cell viability was higher than 85% at both tested concentrations of unloaded CS-NPs, indicating that the surfactant 77KS did not promote significant cytotoxic effects [12].

4. Conclusions

In this work, we prepared and characterized PEGylated and poloxamer-modified DOX-CS-NPs incorporating the pH-sensitive lysine-based surfactant 77KS. NPs showed nanoscale size with relatively high EE%, whereas an improvement on DOX photostability was noticed when NPs were into dry solid forms. All formulations displayed pH-triggered DOX release and can

be stated as switching nanodevices in release kinetics, ranging from slow drug delivery while circulating (pH 7.4) to rapid release kinetics once target sites have been reached (pH 6.6 to 5.4). Finally, cytotoxicity experiments showed the ability of DOX-loaded CS-NPs to kill HeLa tumor cells. However, further studies in MDR cancer cells are needed to enhance our knowledge regarding the role of poloxamer together with 77KS in the sensitization of tumor cells. Altogether, our findings suggested that the pH-responsive DOX-loaded CS-NPs developed here could be potential stimulus-responsive drug delivery systems to target cancer cells by triggering the acidic tumor microenvironment as well as endosomal compartments.

Conflict of interest statement

The authors state that they have no conflict of interest.

Acknowledgments

This research was supported by Projects 447548/2014-0 and 401069/2014-1 of the *Conselho Nacional de Desenvolvimento Científico e Tecnológico* (CNPq - Brazil), 2293-2551/14-0 of *Fundação de Amparo à Pesquisa do Estado do Rio Grande do Sul* (FAPERGS - Brazil) and MAT2012-38047-C02-01 of the *Ministerio de Economía y Competitividad* (Spain) and FEDER (European Union). Laís E. Scheeren and Daniele R. Nogueira thank FAPERGS and PNPD-CAPES (Brazil) for the Masters' and Postdoctoral fellowships, respectively.

References

- [1] P. Vejpongsa, E.T.H. Yeh, JAAC 64 (2014) 938-945. <http://dx.doi.org/10.1016/j.jacc.2014.06.1167>
- [2] M. Dadsetan, K.E. Taylor, C. Yong, Z. Bajzer, L. Lu, M.J. Yaszemski, Acta Biomater. 9 (2013) 5438-5446. <http://dx.doi.org/10.1016/j.actbio.2012.09.019>
- [3] J. Akimoto, M. Nakayama, T. Okano, J. Control. Release 193 (2014) 2-8. <http://dx.doi.org/10.1016/j.jconrel.2014.06.062>
- [4] J. Yahuafai, T. Asai, G. Nakamura, T. Fukuta, P. Siripong, K. Hyodo, H. Ishihara, H. Kikuchi, N. Oku, J. Control. Release 192 (2014) 167-173. <http://dx.doi.org/10.1016/j.jconrel.2014.07.010>
- [5] K.A. Janes, M.P. Fresneau, A. Marazuela, A. Fabra, M.J. Alonsoa, J. Control. Release 73 (2001) 255-267. doi:10.1016/S0168-3659(01)00294-2
- [6] M. Li, Z. Tang, S. Lv, W. Song, H. Hong, X. Jing, Y. Zhang, X. Chen, Biomaterials 35 (2014) 3851-3864. <http://dx.doi.org/10.1016/j.biomaterials.2014.01.018>
- [7] D.A.A. Gewirtz, Biochem. Pharmacol. 57 (1999) 727-741. doi:10.1016/S0006-2952(98)00307-4
- [8] H. Ye, A.A. Karim, X.J. Loh, Mat. Sci. Eng. C 45 (2014) 609-619. <http://dx.doi.org/10.1016/j.msec.2014.06.002>
- [9] J. Liu, Y. Huang, A. Kumar, A. Tan, S. Jin, A. Mozhi, X. Liang, Biotechnol. Adv. 32 (2014) 693-710. <http://dx.doi.org/10.1016/j.biotechadv.2013.11.009>
- [10] E.S. Lee, K.T. Oh, D. Kim, Y.S. Youn, Y.H. Bae, J. Control. Release 123 (2007) 19-26. doi:10.1016/j.jconrel.2007.08.006
- [11] L. Tian, Y.H. Bae, Colloids Surf. B: Biointerfaces 99 (2012) 116-126. doi:10.1016/j.colsurfb.2011.10.039
- [12] D.R. Nogueira, M. Mitjans, M.R. Infante, M.P. Vinardell, Int. J. Pharm. 420 (2011) 51-58. doi:10.1016/j.ijpharm.2011.08.020
- [13] D.R. Nogueira, M. Mitjans, M.R. Infante, M.P. Vinardell, Acta Biomater. 7 (2011) 2846-2856. doi:10.1016/j.actbio.2011.03.017
- [14] D.R. Nogueira, L.B. Macedo, L.E. Scheeren, M. Mitjans, M.R. Infante, C.M.B. Rolim, M.P. Vinardell, J. Appl. Biopharm. Pharmacokinet. 2 (2014) 59-67. doi: <http://dx.doi.org/10.14205/2309-4435.2014.02.02.3>

- [15] M. Prabaharan, Int. J. Biol. Macromol. 72 (2015) 1313-1322.
<http://dx.doi.org/10.1016/j.ijbiomac.2014.10.052>
- [16] S. Mitra, U. Gaur, P.C. Ghosh, A.N. Maitra, J. Control. Release 74 (2001) 317-323.
doi:10.1016/S0168-3659(01)00342-X
- [17] T. Ramasamy, T.H. Tran, H.J. Cho, J.H. Kim, Y.I. Kim, J.Y. Jeon, H. Choi, C.S. Yong, J.O. Kim, Pharm. Res. 31 (2013) 1302-1314. doi:10.1007/s11095-013-1251-9
- [18] G. Unsoy, R. Khodadust, S. Yalcin, P. Mutlu, U. Gunduz, Eur. J. Pharm. Sci. 62 (2014) 243-250. <http://dx.doi.org/10.1016/j.ejps.2014.05.021>
- [19] A. Gabizon, H. Shmeeda, T. Grenader, Eur. J. Pharm. Sci. 45 (2012) 388-398.
doi:10.1016/j.ejps.2011.09.006
- [20] Y. Wu, W. Yang, C. Wang, J. Hu, S. Fu, Int. J. Pharm. 295 (2005) 235-245.
doi:10.1016/j.ijpharm.2005.01.042
- [21] Y. Jeong, D. Kim, M. Jang, J. Nah, Carbohydr. Res. 343 (2008) 282-289.
doi:10.1016/j.carres.2007.10.025
- [22] U. Termsarasab, I. Yoon, J. Park, H.T. Moon, H. Cho, D. Kim, Int. J. Pharm. 464 (2014) 127-134. <http://dx.doi.org/10.1016/j.ijpharm.2014.01.015>
- [23] E.V. Batrakova, A.V. Kabanov, J. Control. Release 130 (2008) 98-106.
doi:10.1016/j.jconrel.2008.04.013
- [24] E.V. Batrakova, S. Li, A.M. Brynskikh, A.K. Sharma, Y. Li, M. Boska, N. Gong, R.L. Mosley, V.Y. Alakhov, H.E. Gendelman, A.V. Kabanov, J. Control. Release 143 (2010) 290-301. doi:10.1016/j.jconrel.2010.01.004
- [25] Y. Zhao, C. Sun, C. Lu, D. Dai, H. Lv, Y. Wu, C. Wan, L. Chen, M. Lin, X. Li, Cancer Lett. 311 (2011) 187-194. doi:10.1016/j.canlet.2011.07.013
- [26] Y. Chen, W. Zhang, Y. Huang, F. Gao, X. Sha, X. Fang, Int. J. Pharm. 488 (2015) 44-58.
<http://dx.doi.org/10.1016/j.ijpharm.2015.04.048>
- [27] L. Sanchez, M. Mitjans, M.R. Infante, M.P. Vinardell, Toxicol. Lett. 161 (2006) 53-60.
doi:10.1016/j.toxlet.2005.07.015
- [28] L. Sanchez, M. Mitjans, M.R. Infante, M.T. García, M.A. Manresa, M.P. Vinardell, Amino Acids 32 (2007) 133-136. PMID: 16729197
- [29] M.A. Vives, M.R. Infante, E. Garcia, C. Selve, M. Maugras, M.P. Vinardell, Chem. Biol. Interact. 118 (1999) 1-18. PII: S0009-2797(98)00111-2

- [30] P. Calvo, C. Remuñán-López, J.L. Vila-Jato, M.J. Alonso, *J. Appl. Polym. Sci.* 63 (1997) 125-132. doi:10.1023/A:1012128907225
- [31] Q. Gan, T. Wang, C. Cochrane, P. McCarron, *Colloids Surf. B: Biointerfaces* 44 (2005) 65-73. doi:10.1016/j.colsurfb.2005.06.001
- [32] S.S. Santos, A. Lorenzoni, N.S. Pegoraro, L.B. Denardi, S.H. Alves, S.R. Schaffazick, L. Cruz, *Colloids Surf. B: Biointerfaces* 116 (2014) 270-276. <http://dx.doi.org/10.1016/j.colsurfb.2014.01.011>
- [33] M.C. Fontana, A. Beckenkamp, A. Buffon, R.C.R. Beck, *Int. J. Nanomed.* 9 (2014) 2979-2991. <http://dx.doi.org/10.2147/IJN.S62857>
- [34] R.W. Korsmeyer, R. Gumy, E. Doelker, P. Buri, N.A. Peppas, *Int. J. Pharm.* 15 (1983) 25-35. doi:10.1016/0378-5173(83)90064-9
- [35] P.L. Ritger, N.A. Peppas, *J. Control. Release* 5 (1987) 23-36. doi:10.1016/0168-3659(87)90034-4
- [36] N.A. Peppas, J.J. Sahlin, *Int. J. Pharm.* 57 (1989) 169-172. doi:10.1016/0378-5173(89)90306-2
- [37] P. Rosa, A.P.S. Salla, C.B. Silva, C.M.B. Rolim, A.I.H. Adams, *AAPS PharmSciTech* 15 (2014) 1155-1162. doi: 10.1208/s12249-014-0149-0
- [38] W. Tiyaboonchai, *Naresuan University Journal* 11 (2003) 51-66.
- [39] T. Kean, M. Thanou, *Adv. Drug Deliv. Rev.* 62 (2010) 3-11. doi:10.1016/j.addr.2009.09.004
- [40] D. Lee, K. Powers, R. Baney, *Carbohydr. Polym.* 58 (2004) 371-377. doi:10.1016/j.carbpol.2004.06.033
- [42] L. Keawchaoon, R. Yoksan, *Colloids Surf. B: Biointerfaces* 84 (2011) 163-171. doi:10.1016/j.colsurfb.2010.12.031
- [42] M.R. Avadi, A.M.M.Sadeghi, N. Mohammadpour, S. Abedin, F. Atyabi, R. Dinarvand, M. Rafiee-Tehrani, *Nanomedicine: Nanotechnol., Biol., Med.* 6 (2010) 58-63. doi:10.1016/j.nano.2009.04.007
- [43] Q. Gan, T. Wang, *Colloids Surf. B: Biointerfaces* 59 (2007) 24-34. doi:10.1016/j.colsurfb.2007.04.009
- [44] D.R. Nogueira, L. Tavano, M. Mitjans, L. Pérez, M. R. Biomaterials 34 (2013) 2758-2772. <http://dx.doi.org/10.1016/j.biomaterials.2013.01.005>

- [45] S. Mao, W. Sun, T. Kissel, *Adv. Drug Deliv. Rev.* 62 (2010) 12-27. doi:10.1016/j.addr.2009.08.004
- [46] L. Tavano, R. Aiello, G. Ioele, N. Picci, R. Muzzalupo, *Colloids Surf. B: Biointerfaces* 118 (2014) 7-13. doi: 10.1016/j.colsurfb.2014.03.016.
- [47] M. Xu, J. Qian, X. Liu, T. Liu, H. Wang, *Mat. Sci. Eng. C* 50 (2015) 341-347. <http://dx.doi.org/10.1016/j.msec.2015.01.098>
- [48] S.S. Kim, Y.M. Lee, *Polymer* 36 (1995) 4497-4501. doi:10.1016/0032-3861(95)96859-7
- [49] H. Hosseinzadeh, F. Atyabi, R. Dinarvand, S.N. Ostad, *Int. J. Nanomed.* 7 (2012) 1851-1863. <http://dx.doi.org/10.2147/IJN.S26365>
- [50] S. Danson, D. Ferry, V. Alakhov, J. Margison, D. Kerr, D. Jowle, M. Brampton, G. Halbert, M. Ranson, *Br. J. Cancer.* 90 (2004) 2085-2091. doi: 10.1038/sj.bjc.6601856
- [51] Y. Jin, H. Hu, M. Qiao, J. Zhu, J. Qi, C. Hu, Q. Zhang, D. Chen, *Colloids Surf. B Biointerfaces* 94 (2012) 184– 191. doi:10.1016/j.colsurfb.2012.01.032
- [52] J. Ji, S. Hao, D. Wu, R. Huang, Y. Xu, *Carbohydr. Polym.* 85 (2011) 803-808. doi:10.1016/j.carbpol.2011.03.051
- [53] J. Park, P.M. Fong, J. Lu, K.S. Russell, C.J. Booth, W.M. Saltzman, T.M. Fahmy, *Nanomed. Nanotechnol.* 5 (2009) 410-418. doi:10.1016/j.nano.2009.02.002
- [54] D.B. Leeper, K. Engin, A.J. Thistlethwaite, H.D. Hitchon, J.D. Dover, D.Li, L. Tupchong, *Int. J. Radiation Oncology Biol. Phys.* 28 (1994) 935-943. doi:10.1016/0360-3016(94)90114-7
- [55] F. Yan, C. Zhang, Y. Zheng, L.Me, L. Tang, C. Song, H. Sun, L. Huang, *Nanomedicine: Nanotechnol., Biol., Med.* 6 (2010) 170-178. doi:10.1016/j.nano.2009.05.004
- [56] L. Mei, Y. Zhang, Y. Zheng, G. Tian, C. Song, D. Yang, H. Chen, H. Sun, Y. Tian, K. Liu, Z. Li, L. Huang, *Nanoscale Res. Lett.* 4 (2009) 1530-1539. doi: 10.1007/s11671-009-9431-6
- [57] R.S.T. Aydin, M. Pulat, *J. Nanomater.* 2012 (2012) 1-10. doi:10.1155/2012/313961
- [58] S.A. Agnihotri, N.N. Mallikarjuna, T.M. Aminabhavi, *J. Control. Release* 100 (2004) 5-28. doi:10.1016/j.conrel.2004.08.010
- [59] J. Berger, M. Reist, J.M. Mayer, O. Felt, N.A. Peppas, R. Gurny, *Eur. J. Pharm. Biopharm.* 57 (2004) 19-34. doi:10.1016/S0939-6411(03)00161-9
- [60] P.L. Ritger, N.A. Peppas, *J. Control. Release* 5 (1987) 37-42. doi:10.1016/0168-3659(87)90035-6

- [61] M. Fazil, S. Md, S. Haque, M. Kumar, S. Baboota, J. Sahni, J. Ali, Eur. J. Pharm. Sci. 47 (2012) 6-15. <http://dx.doi.org/10.1016/j.ejps.2012.04.013>
- [62] J.C. Kasper, G. Winter, W. Friess, Eur. J. Pharm. Biopharm. 85 (2013) 162-169. <http://dx.doi.org/10.1016/j.ejpb.2013.05.019>
- [63] M.K. Lee, M.Y. Kim, S. Kim, J. Lee, J. Pharm. Sci. 98 (2009) 4808-4817. doi:10.1002/jps.21786
- [64] A. Rampino, M. Borgogna, P. Blasi, B. Bellich, A. Cesàro, Int. J. Pharm. 455 (2013) 219-228. <http://dx.doi.org/10.1016/j.ijpharm.2013.07.034>
- [65] T. Cerchiara, A. Abruzzo, M. di Cagno, F. Bigucci, A. Bauer-Brandl, C. Parolin, B. Vitali, M.C. Gallucci, B. Luppi, Eur. J. Pharm. Biopharm. 92 (2015) 112-119. <http://dx.doi.org/10.1016/j.ejpb.2015.03.004>
- [66] M. Luangtana-anan, S. Limmatvapirat J. Nunthanid, R. Chalongsuk, K. Yamamoto, AAPS PharmSciTech 11 (2010) 1376-1382. doi: 10.1208/s12249-010-9512-y

Table 1. Characterization of unloaded and DOX-loaded CS-NPs with or without 77KS. The lyophilized NPs (L-NPs) were analyzed after redispersion in ultra-pure water.

Sample	Particle size (nm) \pm SD [*]	Polydispersity index \pm SD [*]	Zeta potential (mV) \pm SD [*]	pH	EE% \pm SD [*]
CS-NPs (CS:TPP)	170.30 \pm 0.84	0.19 \pm 0.02	25.20 \pm 1.87	5.66	-
DOX-CS-NPs (CS:TPP)	190.35 \pm 1.70	0.22 \pm 0.01	21.90 \pm 1.12	5.70	75.54 \pm 4.98
CS-NPs	176.77 \pm 1.79	0.20 \pm 0.02	24.00 \pm 1.82	5.66	-
DOX-CS-NPs	197.50 \pm 2.30	0.22 \pm 0.01	21.70 \pm 0.81	5.72	66.50 \pm 2.68
PEG-CS-NPs	211.10 \pm 1.55	0.24 \pm 0.01	23.30 \pm 1.96	4.68	-
PEG-DOX-CS-NPs	226.40 \pm 2.33	0.23 \pm 0.01	23.65 \pm 1.06	5.19	66.32 \pm 3.54
Polox-CS-NPs	184.50 \pm 2.00	0.21 \pm 0.02	22.05 \pm 0.91	5.48	-
Polox-DOX-CS-NPs	209.70 \pm 1.35	0.22 \pm 0.03	21.00 \pm 0.85	5.60	62.21 \pm 2.88
L-DOX-CS-NPs	217.45 \pm 4.49	0.33 \pm 0.02	12.40 \pm 0.15	6.14	67.42 \pm 10.85
L-PEG-DOX-CS-NPs	491.60 \pm 32.38	0.73 \pm 0.09	20.45 \pm 0.78	5.91	65.32 \pm 3.18
L-Polox-DOX-CS-NPs	252.80 \pm 7.46	0.40 \pm 0.03	17.50 \pm 0.93	5.98	61.27 \pm 2.28

* SD = standard deviation ($n = 3$)

Table 2. Observed rate constants, correlation coefficients, MSC and half-lives ($t_{1/2}$) obtained by mathematical modeling of DOX release from the different NPs when immersed in PBS buffer at pH 7.4, 6.6 and 5.4. Results are expressed as mean \pm standard deviation (SD) of three experiments.

	pH medium	DOX-CS-NPs	PEG-DOX-CS-NPs	Polox-DOX-CS-NPs
Biexponential				
<i>r</i>		0.99 \pm 0.01	1.00 \pm 0.01	1.00 \pm 0.01
MSC		3.96 \pm 0.36	4.28 \pm 0.25	4.17 \pm 0.45
k_1 (h ⁻¹)		0.44 \pm 0.05	0.67 \pm 0.07	2.84 \pm 1.25
$t_{1/2} k_1$ (h ⁻¹)	7.4	1.58 \pm 0.47	1.02 \pm 0.29	0.24 \pm 0.09
k_2 (h ⁻¹)		0.002 \pm 0.01	0.01 \pm 0.01	0.36 \pm 0.36
$t_{1/2} k_2$ (h ⁻¹)		407.64 \pm 33.76	93.64 \pm 9.12	1.91 \pm 0.38
<i>a</i>		0.74 \pm 0.04	0.70 \pm 0.03	0.31 \pm 0.08
<i>b</i>		0.23 \pm 0.04	0.26 \pm 0.02	0.68 \pm 0.08
Monoexponential				
<i>r</i>		0.99 \pm 0.01	0.99 \pm 0.01	0.98 \pm 0.01
MSC	6.6	3.74 \pm 0.32	3.46 \pm 0.63	3.13 \pm 0.35
k (h ⁻¹)		0.64 \pm 0.04	1.23 \pm 0.08	1.05 \pm 0.08
$t_{1/2}$ (h ⁻¹)		1.07 \pm 0.05	0.56 \pm 0.03	0.65 \pm 0.14
<i>r</i>		1.00 \pm 0.01	0.99 \pm 0.01	1.00 \pm 0.00
MSC	5.4	4.68 \pm 0.29	3.31 \pm 0.31	5.07 \pm 0.25
k (h ⁻¹)		0.76 \pm 0.03	0.98 \pm 0.07	0.91 \pm 0.03
$t_{1/2}$ (h ⁻¹)		0.90 \pm 0.10	0.71 \pm 0.20	0.76 \pm 0.19

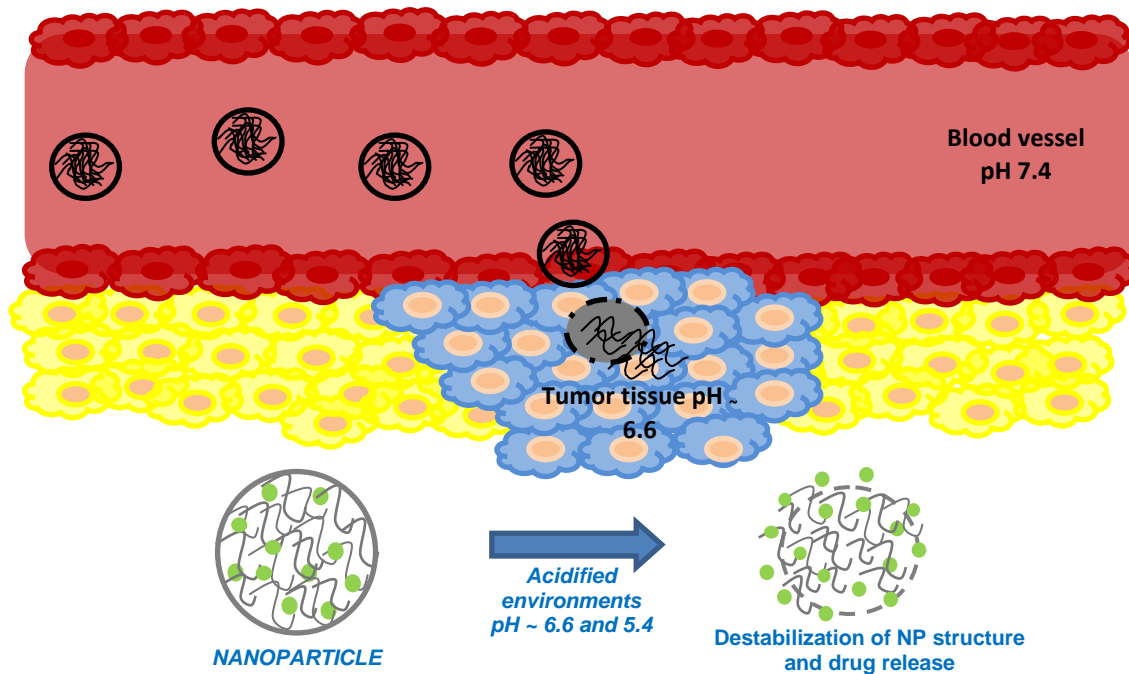


Fig. 1. Design of pH-responsive DOX-loaded CS-NPs to facilitate target drug release at the tumor site.

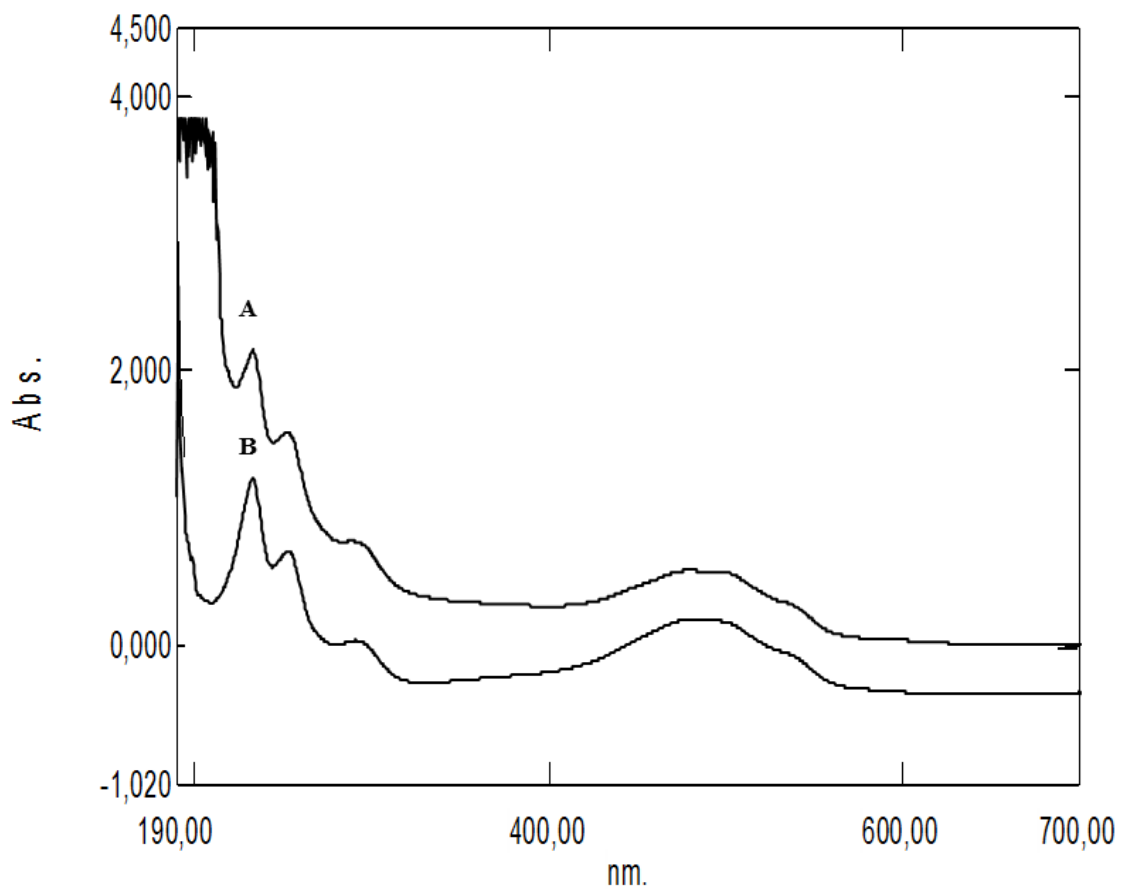


Fig. 2. UV-Vis absorption spectra of the DOX extracted from NPs (A) and DOX aqueous solution (B).

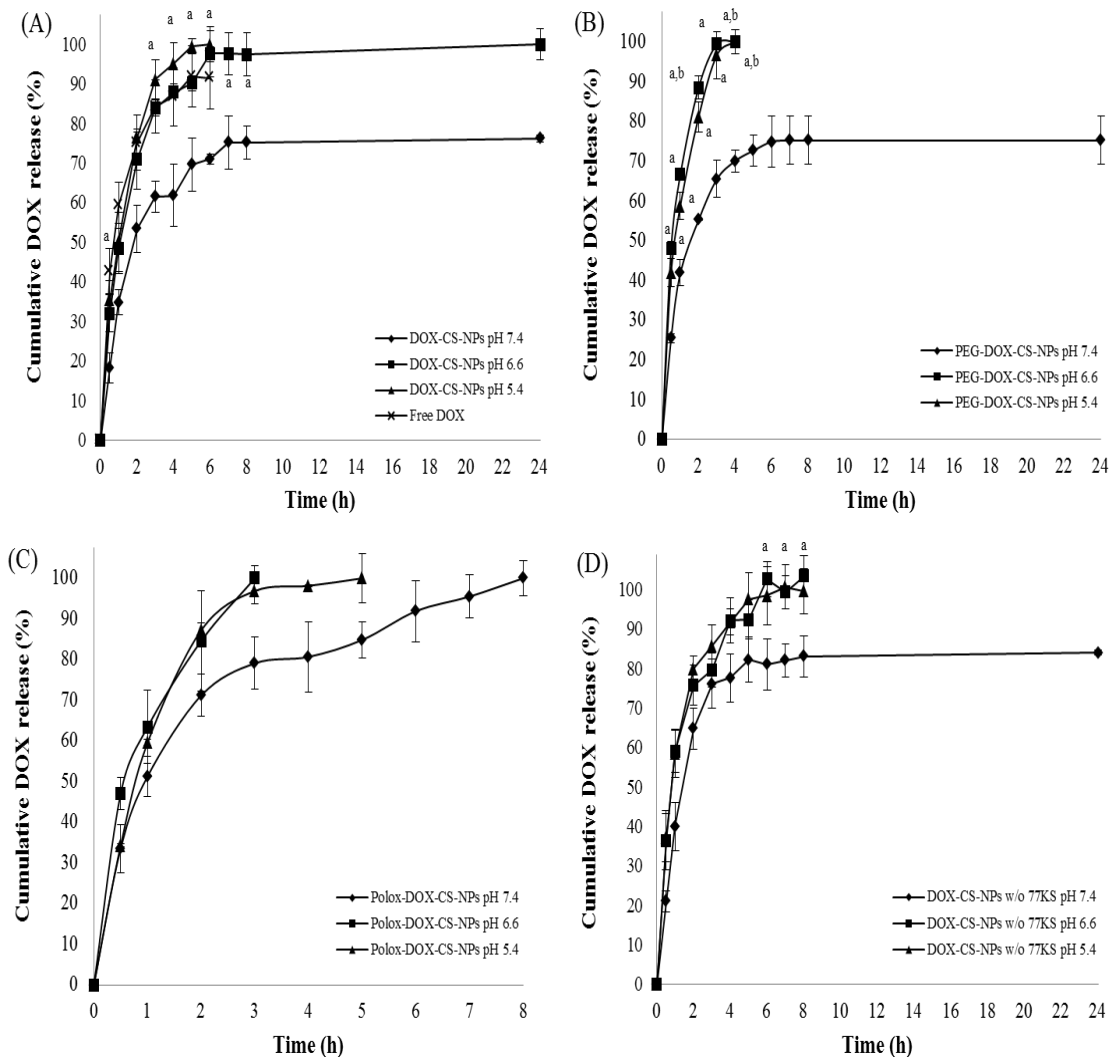


Fig. 3. pH-dependent *in vitro* cumulative DOX release from NPs in PBS buffer at pH 7.4, 6.6 and 5.4. (A) DOX-CS-NPs, (B) PEG-DOX-CS-NPs, (C) Polox-DOX-CS-NPs and (D) DOX-CS-NPs without 77KS. Results are expressed as the mean \pm SE of three independent experiments. Statistical analyses were performed using ANOVA followed by Tukey's multiple comparison test. ^a Significant difference from PBS pH 7.4 ($p < 0.05$), ^b highly significant difference from PBS pH 7.4 ($p < 0.01$).

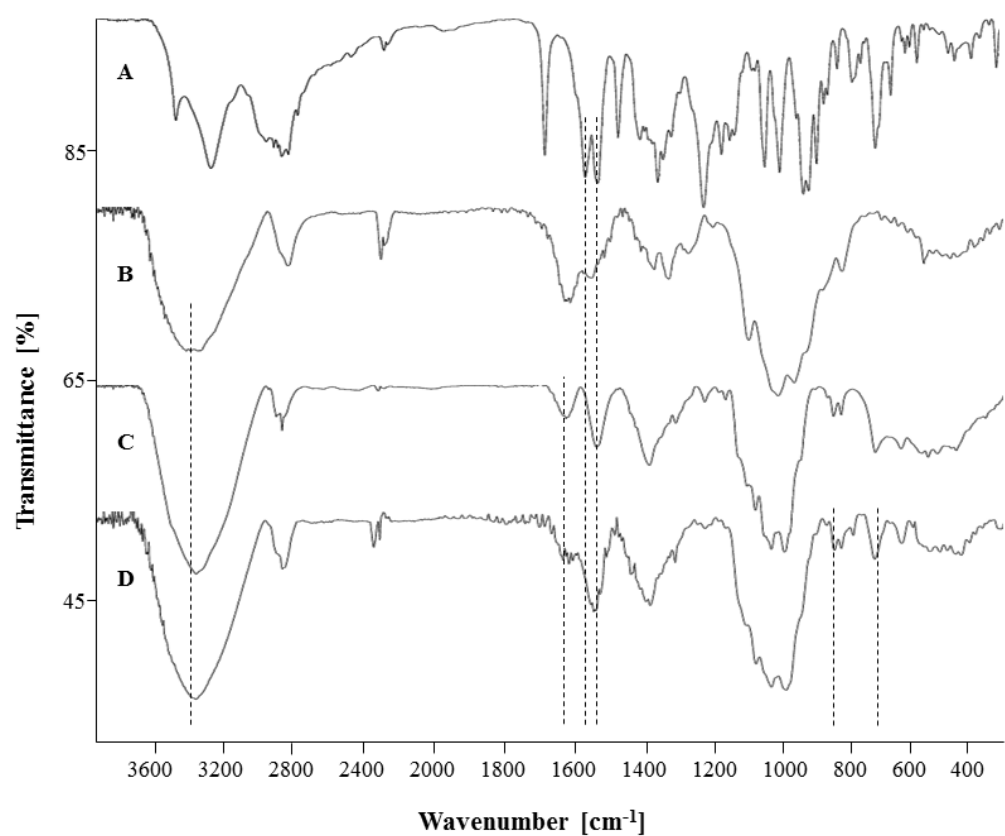


Fig. 4. FT-IR spectra of pure DOX (A), CS raw material (B), DOX-CS-NPs (C) and PEG-DOX-CS-NPs (D).

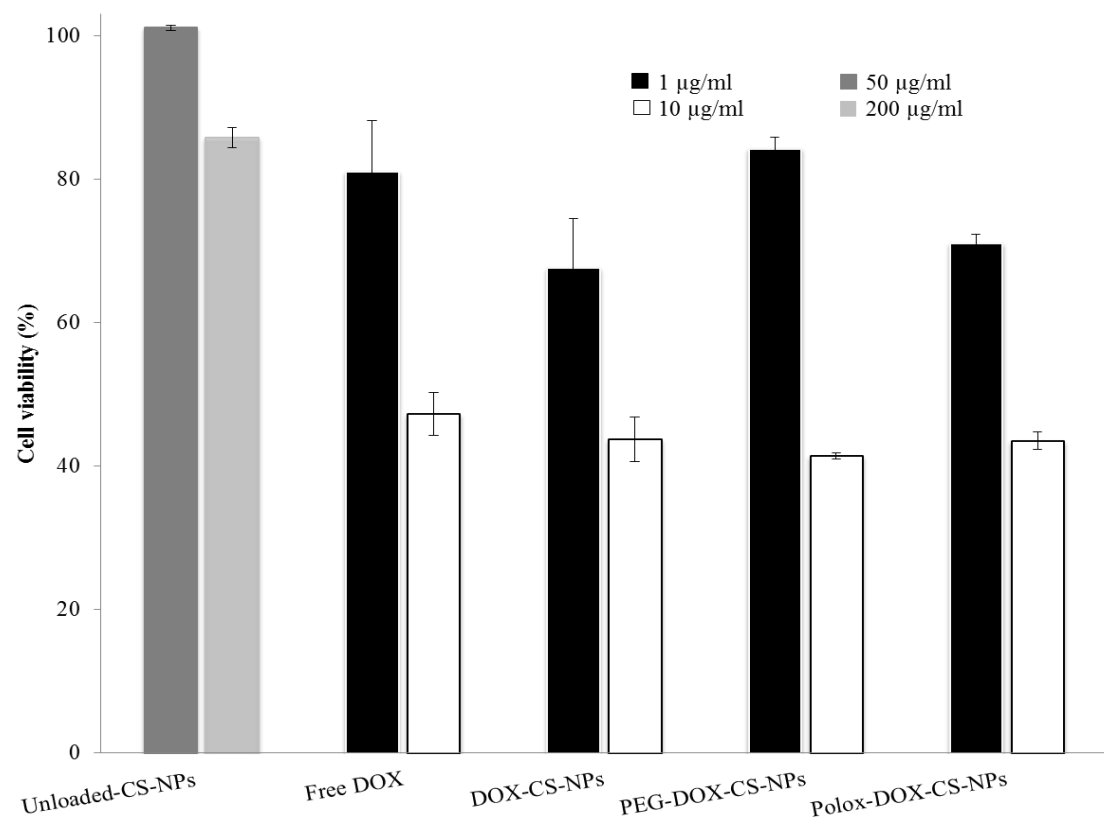


Fig. 5. *In vitro* antitumor activity of unloaded-CS-NPs, free DOX and DOX-loaded CS-NPs in HeLa cell line.

6. ARTIGO CIENTÍFICO III:

“Chitosan nanoparticles functionalized with a pH-responsive surfactant improved the *in vitro* antineoplastic effects of doxorubicin”

O presente manuscrito está disposto no formato de submissão ao periódico *Chemico-Biological Interactions* (Fator de impacto 2,577. WebQualis A2).

APRESENTAÇÃO EM PORTUGUÊS

Nanopartículas de quitosana incorporando um tensoativo pH-sensível melhoraram a atividade antineoplásica *in vitro* da doxorrubicina

Conforme demonstrado em estudo prévio, o tensoativo 77KS apresenta propriedade de romper membranas biológicas de forma pH-dependente. Além disso, as CS-NPs incorporando este tensoativo mostraram-se capazes de promover a liberação acelerada da DOX encapsulada em meios acidificados. Sendo assim, a fim de aprofundar nosso conhecimento acerca do potencial terapêutico/tóxico das NPs incorporando o 77KS, com ou sem os modificadores PEG e poloxamer, neste trabalho foram conduzidos estudos de citotoxicidade *in vitro*, bem como estudos de hemólise para verificar a capacidade lítica de membrana e a hemocompatibilidade das NPs. Para os estudos de citotoxicidade, utilizaram-se três linhagens celulares, sendo uma não-tumoral (fibroblastos 3T3), servindo como controle da atividade inespecífica das NPs, e duas linhagens tumorais (HeLa e MCF-7). Os ensaios MTT e NRU foram aplicados para a determinação da viabilidade celular. As CS-NPs contendo DOX tiveram sua atividade antitumoral comparada ao fármaco não-encapsulado. Os diferentes tratamentos foram aplicados utilizando-se meio de cultivo com pH normal, por 24 e 48 horas, além de pH levemente acidificado, simulando as condições do microambiente tumoral ($pH_e \sim 6,6$), por 24 horas. As CS-NPs exibiram efeitos citotóxicos maiores nas linhagens celulares tumorais, principalmente quando em meio acidificado (pH 6,6), e baixa atividade contra as células não tumorais. O ensaio de hemólise, com o eritrócito como modelo de membrana endossomal, foi realizado para verificar a atividade lítica de membrana das NPs de acordo com o tempo de exposição, concentração das NPs e pH do meio (7,4, 6,6 e 5,4). Demonstrou-se que as NPs contendo o 77KS apresentaram atividade lítica significativamente maior em relação às NPs sem o 77KS em pH 6,6 e 5,4, indicando que o tensoativo é, claramente, o responsável pela atividade pH-sensível das NPs. Este resultado poderia ser explicado pela protonação da molécula do 77KS quando em pH ácido, o que aumentaria a sua hidrofobicidade e, consequentemente, sua interação com as membranas celulares. Por fim, o teste de hemólise também foi utilizado para verificar a hemocompatibilidade das NPs, uma vez que estas são pretendidas para administração endovenosa.

Chitosan nanoparticles functionalized with a pH-responsive surfactant improved the *in vitro* antineoplastic effects of doxorubicin

ABSTRACT

Stimuli-responsive delivery systems that release a therapeutic molecule in a controlled manner are highly desirable for the antineoplastic therapy. Of particular interest are pH-responsive nanocarriers because they allow the exploitation of the various pH gradients within the body, for example, between healthy tissue and tumor tissue, or between the extracellular tissue and some cell compartments. Likewise, modifications in nanocarriers with polyethylene glycol (PEG) and poloxamer have been exploiting in an attempt to improve the effectiveness of cancer treatments. Here, we prepared pH-responsive DOX-loaded chitosan-tripolyphosphate nanoparticles (NPs), modified or not with PEG or poloxamer, for target delivery to tumor cells. The pH-sensitive surfactant 77KS, derived from the amino acid lysine, was used as a potential bioactive adjuvant for intracellular drug delivery. Owning to the pH-sensitivity of 77KS, the CS-NPs showed pH-responsive membranolytic behavior upon reducing the pH value of surrounding media to 6.6 and 5.4. The *in vitro* antiproliferative assays with MCF-7 and HeLa tumor cells indicated that the NPs themselves had no associated significant cytotoxicity, while DOX-loaded modified and unmodified NPs possessed higher cytotoxicity than free drug. Additionally, DOX-loaded CS-NPs displayed greater selectivity to tumor cells than to the non-tumor 3T3 fibroblasts. Finally, the feasibility of using these NPs to target tumor microenvironment was proven, as cytotoxicity against cancer cells was higher in a mildly acidic environment. Altogether, the results suggest that the combination of endosomal acidity with the endosomolytic capability of these pH-responsive nanocarriers could increase the intracellular delivery of DOX, which thus might enhance its antineoplastic efficacy. Therefore, the designed pH-responsive CS-NPs may offer a promising pattern to accurately deliver DOX payload to tumor cells for cancer therapy.

Keywords: Chitosan-based nanoparticles; Doxorubicin; *In vitro* antitumor activity; Lysine-based surfactant; pH-sensitive membranolytic behavior

1. Introduction

Increasing efforts have been made to exploit physiological signals such as pH and temperature for targeted drug delivery applications [1,2]. Of the various stimuli, pH has been widely investigated for the treatment of solid tumors. A response to pH change is of great importance, since defined pH gradients exist in biological systems. Neoplastic tissues could exhibit a lower pH value (acidosis) than healthy tissue and, therefore, drug targeting to solid tumors can be achieved by designing stimuli-sensitive drug carriers [3]. The slight acidosis in tumor tissue, with pH values ranging from 6.5 to 7.2, is attributed to a combination of elevated aerobic glycolysis and reduced blood flow [4]. Likewise, the early and late endosomal compartments have acidic pH of about 6.6 and 5.4, respectively [5].

Cancer is one of the main causes of mortality worldwide and doxorubicin (DOX) is a potent chemotherapeutic drug applied in the clinics for the treatment of various human cancers. DOX is a hydrophilic drug that binds to DNA by intercalation and induces a series of biochemical events, leading to apoptosis in tumor cells [6]. The clinical efficacy of the conventional treatments with DOX is often compromised by the acquisition of resistance in cancer cells and/or by the generation of several side effects to the patients, especially a cumulative dose-dependent cardiotoxicity [7-9]. Moreover, conventional drugs usually easily escape from tumors, but the accumulation in the tumor tissue can increase significantly when encapsulated into a nanostructure [10].

Upon this sense, investigations on nanocarriers for antitumor therapy are dominating the field and growing rapidly. Polymeric NPs responsive to pH that are capable of retaining drug during circulation while actively releasing it at the tumor site and/or inside the target tumor cells have received an overwhelming interest for tumor-targeting cancer chemotherapy [11,12]. Moreover, when vectorized, DOX would be favored to accumulate on the site of action, limiting thus its dispersion into healthy tissues [13].

Chitosan (CS) is a naturally occurring polymer that has been attracting increasing attention in pharmaceutical and biomedical applications because of its biocompatibility, biodegradability, non-toxicity, cationic properties and bioadhesive characteristics [14,15]. Therefore, CS nanoparticles (NPs) are of great interest as drug delivery systems, including applications for cancer therapy [16,17]. Considering DOX encapsulation, the challenge was to entrap a cationic, hydrophilic molecule into NPs formed by ionic gelation of the positively charged polysaccharide CS. A previous study has reported the use of the polyanionic dextran sulphate to mask the positive charge in DOX [18]. Here, we used the polyanion pentasodium tripolyphosphate to form the NPs by ionic complexation with CS, which can also aid DOX

encapsulation by electrostatic interactions [19]. Moreover, several modifications can be envisioned to further improve and tune CS-based colloidal drug delivery systems. Here, we reported a simple strategy for preparation of pH-responsive CS-NPs encapsulating DOX by using the ionic gelation method. Without crosslinkers and/or organic solvents, a bioactive amino acid-based surfactant with sodium counterion (77KS) was incorporated into NP matrix to give it a pH-sensitive behaviour [20].

It is well known that DOX is found to be glycoprotein P (P-gp) substrate, which is likely to develop the multidrug resistance (MDR). In an attempt to achieve MDR reversal capacity, poloxamer-modified NPs have been studied [21,22]. Poloxamers are approved by the Food and Drug Administration (FDA) and are well tolerated upon repeated exposure [23]. The key attribute for the biological activity of poloxamers is their capability to incorporate into membranes, affecting various cellular functions, which in turn cause drastic sensitivity of MDR tumors to various antitumor drugs [21]. Additionally, PEG modification technology of NPs has been shown not only to provide prolonged *in vivo* circulation, but also lower clearance of the encapsulated drug [24]. This behaviour, in turn, contributes to the great success of the anticancer therapy.

Therefore, the aim of this study was to assess the *in vitro* antiproliferative activity of the pH-responsive CS-based NPs in comparison with free DOX. We used HeLa and MCF-7 tumor cell models and 3T3 fibroblasts as non-tumor control cells. Moreover, we studied the feasibility of using these NPs to target acidic tumor extracellular environment using also *in vitro* endpoints. Finally, the role of pH in the membrane-lytic activity of CS-based NPs incorporating 77KS, containing or not the modifiers PEG and poloxamer, was evaluated by the hemolysis assay with the erythrocyte as a model for the endosomal membrane.

2. Experimental

2.1. Chemicals and reagents

Chitosan (CS) of low molecular weight (LMW) (deacetylation degree, 75-85%; viscosity, 20-300 cP according to the manufacturer's data sheet), pentasodium tripolyphosphate (TPP), polyethylene glycol methyl ether (mPEG, $M_n = 5,000$), poloxamer 188 solution (10%, w/v), 2,5-diphenyl-3,-(4,5-dimethyl-2-thiazolyl) tetrazolium bromide (MTT), neutral red (NR) dye, dimethyl sulfoxide (DMSO), phosphate buffered saline (PBS) and trypsin-EDTA solution (0.5 g porcine trypsin and 0.2 g EDTA • 4Na per liter of Hanks'

Balanced Salt Solution) were obtained from Sigma-Aldrich (St. Louis, MO, USA). Doxorubicin (DOX, state purity 98.32%) was purchased from Zibo Ocean International Trade (Zibo, Shangdong, P.R., China). Fetal bovine serum (FBS) and Dulbecco's Modified Eagle's Medium (DMEM), supplemented with L-glutamine (584 mg/l) and antibiotic/antimicotic (50 mg/ml gentamicin sulphate and 2 mg/l amphotericin B), were purchased from Vitrocell (Campinas, SP, Brazil). All other reagents were of analytical grade.

The anionic amino acid-based surfactant derived from N^a,N^c-dioctanoyl lysine and with an inorganic sodium counterion (77KS) was included in the NP formulations as a bioactive and pH-sensitive adjuvant. Two alkyl chains form its chemical structure, each one with eight carbon atoms. It has a molecular weight of 421.5 g/mol and a critical micellar concentration (CMC) of 3×10^3 µg/ml [25]. This surfactant was previously synthesized as described elsewhere [26].

2.2. Nanoparticle preparation

CS-NPs were obtained by ionotropic gelation method, according to Calvo et al. [27]. Firstly, a CS solution (0.1% w/v) was prepared by dissolving LMW-CS in 1% (v/v) acetic acid solution. The pH of the CS final solution was adjusted to 5.5 with 1 M NaOH [28]. Then, unloaded-CS NPs were formed spontaneously upon dropwise addition of a premixed solution containing the cross-linker TPP and the surfactant 77KS (at 0.2% and 0.05%, w/v, respectively) over the CS solution under magnetic stirring at room temperature for 20 min. The final selective ratio of NPs was CS:TPP:77KS ratio of 5:2:0.5 (w/w/w). Similarly, DOX-loaded CS NPs (DOX-CS-NPs) were prepared following the same procedure, but first adding DOX to the CS solution (CS:DOX ratio 5:0.5, w/w) under 1000 rpm magnetic stirring for 10 min. Furthermore, PEGylated DOX-CS-NPs (PEG-DOX-CS-NPs) were obtained by first preparing a mixed solution of CS and PEG (0.1 and 1% w/v, respectively) in 1 % (v/v) acetic acid. Poloxamer-modified DOX-CS-NPs (Polox-DOX-CS-NPs) were reached by adding TPP:77KS solution to CS solution containing 0.5% (w/v) of poloxamer. All procedures involving DOX were conducted in a low incidence of light. The resulting DOX-loaded NPs were purified by dialysis for 1 h in distilled water (dialysis bag - Sigma-Aldrich, 14,000 MWCO), in order to remove the non-encapsulated drug.

2.3. Nanoparticle characterization

The mean hydrodynamic diameter and the polydispersity index (PDI) of the NP suspensions in water and also dispersed in cell culture medium were determined by dynamic

light scattering (DLS) using a Malvern Zetasizer ZS (Malvern Instruments, Malvern, UK). The samples were diluted in cell culture medium with 5% (v/v) FBS before the corresponding measurements and the dynamic evolution of particle distribution was investigated by monitoring particle size over time. Readings were taken at 25°C immediately after dilution ($t = 0$ h) and after 24 h incubation at 37°C ($t = 24$ h), simulating the environment found during the *in vitro* cytotoxicity experiments. Each measurement was performed using at least three sets of ten runs. The zeta potential (ZP) of NPs was assessed by determining the electrophoretic mobility with the Malvern Zetasizer ZS equipment. The measurements were performed after dilution of the formulations in 10 mM NaCl aqueous solution (1:10 volume per volume), using at least three sets of 10 runs.

2.4. Preparation of red blood cells suspensions

Erythrocytes were isolated from human blood, which was obtained from discarding samples of the Clinical Analysis Laboratory of the University Hospital of Santa Maria. Tubes containing EDTA as anticoagulant were used for blood collection. Red blood cells were isolated by centrifugation at 3,000 rpm for 10 min, and washed three times in an isotonic phosphate buffer solution (PBS) containing 123.3 mM NaCl, 22.2 mM Na₂HPO₄ and 5.6 mM KH₂PO₄ in distilled water (pH 7.4; 300 mOsmol/l). These washing steps are necessary to remove other cells and traces of plasma. The cell pellets were then suspended in PBS at a cell density of 8×10^9 cell/ml.

2.5. Hemocompatibility studies

The hemolysis assay was performed following the previously described procedure [29]. Twenty-five microliter aliquots of erythrocyte suspension were exposed to unloaded-CS-NPs at concentrations of 150, 300 and 600 µg/ml (concentrations based on the total composition of the formulation), and to DOX-loaded CS-NPs or free DOX at concentrations of 10, 20 and 40 µg/ml (concentrations based on the total amount of DOX). Each formulation was suspended in PBS buffer at pH 7.4 in a total volume of 1 ml. Two controls were prepared by resuspending erythrocyte suspension either in buffer alone (negative control) or in distilled water (positive control). The samples were incubated at room temperature for 10 minutes or 1 h and then centrifuged at 10000 rpm for 5 min to stop the reaction. Absorbance of the hemoglobin released in supernatants was measured at 540 nm by a double-beam UV-VIS spectrophotometer (Shimadzu, Kyoto, Japan), model UV-1800. The percentage of hemolysis of each sample was determined by comparison with the positive control samples.

2.6. pH-dependent membrane-lytic activity of nanoparticles

The pH-dependent membrane-lytic activity of the NPs was assessed using the hemolysis assay, with the erythrocytes as model of the endosomal membrane [30,31]. PBS buffers of pH 7.4, 6.6 and 5.4 were prepared to be isosmotic to the inside of the erythrocyte and cause negligible hemolysis. The extent and kinetics of hemolysis were assessed as reported earlier [20].

2.7. *In vitro* antitumor activity of free and encapsulated drug

2.7.1. Cell cultures and treatments

The tumor cell lines HeLa (human epithelial cervical cancer) and MCF-7 (human breast cancer) were used as *in vitro* models to study the antitumor activity of DOX in its free and nanoencapsulated forms. Moreover, the non-tumor cell line 3T3 (murine Swiss albino fibroblasts) were used as negative control of the antitumor activity. All cells were grown in DMEM medium (4.5 g/l glucose), supplemented by 10% (v/v) FBS, at 37°C with 5% CO₂. They were routinely cultured in 75 cm² culture flasks and harvested using trypsin-EDTA when the cells reached approximately 80% confluence.

HeLa (7.5×10^4 cells/ml), MCF-7 (1×10^5 cells/ml) and 3T3 (1×10^5 cells/ml) cells were seeded into the 60 central wells of 96-well cell culture plates in 100 µl of complete culture medium. Cells were incubated for 24 h under 5% CO₂ at 37°C and the medium was then replaced with 100 µl of fresh medium supplemented by 5% (v/v) FBS containing the treatments. Unloaded-CS-NPs were assayed in the 25-200 µg/ml concentration range, being these concentrations based on the total composition of the formulation. In contrast, cells incubated with DOX-CS-NPs and free DOX were assessed at µg/ml equivalent drug concentration range (0.1-10 µg/ml). Untreated control cells were exposed to medium with 5% (v/v) FBS only. The cell lines were exposed for 24 h or 48 h to each treatment, and their viability was assessed by two different assays, as described below.

To assess the cytotoxic effects of the NPs as a function of the pH, the cells were exposed to treatments at pH 6.6, which mimics the acidic extracellular environment of tumors (pH_e) [32]. To obtain an acidified medium, DMEM 5% FBS was mixed with 1 M HEPES buffer pH 6.2 (acidified with 5 M HCl) at a ratio of 4:1. Thereafter, the resulting mixture, with an experimental pH of 6.6, was applied for tumor cell treatments with NPs and free drug for 24 h. Here, untreated control cells were exposed to the acidified medium.

2.7.2. Cytotoxicity assays

The endpoints MTT and Neutral Red Uptake (NRU) were used to assess cell viability in the *in vitro* cytotoxicity assays. The first one is a measurement of cell metabolic activity, while the later reflects the functionality of the lysosomes and cell membranes. After complete the cell treatment time, the medium was removed, and 100 µl of MTT in PBS (5 mg/ml) diluted 1:10 in medium without FBS was then added to each well. Similarly, 100 µl of 50 µg/ml NR solution in DMEM without FBS was added to each well for the NRU assay. The microplates were further incubated for 3 h under 5% CO₂ at 37°C, after which the medium was removed, and the wells of the NRU assay were washed once with PBS. Thereafter, 100 µl of DMSO was added to each well to dissolve the purple formazan product (MTT assay) or, similarly, 100 µl of a solution containing 50% ethanol absolute and 1% acetic acid in distilled water was added to extract the NR dye (NRU assay). After 10 min shaking at room temperature, the absorbance of the resulting solution was measured at 550 nm using a SpectraMax M2 (Molecular Devices, Sunnyvale, CA, USA) microplate reader. Cell viability for MTT and NRU was calculated as the percentage of tetrazolium salt reduced by viable cells in each sample or as the percentage of uptake of NR dye by lysosomes, respectively.

The cytotoxicity of each NP in each cell line was expressed as percentage of viability with regard to untreated control cells (the mean optical density of untreated cells was set at 100% viability) in terms of its IC₅₀ (concentration causing 50% death of the cell population), calculated from concentration-response curves.

2.7.3. Selectivity index

The degree of selectivity of the NPs against tumor cell lines is expressed by the Selectivity index (SI) [33], which was calculated as follows:

$$\text{Selectivity index (SI)} = \text{IC}_{50} \text{ in non-tumor cell line} / \text{IC}_{50} \text{ in tumor cell line}$$

2.8. Statistical analysis

Results are expressed as mean ± standard error (SE) and statistical analyses were performed using one-way analysis of variance (ANOVA) to determine the differences between the datasets, followed by Tukey's or Dunnett's post-hoc tests for multiple comparisons, using SPSS® software (SPSS Inc., Chicago, IL, USA). All *in vitro* experiments were performed at least three times, using three replicate samples for each formulation

concentration tested. $p < 0.05$ and $p < 0.005$ were considered significant and highly significant, respectively.

3. Results and discussion

In this study, an acid-triggered drug carrier system with potential ability of rapid intracellular drug release was investigated for potential tumor therapy (Fig. 1). It should further be noted that a fast DOX release feature renders pH-responsive NPs also particularly appealing for treatment of multidrug-resistant (MDR) cancers, as initially sensitive tumor cells can become resistant due to slow drug release at the site of action [32].

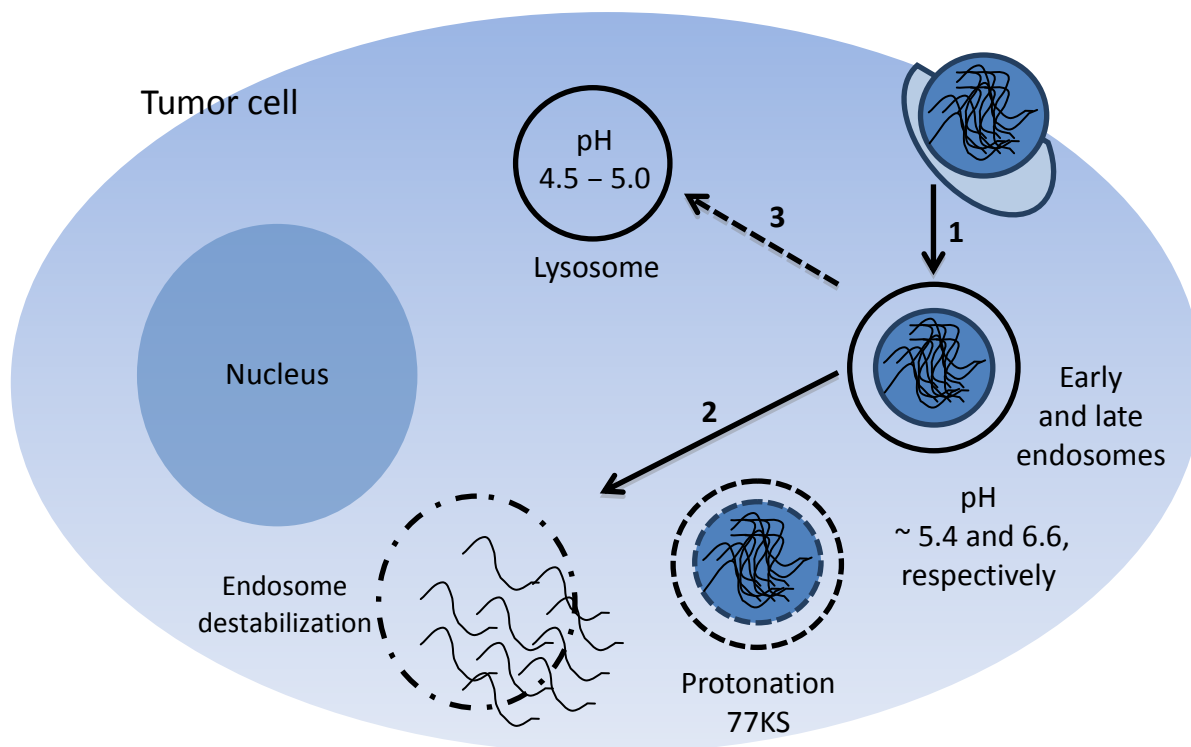


Fig. 1 Schematic representation of a proposed mechanism for the cellular uptake and drug release of pH-responsive CS-NPs. (1) Internalization of NPs by endocytosis, (2) Under mildly acidic environments found in endosomes, the carboxylic group of 77KS would become protonated, which would enhance its hydrophobicity and cause the disruption of endosomal membranes, releasing thus the loaded drug into the cytoplasm, and (3) without a specific mechanism for endosomal escape, DOX-loaded CS-NPs would be trafficked to lysosomes, where degradation of the drug may occur.

The ionotropic gelation between CS as the polycation and TPP as the polyanionic partner was chose as a simple and rapid methodology to prepare NPs responsive to pH [27].

This procedure is a solvent-free approach to prepare colloidal systems with good capacity to encapsulate hydrophilic drugs such as DOX. The pH-sensitivity of NPs was achieved by incorporation of the surfactant 77KS. Without crosslinkers and/or organic solvents, it was included in the complexation process during NP preparation. It is worth mentioning that our previous findings supported the selection of this amphiphile as a bioactive excipient. We have demonstrated its pH-sensitive membranolytic activity, especially in the endosomal pH range, as well as its low cytotoxic potential [20,34].

Furthermore, besides the looking for pH-responsive drug delivery systems, increasing attention has been given to nanocarriers modified with PEG and poloxamer regarding their potential to improve the effectiveness of cancer therapy. PEGylation was shown not only to provide prolonged *in vivo* circulation, but also lower clearance of the loaded drug [24]. On the other hand, poloxamer was shown to interact with MDR cancer cells, resulting in drastic sensitization of tumors with respect to anticancer agents [35]. In this context, we prepared pH-responsive DOX-loaded CS-NPs modified or not with PEG or poloxamer, and evaluated the effects of these modifiers, together with the pH-sensitivity, on the *in vitro* membranolytic and antitumor activity of these nanostructures.

The 5:2 CS to TPP ratio was confirmed as a suitable ratio to carry out the following studies. The complete optimization procedures on the design of the NP formulation were reported previously (unpublished data) and, here, we focused on the evaluation of the biological properties and pH-responsive behavior. The obtained NPs have a positive surface, which is also important for triggering membrane disruption despite the NP pH-sensitivity. It is well known that cationic particles interact more efficiently with the negatively charged cell membranes [36].

3.1. Characterization of nanoparticles

Before cell viability evaluation, the colloidal stability of CS-based NPs in cell culture medium was investigated. Here, we analyzed how suspending CS-NPs in cell culture medium supplemented with 5% FBS influenced their size and ZP values. DLS measurements were performed right after suspending CS-NPs as well as after 24 hours of storage in medium. Fig. 2 shows the characterization parameters of the NPs obtained under standard conditions and after dispersion in cell culture medium. DLS measurements showed that fresh prepared unloaded and DOX-loaded CS-NPs dispersed in ultra-pure water had an average hydrodynamic size between 170 and 227 nm (Fig. 2a). In contrast, when NPs were dispersed in cell culture medium, the size increase was remarkable by 0 h (Fig. 2b), which indicates that

NP agglomeration took place. After 24 h incubation under cell culture conditions ($t = 24$ h), CS-NPs presented a size distribution with smaller particles than those obtained at $t = 0$ h. It is clear that CS-NPs did not retain their size for both blank and loaded NPs. Therefore, the results indicate that the dispersion medium plays a key role in the aggregation behavior of CS-based NPs under standard cell culture conditions. Concerning the NP surface charge, positive ZP values (~ 23 mV) were detected for all formulations under standard conditions (Fig. 2c). ZP is a measurement of the electric charge at the surface of the particles and indicates the physical stability of colloidal systems. However, when suspended in cell culture medium, the NPs displayed ZP values closed to the neutrality (Fig. 2d). This behavior can explain, in part, the aggregation tendency of NPs.

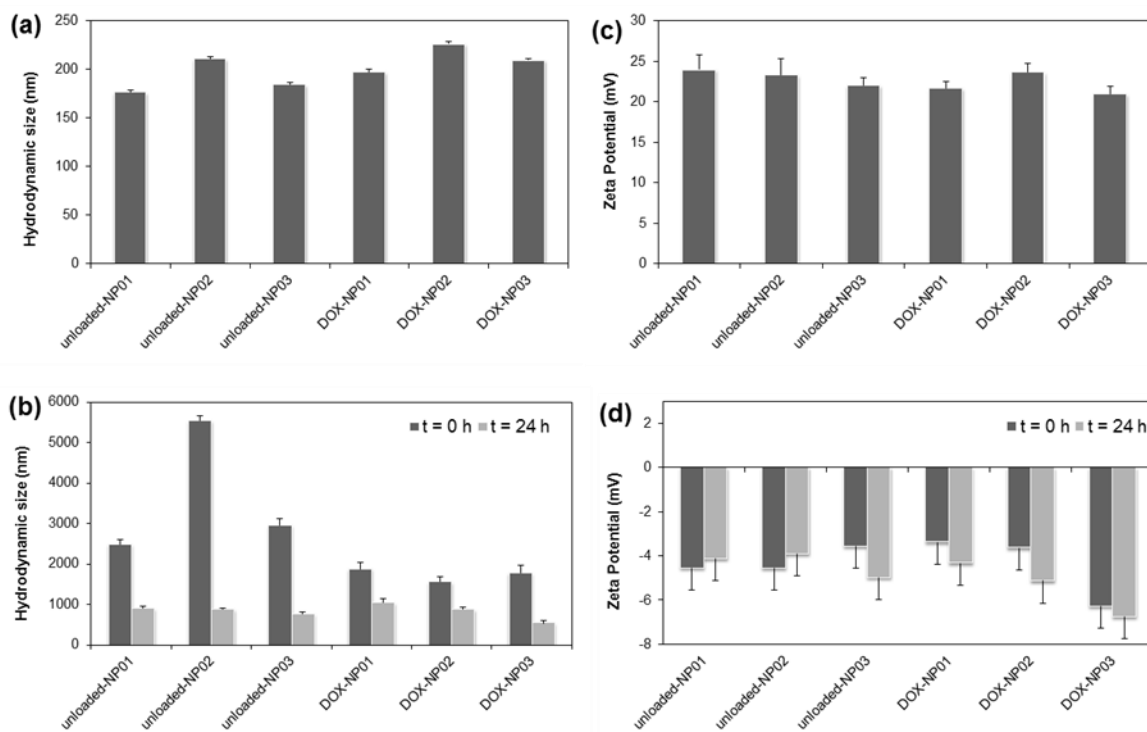


Fig. 2 Characterization of unloaded and DOX-loaded CS-NPs in water and cell culture medium: (a) and (b) Hydrodynamic diameters, and (c) and (d) zeta potential values, of fresh prepared NP suspensions and of NPs suspending in cell culture medium, respectively. The measurements in cell culture medium were performed right after dispersion as well as after 24 hours of storage at 37°C . DOX-NP01, DOX-NP02 and DOX-NP03 represent DOX-CS-NPs, PEG-DOX-CS-NPs and Polox-DOX-CS-NPs, respectively. Unloaded-NPs represent the same formulations without the drug.

The increase in measured particle size in protein-containing medium may be due to protein coating of the particles and aggregation, rather than further growth of the individual particle size after its initial formation [30,37]. It is widely reported that NPs are easily

aggregated or agglomerated in a cell culture medium for *in vitro* assessments because the high ionic nature of the solution and the electrostatic/van der Waals interaction between protein and NPs result in the formation of secondary particles [38-40]. Considering this relevant behavior in cell culture medium, the size of the secondary NPs should be used as a characteristic parameter to determine the *in vitro* activity of NPs [41]. It is worth mentioning that these secondary NPs are also taken up into the cell by endocytosis. Moreover, previously studies have demonstrated that the secondary NP size did not affect the cell viability and efficiency of endocytosis [42].

At the pH of the cell culture medium (~ 7.4), there is a considerable reduction in the degree of protonation at the NPs surface (confirmed by the ZP values), which decreases electrostatic repulsion between the particles and, thereby, increases the probability of particle aggregation. However, the decreasing protonation state of the CS molecule in the particle surface might lead to desorption of the superficial molecules, due to reduced ionic interaction with both TPP and 77KS. This process probably has a slow equilibration, which may justify the shaping of smaller NPs after 24 h incubation in the cell culture medium.

3.2. pH-dependent membrane-lytic activity of nanoparticles

Cells usually take up colloidal systems via endocytosis and an important challenge for the intracellular delivery of therapeutic compounds is to circumvent the non-productive trafficking from endosomes to lysosomes, where degradation may occur [43]. Therefore, the ongoing development of stimuli-responsive colloidal systems has afforded an opportunity to design nanocarriers responsive to pH that efficiently facilitate the drug release into the cytosol by destabilizing endosomal membranes under mildly acidic conditions [44].

Acid-sensitive NPs that are prone to swelling, dissolution or degradation at endosomal pH (5.4–6.6) are a promising approach to obtain fast intracellular DOX release in tumor cells. Therefore, for understanding the pH-sensitivity behavior of NPs, we firstly performed swelling studies by soaking CS-NPs into PBS buffer pH 7.4 and 5.4 that mimic extracellular and endosomal environments. After 3 h incubation, it was noticed a considerable increase of particle size with decrease of buffer pH from 7.4 to 5.4 (178.9 nm and 309.7 nm, respectively). This pH-sensitive swelling behavior, attributed to the increased repulsion forces between cross-linked CS chains, demonstrated that the NPs tend to destabilize at acidic conditions and DOX can be successfully released.

Additionally, the pH-dependent hemolysis assay of CS-NPs, with the erythrocyte as a model for the endosomal membrane [44-46], was applied herein to assess whether the

presence of 77KS provides to the NPs a pH-responsive membranolytic behavior. The membrane-destabilizing activity was assessed at pH 7.4, 6.6 and 5.4. These conditions were chosen to mimic the extracellular environment in the body, as well as the acidic conditions of cell compartments.

The membrane-lytic activity of the unloaded and DOX-loaded NPs was evaluated as a function of concentration, and with varying pH and incubation time (Figs. 3 and 4, respectively). Primarily, we evaluated the hemolysis of non-encapsulated DOX, but insignificant membrane lysis was obtained in the entire pH range (Fig. 4a). As a next step, the membrane lysis induced by unloaded and DOX-loaded CS-NPs without 77KS was assessed (Fig. 3a and 4b, respectively). Negligible or low hemolysis rates were obtained in all tested conditions, proving the lack of pH-responsive behavior of these NPs in the absence of the bioactive surfactant. Therefore, these colloidal systems do not seem to have any ability to facilitate endosomal destabilization.

On the other hand, modified and unmodified CS-NPs incorporating 77KS displayed a clear membranolytic activity dependent on pH. Moreover, this behavior was maintained regardless of the presence of the drug. Both unloaded (Fig. 3b to d) and DOX-loaded CS-NPs (Fig. 4c to e) were non-hemolytic at physiological pH and showed increasing membrane-lytic activity as the pH decrease to 6.6 and 5.4. At physiological pH, negligible hemolysis was observed after 10 min incubation, while maximum hemolysis of 5.7 and 12.5% was observed after 60 min incubation with NPs loading or not the drug, respectively. As the pH decreased to 6.6 and 5.4, the membrane-lytic activity of unloaded and DOX-loaded CS-NPs increased significantly ($p < 0.05$) in a time- and dose-dependent manner. After 60 min incubation, unloaded-CS-NPs were 1.97- and 5.99-fold more hemolytic at pH 6.6 and 5.4 than at pH 7.4, respectively (Fig. 3b). Likewise, DOX-CS-NPs were 1.84- and 3.66-fold more membranolytic in environments simulating early and late endosomal compartments, respectively (Fig. 4c). Considering the PEGylated CS-NPs, similar pH-dependent behavior was observed, with blank and drug-loading NPs showing maximum hemolysis of 70.28 and 90.90, and 82.87 and 90.36%, at pH 6.6 and 5.4, respectively (Figs. 3c and 4d). Finally, it was noticed that the pH-sensitivity of poloxamer-modified CS-NPs was less prominent. The hemolytic activity at acidic conditions was higher than at pH 7.4, but in a lesser extent when comparing to the other formulations. Maximum hemolysis of 12.64 and 62.35% was observed at pH 6.6 and 5.4 with unloaded NPs, whereas 36.52 and 85.48% hemolysis was obtained with NPs encapsulating DOX (Figs. 3d and 4e). This lower membranolytic activity of NPs modified with poloxamer might be due to the fact that poloxamer 188 can increase the structural

stability and resealing of the plasma membrane [23]. The mechanisms underlying this behavior are not entirely clear, however poloxamer 188 may act by increasing the lipid packing density [47].

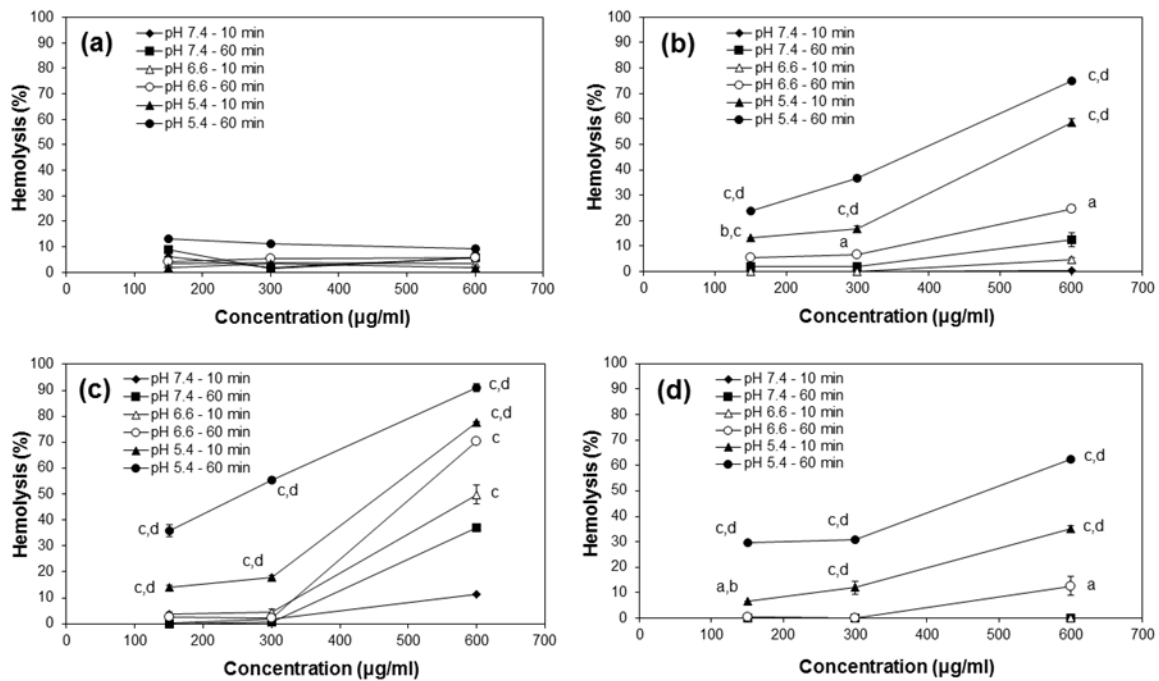


Fig. 3 pH-responsive membranolytic behavior of unloaded CS-NPs: (a) CS-NPs without 77KS, (b) CS-NPs with 77KS, (c) PEG-CS-NPs with 77KS and (d) Polox-CS-NPs with 77KS. NP-induced membrane-lysis is expressed as a function of pH, concentration and incubation time. Results are expressed as the mean \pm SE of three independent experiments. Statistical analyses were performed using ANOVA followed by Tukey's multiple comparison test. ^a Significantly different from pH 7.4 ($p < 0.05$), ^b from pH 6.6 ($p < 0.05$), ^c from pH 7.4 ($p < 0.005$) and ^d from pH 6.6 ($p < 0.005$).

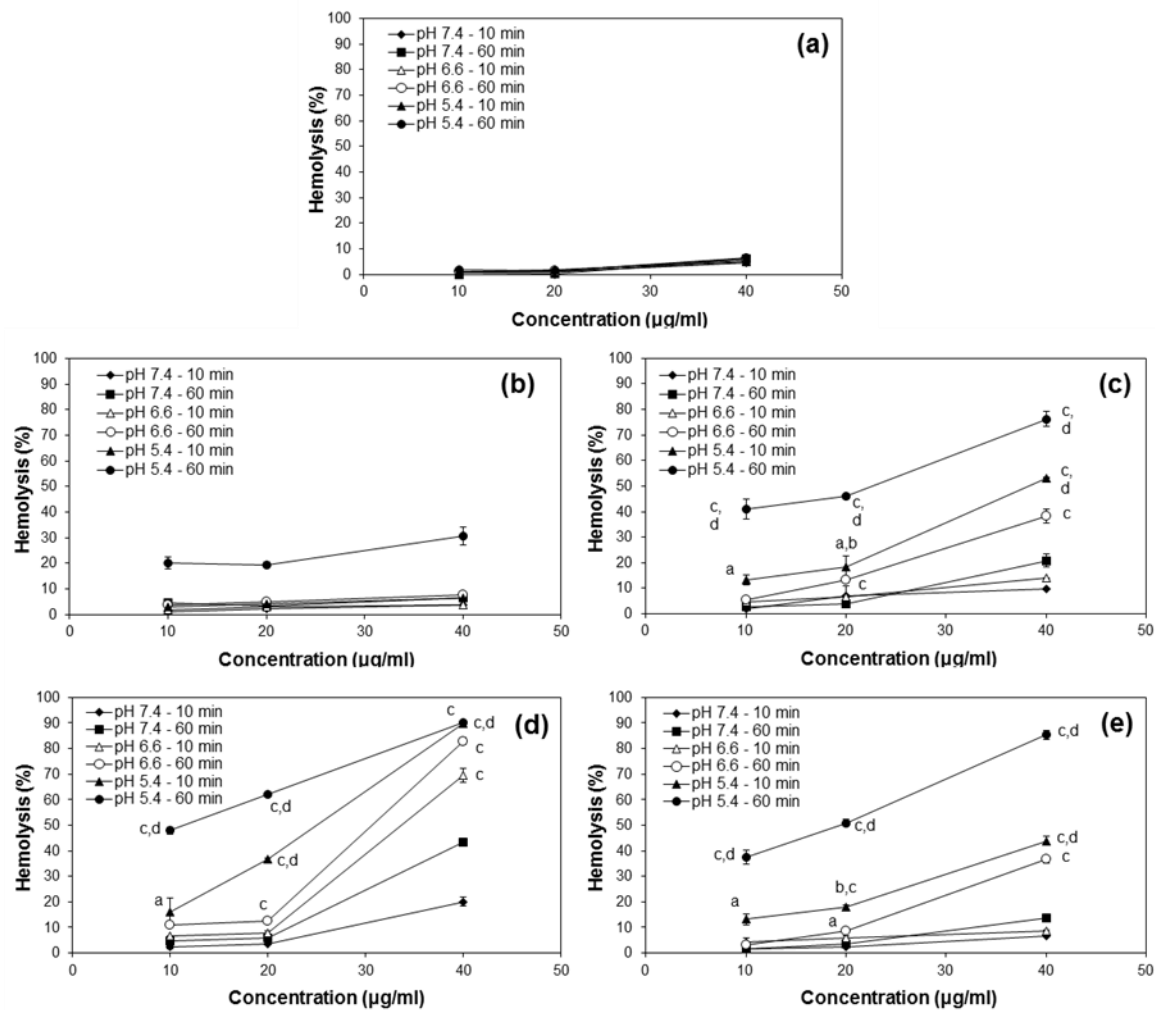


Fig. 4 pH-responsive membranolytic behavior of free drug and DOX-loaded CS-NPs: (a) free DOX, (b) DOX-CS-NPs without 77KS, (c) DOX-CS-NPs with 77KS, (d) PEG-DOX-CS-NPs with 77KS and (e) Polox-DOX-CS-NPs with 77KS. NP-induced membrane-lysis is expressed as a function of pH, concentration and incubation time. Results are expressed as the mean \pm SE of three independent experiments. Statistical analyses were performed using ANOVA followed by Tukey's multiple comparison test. ^a Significantly different from pH 7.4 ($p < 0.05$), ^b from pH 6.6 ($p < 0.05$), ^c from pH 7.4 ($p < 0.005$) and ^d from pH 6.6 ($p < 0.005$).

The strong dependence of 77KS ionization with pH makes this compound an interesting candidate to be used for the design of pH-sensitive devices [20]. Upon this sense, we prepare polymeric NPs incorporating the amphiphile 77KS, which showed a clear membranolytic behavior in a pH-dependent fashion. Therefore, it can be inferred that the most significant hemolysis at acidic environments must be due to a modification in the hydrophobic/hydrophilic balance of 77KS at the acidic pH range. The carboxylic group of 77KS seems to become protonated at acidic conditions, which makes it non-ionic and enhances its hydrophobicity. These hydrophobic segments can insert into lipophilic regions of

lipid bilayers, causing membrane solubilization or altering the permeability of the membrane, inducing, hence, cell lysis [20,48].

3.3. *In vitro* assessments of antitumor activity

The *in vitro* cytotoxicity of drug alone and blank and DOX-loaded CS-NPs was investigated by MTT and NRU assays on HeLa and MCF-7 tumor cell lines. Here, *in vitro* model systems were chose, as they provide a rapid and effective means to assess NPs for a number of toxicological endpoints and mechanism-driven responses. Moreover, an initial animal-based screening approach is not reasonable with regard to laboratory capacities and costs and, especially, from an animal welfare viewpoint [49].

The results from the viability assays are presented in Fig. 5 After 24 h, blank NPs have slight toxic effects on applied cells (Fig 5a), but with DOX-loaded CS-NPs the cell viability systematically decreased with increasing concentrations and was more inhibited than by free DOX, in both tumor cell lines (Fig 5c to e). The more prominent results were obtained with the higher concentrations tested. For example, the HeLa cell viability determined by the NRU assay after 24 h incubation at 10 µg/ml drug concentration (Fig. 5d) was decreased from 60.12% for free DOX to 38.71, 36.68 and 43.92% (i.e. a 53.69, 58.78 and 40.62% increase in cytotoxicity, $p < 0.05$) for DOX-CS-NPs, PEG-DOX-CS-NPs and Polox-DOX-CS-NPs, respectively. In contrast, the non-tumor cell line 3T3 was much less sensitive to the antiproliferative and toxic effects of DOX-loaded NPs, with viabilities higher than 60%. Likewise, free DOX showed cytotoxicity of less than 30% to the 3T3 cells (Fig 5b). Finally, it was observed that DOX-loaded NPs affected cell viability in a time-dependent manner. Fig. 5g and h shown that viability was significantly lower ($p < 0.05$) after 48 h incubation; however, in this case, free and encapsulated DOX showed similar cytotoxic behavior ($p > 0.05$). Therefore, it was straightforward to understand that both incubation time and concentration played a major role in the *in vitro* antiproliferative activity of DOX, where higher drug concentration and longer incubation time would cause lower cell viability.

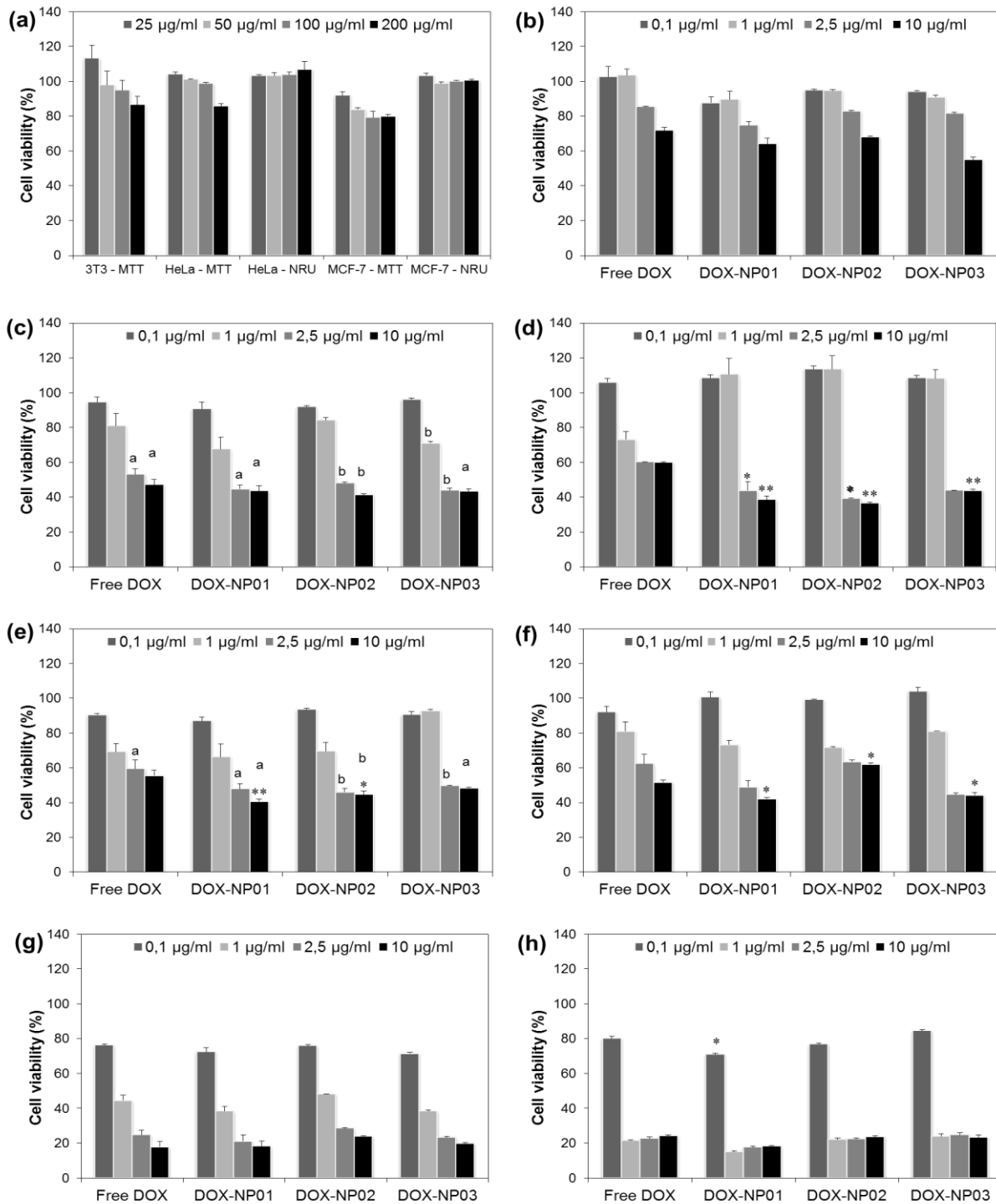


Fig. 5 Cytotoxicity of varying concentrations of CS-NPs and free drug after 24 h incubation: (a) unloaded-CS-NPs in 3T3, HeLa and MCF-7 cell lines; (b) free drug and DOX-loaded CS-NPs in 3T3 cells by MTT assay, (c) in HeLa cells by MTT assay, (d) in HeLa cells by NRU assay, (e) in MCF-7 cells by MTT assay, and (f) in MCF-7 cells by NRU assay. (g) and (h) expressed CS-NPs and free drug in HeLa and MCF-7 cells by MTT assay, respectively, after 48 h incubation. Data are expressed as the mean of three independent experiments \pm SE. Statistical analyses were performed using ANOVA followed by Tukey's or Dunnett's multiple comparison tests. ^a Significant ($p < 0.05$) and ^b highly significant ($p < 0.005$)

difference from 3T3 cells. * $p < 0.05$ and ** $p < 0.005$ denote significant differences from free DOX. DOX-NP01, DOX-NP02 and DOX-NP03 represent DOX-CS-NPs, PEG-DOX-CS-NPs and Polox-DOX-CS-NPs, respectively.

From the measurements of IC₅₀, defined as the concentration inhibiting 50% cell proliferation, it was corroborated the significantly higher activity of DOX-loaded NPs. Table 1 shows that modified and unmodified DOX-loaded CS-NPs possess lower IC₅₀ values than free drug after a 24-h treatment. In contrast, after 48-h treatment, the IC₅₀ values decreased to ~0.8 and 0.4 µg/ml for HeLa and MCF-7 cells, respectively; however, did not differ significantly ($p > 0.05$) between free and encapsulated drug. It is worth mentioning that the IC₅₀ values obtained in all tested conditions were statistically similar ($p > 0.05$) when comparing modified and unmodified CS-NPs. These results indicated that PEG and poloxamer did not affect the antitumor potential of DOX-loaded NPs.

Table 1. Antitumor activity of free drug and DOX-loaded CS-NPs expressed as IC₅₀ (µg/ml) and SI values.

Cell line – assay conditions	IC ₅₀ (µg/ml) ± SE ^a			
	Free DOX	DOX-CS-NPs	PEG-DOX-CS-NPs	Polox-DOX-CS-NPs
3T3 – 24 h - MTT	19.72 ^b ± 3.43	17.49 ^b ± 1.48	18.78 ^b ± 3.54	11.64 ^b ± 3.56
HeLa – 24 h - MTT	8.04 ^Φ ± 2.03	2.09 ^{*,Ψ} ± 1.56	2.51 ^{*,Ψ} ± 1.23	2.10 ^{*,Φ} ± 3.56
MCF-7 – 24 h - MTT	11.74 ^{b,Φ} ± 1.89	2.29 ^{*,Ψ} ± 0.59	2.19 ^{*,Ψ} ± 2.09	2.71 ^{*,Φ} ± 3.25
HeLa – 24 h - NRU	13.91 ^b ± 1.96	2.29 ^{**} ± 0.98	2.16 ^{**} ± 1.47	2.29 ^{**} ± 2.84
MCF-7 – 24 h - NRU	10.38 ^b ± 2.35	2.39 [*] ± 2.96	14.40 ^b ± 2.69	2.23 [*] ± 1.34
HeLa – 48 h - MTT	0.91 ± 0.78	0.69 ± 1.12	1.05 ± 1.45	0.71 ± 2.74
MCF-7 – 48 h - MTT	0.42 ± 1.02	0.30 ± 2.57	0.41 ± 1.45	0.47 ± 0.78
HeLa – 24 h (pH _e 6.6) - MTT	11.57 ^b ± 2.51	1.61 ^{**} ± 3.47	1.79 ^{**} ± 2.56	1.87 ^{**} ± 1.25
MCF-7 – 24 h (pH _e 6.6) - MTT	15.57 ^b ± 1.65	3.8 ^{**} ± 4.01	4.32 ^{**} ± 2.45	4.64 ^{**} ± 1.78
Selectivity Index (SI) ^c				
HeLa – 24 h - MTT	2.45	8.37	7.48	5.54
MCF-7 – 24 h - MTT	1.68	7.64	8.57	4.29

^a = Standard error of the mean; ^b = estimated values; ^c = SI = IC₅₀ in non-tumor cell line (3T3)/IC₅₀ in tumor cell line (HeLa or MCF-7).

Statistical analyses were performed using ANOVA followed by Dunnett's multiple comparison tests. ^{*} = Significant ($p < 0.05$) and ^{**} highly significant ($p < 0.005$) difference from free DOX; [¶] = Significant ($p < 0.05$) and [¤] highly significant ($p < 0.005$) difference from 3T3 non-tumor cells.

The effect of the medium's pH during cell treatment on the cytotoxic responses of free and encapsulated DOX were evaluated by MTT assay (Fig. 6). Free DOX showed reduced activity against both tumor cell lines when incubated in conditions simulating the tumor microenvironment (pH_e ~ 6.6) in regard to physiological conditions. In contrast, both modified and unmodified DOX-loaded CS-NPs showed significantly higher cytotoxic effects ($p < 0.05$) to HeLa cells when incubated in a mildly acidic environment (Fig. 6a). The IC₅₀ values changed from 8.04 and ~2.20 µg/ml to 11.57 and ~1.70 µg/ml for free drug and DOX-loaded CS-NPs, respectively, representing a ~2-fold increase in the NP activity (Table 1). On the other hand, the cytotoxicity of free DOX on MCF-7 cells was somewhat reduced at pH 6.6 (Fig. 6b). However, here the antitumor activity of NPs containing DOX is still much higher than free drug, i.e. 79% and 58% cell viability with free DOX and DOX-CS-NPs, respectively, at 2.5 µg/ml, representing a 100% increase in the NP cytotoxic potential. Following the same test conditions, the antitumor effects observed in standard physiological environment are proportionately reduced, i.e. 59% and 47% cell viability were found with free DOX and DOX-CS-NPs, respectively, at 2.5 µg/ml, representing only a 29.27% increase in the NP cytotoxicity.

The absorbance measured using MTT assay reflects the total metabolic activity of a cell population and is therefore also an indirect measurement of cell proliferation [50]. On the other hand, the NRU assay reflects the functionality of the lysosomes and cell membranes [51]. Here we found non-significant differences ($p > 0.05$) between the endpoints, suggesting thus that both free drug and DOX-loaded CS-NPs exerted toxicity on cell membranes and mitochondrial compartments by affecting cell metabolism.

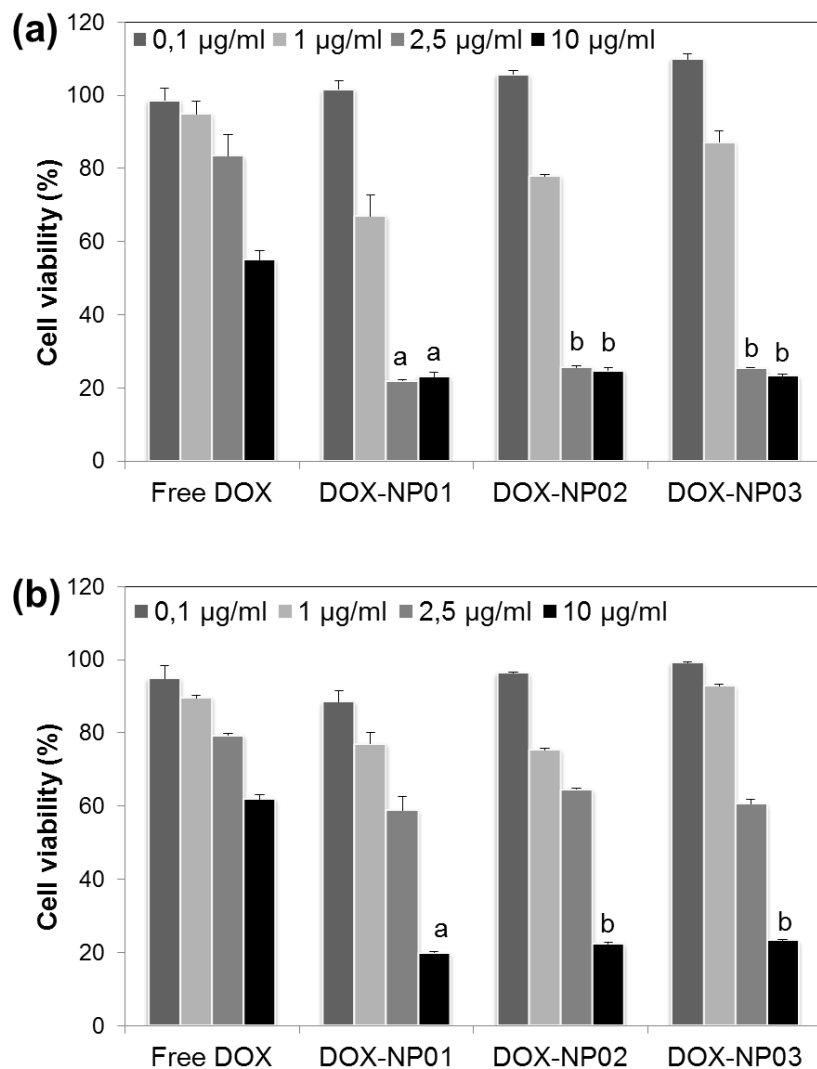


Fig. 6 *In vitro* cell viability by MTT assay in tumor cell lines following 24 h-treatment with free drug and DOX-loaded CS-NPs at pH_e 6.6, simulating the pH of the tumor microenvironment: (a) HeLa and (b) MCF-7 cells. Data are expressed as the mean of three independent experiments \pm SE. Statistical analyses were performed using ANOVA followed by Tukey's multiple comparison tests. ^a Significant ($p < 0.05$) and ^b highly significant ($p < 0.005$) difference from cytotoxicity at pH 7.4 (data reported in Fig. 5c and e). DOX-NP01, DOX-NP02 and DOX-NP03 represent DOX-CS-NPs, PEG-DOX-CS-NPs and Polox-DOX-CS-NPs, respectively.

The rather unexpected absence of noticeable difference between the cytotoxic effect of DOX-loaded CS-NPs prepared with CS alone and CS + poloxamer ($\text{IC}_{50} = 2.09$ and $2.10 \mu\text{g}/\text{ml}$ for HeLa cells, and 2.29 and $2.71 \mu\text{g}/\text{ml}$ for MCF-7 cells, respectively). Therefore, it can be concluded that incorporation of poloxamer into NP matrix does not influence the cytotoxic of NPs in these cancer cells. Similar results were found for CS-Pluronic NPs encapsulating

gemcitabine on colon carcinoma cell line [52]. Therefore, we can state that the potential effects of poloxamer as tumor sensitizers depend on the presence of MDR cells. Previously studies reported that poloxamers interact with MDR tumors resulting in their sensitization with respect to various anticancer agents, especially, anthracycline antibiotics [53].

The selectivity index (SI), calculated as the ratio between the IC₅₀ of NPs in non-tumor cells and IC₅₀ in tumor cells, is greater than 4.20 in both cancer cell lines for all designed formulations (Table 1). The SI demonstrates the differential activity of NPs, where values lower than 2.0 indicate the general toxicity of the tested product [54]. Therefore, the SI values clearly reflect the high degree of selectivity of DOX-loaded NPs to tumor cells. In contrast, free DOX have SI values around 2.0 for both HeLa and MCF-7 cells, which indicates its low selective cytotoxicity. These differences of selectivity between tumor and non-tumor cells might be related to the different internalization pathways depending on the cell characteristics and/or proliferative status. Unexpectedly, the poloxamer-modified NPs displayed the lower values of SI among the designed formulations. This can be attributed to the fact that the model cancer cell lines used in this study are non-MDR and poloxamer is stated to act as a chemosensitizer, with energydepleting effects, especially in MDR tumor cells [55].

DOX exerts its antineoplastic effect via cytotoxic mechanisms of action, especially intercalation into DNA and inhibition of the enzyme topoisomerase II. Some secondary mechanisms underlying DOX action have been described, i.e. formation of reactive oxygen species (ROS). All of these have a deleterious effect on DNA synthesis, as the intercalation of DOX molecule leads to an inhibition of RNA and DNA polymerases by means of disturbances in base recognition and sequence specificity [9,13]. In recent studies it has been reported that free DOX showed greater cytotoxicity than nanostructures encapsulating DOX [9,56,57]. Some authors attributed these results to the different transport mechanisms, as free DOX passes from the extracellular to intracellular compartments by simple passive diffusion, while NPs have to be internalized and thereafter release the drug content to play its cytotoxic effects [58]. In contrast, as we observed here, several publications described the design of DOX-loaded NPs with higher activity against tumor cells than the free drug [12,19,59]. This behavior can be explained by the fact that despite free DOX can cross the cell membrane by a passive diffusion mechanism, its transport into the cells can be limited by the ionization state at physiological pH, as most of drug molecules are protonated at pH 7.4 (DOX pKa = 8.2). In addition, since the molecular weight of conventional drugs is only a few hundred Daltons, they easily escape from tumors [10]. However, when encapsulated into a nanocarrier, the

increased size allows entrance into the tumor vasculature but inhibits escape, leading to accumulation in the tumor tissue.

The enhanced cytotoxicity of DOX via the nano-sized particles means that a reverse effect of drug resistance took place. It seems that the pH-sensitive NPs could reduce the MDR effects that characterize a wide range of chemotherapeutics. The pH-sensitivity of NPs probably allowed the rapid escape of DOX from the endosomes after cell internalization, which might aid the drug to reach the nucleus easily. This behavior is more remarkable when the cytotoxic activity of the pH-responsive CS-NPs was investigated at acidic pH ($pH_e \sim 6.6$) found in the tumor microenvironment. Free DOX have no enhanced and even lower activity at this pH, whereas DOX-loaded NPs displayed higher activity against MCF-7 and HeLa tumor cells, regardless of the presence of the modifiers PEG and poloxamer. This higher activity at acidic pH may be due to the combined effect of increased protonation of CS and 77KS [29]. Firstly, the higher protonation of CS increases binding to the cell membrane, which is negatively charged. Secondly, the protonation of 77KS makes it non-ionic, leading to an enhanced hydrophobicity, which would also increase binding to the cell membrane and trigger greater internalization, enhancing thus the cytotoxic effects. Altogether, these mechanisms could enhance cell internalization of NPs and, thus, DOX cytotoxic effects.

3.4. Hemocompatibility studies

The intravenous administration of nanocarriers allows systemic delivery of the encapsulated drugs to achieve specific and targeted organs. However, for frequent intravenous dosing, it is necessary to assess if and how the NPs interact with blood components [60]. Here, we evaluated whether the unmodified and modified CS-NPs are hemocompatibles. By assessing the hemolytic potential, we can determine the NP toxicity in the blood with regards to the integrity of red blood cells [61].

The release of hemoglobin was used to quantify the erythrocyte-damaging properties of NPs (Fig. 7). Regardless of the presence of the modifiers PEG and poloxamer, DOX-loaded CS-NPs (at 10 and 20 $\mu\text{g}/\text{ml}$) were non-hemolytic (less than 5%) after 10 min incubation and showed slight hemolysis (less than 10%) after 1 h incubation. In contrast, at the highest concentration tested (40 $\mu\text{g}/\text{ml}$), the NPs induced considerably higher hemolysis after 1 h incubation. The free DOX was non-hemolytic in all tested conditions. Altogether, the obtained results suggest the hemocompatibility of the designed pH-sensitive NPs at concentrations up to 20 $\mu\text{g}/\text{ml}$. It is worth mentioning that the NPs already presented remarkable *in vitro* antitumor activity at these non-hemolytic concentrations, as the

haemolytic concentration of 40 µg/ml is about 20 times higher than the IC₅₀ calculated in cancer cells.

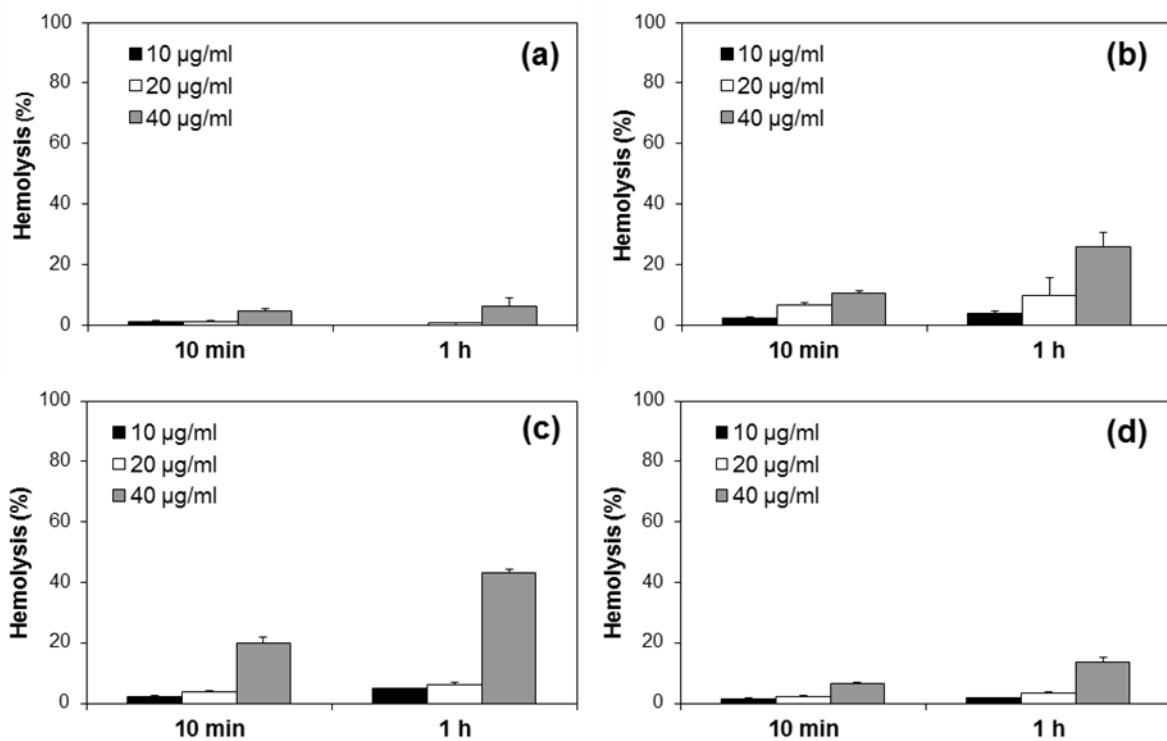


Fig. 7 Percentage of hemolysis caused by free drug and DOX-loaded CS-NPs after 10 and 60 min of incubation with human erythrocytes: (a) free DOX, (b) DOX-CS-NPs, (c) PEG-DOX-CS-NPs and (d) Polox-DOX-CS-NPs. Each value represents the mean \pm SE of three experiments.

4. Conclusions

We have demonstrated a simple and solvent-free approach to prepare pH-responsive CS-NPs by incorporating a biocompatible lysine-based amphiphile in the ionotropic gelation process. The inclusion of 77KS on the formulation clearly gives it a pH-sensitive membranolytic behavior, regardless of the presence of the modifiers PEG and poloxamer. Moreover, the designed pH-responsive CS-NPs significantly improved the *in vitro* antitumor activity of DOX with respect to the free drug, especially in mildly acidic conditions simulating the tumor microenvironment. Outstandingly, DOX-loaded CS-NPs also displayed greater selectivity to tumor cells than to the non-tumor 3T3 fibroblasts. Finally, by using a hemolysis assay, it was demonstrated the hemocompatibility of these NPs. Based on the overall results, it can be concluded that the enhanced *in vitro* antitumor activity of DOX-

loaded NPs might be ascribed to their pH-responsive behavior. Therefore, these nanosystems are potential intracellular delivery carriers, representing a promising strategy for the administration of antitumor drugs in cancer therapy. The remarkable results obtained here merit further investigations under *in vivo* conditions to confirm this evidence.

Conflict of interest statement

The authors state that they have no conflict of interest.

Acknowledgments

This research was supported by Projects 447548/2014-0 and 401069/2014-1 of the *Conselho Nacional de Desenvolvimento Científico e Tecnológico* (CNPq - Brazil), 2293-2551/14-0 of *Fundação de Amparo à Pesquisa do Estado do Rio Grande do Sul* (FAPERGS - Brazil) and MAT2012-38047-C02-01 of the *Ministerio de Economía y Competitividad* (Spain). Daniele R. Nogueira and Laís E. Scheeren thank PNPD-CAPES (Brazil) and FAPERGS for the Postdoctoral and Masters' fellowships, respectively.

References

- [1] A.E. Felber, M.H. Dufresne, J.C. Leroux, pH-sensitive vesicles, polymeric micelles, and nanospheres prepared with polycarboxylates, *Adv. Drug Deliv. Rev.* 64 (2012) 979–992.
- [2] W. Gao, J. Chan, O.C. Farokhzad, pH-responsive nanoparticles for drug delivery, *Mol. Pharm.* 7 (2010) 1913–1920.
- [3] E.S. Lee, Z. Gao, Y.H. Bae, Recent progress in tumor pH targeting nanotechnology, *J. Control. Release* 132 (2008) 164–170.
- [4] J. Kim, C.V. Dang, Cancer's molecular sweet tooth and the warburg effect, *Cancer Res.*, 66 (2006) 8927–8930.
- [5] N.M. Moore, C.L. Sheppard, T.R. Barbour, S.E. Sakiyama-Elbert, The effect of endosomal escape peptides on in vitro gene delivery of polyethylene glycol-based vehicles, *J. Gene Med.* 10 (2008) 1134–1149.
- [6] X-B. Xiong, Z. Ma, R. Lai, A. Lavasanifar, The therapeutic response to multifunctional polymeric nano-conjugates in the targeted cellular and subcellular delivery of doxorubicin, *Biomaterials* 31 (2010) 757–768.
- [7] X. Dong, R.J. Mumper, Nanomedicinal strategies to treat multidrug-resistant tumors: current progress, *Nanomedicine* 5 (2010) 597–615.
- [8] H.D. Han, C.K. Song, Y.S. Park, K.H. Noh, J.H. Kim, T. Hwang, T.W. Kim, B.C. Shin, A chitosan hydrogel-based cancer drug delivery system exhibits synergistic antitumor effects by combining with a vaccinia viral vaccine, *Int. J. Pharm.* 350 (2008) 27–34.
- [9] K. Tomankova, K. Polakova, K. Pizova, S. Binder, M. Havrdova, M. Kolarova, E. Kriegova, J. Zapletalova, L. Malina, J. Horakova, J. Malohlava, A. Kolokithas-Ntoukas, A. Bakandritsos, H. Kolarova, R. Zboril, In vitro cytotoxicity analysis of doxorubicin-loaded/superparamagnetic iron oxide colloidal nanoassemblies on MCF7 and NIH3T3 cell lines, *Int. J. Nanomedicine* 10 (2015) 949–961.
- [10] D. Peer, J.M. Karp, S. Hong, O.C. Farokhzad, R. Margalit, R. Langer, Nanocarriers as an emerging platform for cancer therapy, *Nat. Nanotechnol.* 2 (2007) 751–760.
- [11] M.D. Chavanpatil, A. Khadair, J. Panyam, Surfactant-polymer nanoparticles: a novel platform for sustained and enhanced cellular delivery of water-soluble molecules, *Pharm. Res.* 24 (2007) 803–810.
- [12] H.Y. Tsai, C.C. Chiu, P.C. Lin, S.H. Chen, S.J. Huang, L.F. Wang, Antitumor efficacy of doxorubicin released from crosslinked nanoparticulate chondroitin sulfate/chitosan polyelectrolyte complexes, *Macromol. Biosci.* 11 (2011) 680–688.
- [13] J. Gautier, E. Munnier, A. Paillard, K. Hervé, L. Douziech-Eyrolles, M. Soucé, P. Dubois, I. Chourpa, A pharmaceutical study of doxorubicin-loaded PEGylated nanoparticles for magnetic drug targeting, *Int. J. Pharm.* 423 (2012) 16–25.

- [14] H. Bao, L. Li, H. Zhang, Influence of cetyltrimethylammonium bromide on physicochemical properties and microstructures of chitosan-TPP nanoparticles in aqueous solutions, *J. Colloid Interface Sci.* 328 (2008) 270-277.
- [15] W. Fan, W. Yan, Z. Xu, H. Ni, Formation mechanism of monodisperse, low molecular weight chitosan nanoparticles by ionic gelation technique, *Colloids Surf. B Biointerfaces* 90 (2012) 21-27.
- [16] J. Chen, L. Huang, H. Lai, C. Lu, M. Fang, Q. Zhang, X. Luo, Methotrexate-loaded PEGylated chitosan nanoparticles: synthesis, characterization, and in vitro and in vivo antitumoral activity, *Mol. Pharm.* 11 (2014) 2213-2223.
- [17] X. Deng, M. Cao, J. Zhang, K. Hu, Z. Yin, Z. Zhou, X. Xiao, Y. Yang, W. Sheng, Y. Wu, Y. Zeng, Hyaluronic acid-chitosan nanoparticles for co-delivery of MiR-34a and doxorubicin in therapy against triple negative breast cancer, *Biomaterials* 35 (2014) 4333-4344.
- [18] K.A. Janes, M.P. Fresneau, A. Marazuela, A. Fabra, M.J. Alonso, Chitosan nanoparticles as delivery systems for doxorubicin, *J. Control. Release*, 73 (2001) 2552-2567.
- [19] T. Ramasamy, T.H. Tran, H.J. Cho, J.H. Kim, Y.I. Kim, J.Y. Jeon, H.G. Choi, C.S. Yong, J.O. Kim, Chitosan-based polyelectrolyte complexes as potential nanoparticulate carriers: physicochemical and biological characterization, *Pharm. Res.* 31 (2013) 1302-1314.
- [20] D.R. Nogueira, M. Mitjans, M.R. Infante, M.P. Vinardell, The role of counterions in the membrane-disruptive properties of pH-sensitive lysine-based surfactants, *Acta Biomater.* 7 (2011) 2846-2856.
- [21] Y.Z. Zhao, C.Z. Sun, C.T. Lu, D.D. Dai, H.F. Lv, Y. Wu, C.W. Wan, L.J. Chen, M. Lin, X.K. Li, Characterization and anti-tumor activity of chemical conjugation of doxorubicin in polymeric micelles (DOX-P) in vitro, *Cancer Lett.* 311 (2011) 187-194.
- [22] Y. Chen, W. Zhang, Y. Huang, F. Gao, X. Sha, X. Fang, Pluronic-based functional polymeric mixed micelles for co-delivery of doxorubicin and paclitaxel to multidrug resistant tumor, *Int. J. Pharm.* 488 (2015) 44-58.
- [23] J.G. Moloughney, N. Weisleder, Poloxamer 188 (p188) as a membrane resealing reagent in biomedical applications, *Recent Pat. Biotechnol.* 6 (2012) 200-211.
- [24] H.J. Cho, I.S. Yoon, H.Y. Yoon, H. Koo, Y.J. Jin, S.H. Ko, J.S. Shim, K. Kim, I.C. Kwon, D.D. Kim, Polyethylene glycol-conjugated hyaluronic acid-ceramide self-assembled nanoparticles for targeted delivery of doxorubicin, *Biomaterials* 33 (2012) 1190-1200.
- [25] L. Sánchez, M. Mitjans, M.R. Infante, M.T. García, M.A. Manresa, M.P. Vinardell, The biological properties of lysine-derived surfactants, *Amino Acids* 32 (2007) 133-136.
- [26] M.A. Vives, M.R. Infante, E. Gracia, C. Selve, M. Maugras, M.P. Vinardell, Erythrocyte hemolysis and shape changes induce by new lysine-derivate surfactants, *Chem. Biol. Interact.* 118 (1999) 1-18.

- [27] P. Calvo, C. Remuñan-López, J.L. Vila-Jato, M.J. Alonso, Chitosan and chitosan/ethylene oxide-propylene oxide block copolymer nanoparticles as novel carriers for proteins and vaccines, *Pharm. Res.* 14 (1997) 1431-1436.
- [28] Q. Gan, T. Wang, C. Cochrane, P. McCarron, Modulation of surface charge, particle size and morphological properties of chitosan-TPP nanoparticles intended for gene delivery, *Colloids Surf. B Biointerfaces* 44 (2005) 65-73.
- [29] D.R. Nogueira, L. Tavano, M. Mitjans, L. Pérez, M.R. Infante, M.P. Vinardell, In vitro antitumor activity of methotrexate via pH-sensitive chitosan nanoparticles, *Biomaterials* 34 (2013) 2758-2772.
- [30] T. Akagi, H. Kim, M. Akashi, pH-dependent disruption of erythrocyte membrane by amphiphilic poly(amino acid) nanoparticles, *J. Biomater. Sci. Polym. Ed.* 21 (2010) 315-328.
- [31] X-L. Wang, S. Ramusovis, T. Nguyen, Z-R. Lu, Novel polymerizable surfactants with pH-sensitive amphiphilicity and cell membrane disruption for efficient siRNA delivery, *Bioconjugate Chem.* 18 (2007) 2169-2177.
- [32] K. Na, E.S. Lee, Y.H. Bae, Adriamycin loaded pullulan acetate/sulfonamide conjugate nanoparticles responding to tumor pH: pH-dependent cell interaction, internalization and cytotoxicity in vitro, *J. Control. Release* 87 (2003) 3-13.
- [33] R.B. Badisa, L.T. Ayuk-Takem, C.O. Ikediobi, E.H. Walker, Selective anticancer activity of pure licamichauxiioic-B acid in cultured cell lines, *Pharm. Biol.* 44 (2006) 141–145
- [34] D.R. Nogueira, M. Mitjans, M.R. Infante, M.P. Vinardell, Comparative sensitivity of tumor and non-tumor cell lines as a reliable approach for in vitro cytotoxicity screening of lysine-based surfactants with potential pharmaceutical applications, *Int. J. Pharm.* 420 (2011) 51-58.
- [35] Y. Wang, L. Yu, L. Han, X. Sha, X. Fang, Difunctional Pluronic copolymer micelles for paclitaxel delivery: synergistic effect of folate-mediated targeting and Pluronic-mediated overcoming multidrug resistance in tumor cell lines, *Int. J. Pharm.* 337 (2007) 63-73.
- [36] J.S. Park, T.H. Han, K.Y. Lee, S.S. Han, J.J. Hwang, D.H. Moon, S.Y. Kim, Y.W. Cho, N-acetyl histidine-conjugated glycol chitosan self-assembled nanoparticles for intracytoplasmic delivery of drugs: endocytosis, exocytosis and drug release, *J. Control. Release* 115 (2006) 37-45.
- [37] S.J. Duthie, Folic-acid-mediated inhibition of human colon-cancer cell growth, *Nutrition* 17 (2001) 736-737.
- [38] D. Dutta, S.K. Sundaram, J.G. Teeguarden, B.J. Riley, L.S. Fifield, J.M. Jacobs, S.R. Addleman, G.A. Kaysen, B.M. Moudgil, T.J. Weber, Adsorbed proteins influence the biological activity and molecular targeting of nanomaterials, *Toxicol. Sci.* 100 (2007) 303–315.

- [39] M. Horie, K. Nishio, K. Fujita, S. Endoh, A. Miyauchi, Y. Saito, H. Iwahashi, K. Yamamoto, H. Murayama, H. Nakano, N. Nanashima, E. Niki, Y. Yoshida, Protein adsorption of ultrafine metal oxide and its influence on cytotoxicity toward cultured cells, *Chem. Res. Toxicol.* 22 (2009) 543–553.
- [40] H. Kato, In vitro assays: Tracking nanoparticles inside cells, *Nat. Nanotechnol.* 6 (2011) 139–140.
- [41] M. Horie, H. Kato, K. Fujita, S. Endoh, H. Iwahashi, In vitro evaluation of cellular response Induced by manufactured nanoparticles, *Chem. Res. Toxicol.* 25 (2012) 605–619.
- [42] Z.P. Chen, Y. Zhang, K. Xu, R.Z. Xu, J.W. Liu, N. Gu, Stability of hydrophilic magnetic nanoparticles under biologically relevant conditions, *J. Nanosci. Nanotechnol.* 8 (2008) 6260–6265.
- [43] P.S. Stayton, A.S. Hoffman, N. Murthy, C. Lackey, C. Cheung, P. Tan, L.A. Klumb, A. Chilkoti, F.S. Wilbur, O.W. Press, Molecular engineering of proteins and polymers for targeting and intracellular delivery of therapeutics, *J. Control. Release* 65 (2000) 203–220.
- [44] R. Chen, S. Khormaei, M.E. Eccleston, N.K.H. Slater, The role of hydrophobic amino acid grafts in the enhancement of membrane-disruptive activity of pH-responsive pseudo-peptides, *Biomaterials* 30 (2009) 1954–1961.
- [45] Y-J. Lee, G. Johnson, J-P. Pellois, Modeling of the endosomolytic activity of HA2-TAT peptides with red blood cells and ghosts, *Biochemistry* 49 (2010) 7854–7866.
- [46] J.T. Wilson, A. Postma, S. Keller, A.J. Convertine, G. Moad, E. Rizzardo, L. Meagher, J. Chiefari, P.S. Stayton, Enhancement of MHC-I antigen presentation via architectural control of pH-responsive, endosomolytic polymer nanoparticles, *AAPS J.* 17 (2015) 358–369.
- [47] S.A. Maskarinec, J. Hannig, R.C. Lee, K.Y. Lee, Direct observation of poloxamer 188 insertion into lipid monolayers, *Biophys. J.* 82 (2002) 1453–1459.
- [48] A. Pinazo, L. Pérez, M.R. Infante, R. Pons, Unconventional vesicle-to-ribbon transition behaviour of diacyl glycerol amino acid based surfactants in extremely diluted systems induced by pH-concentration effects, *Phys. Chem. Chem. Phys.* 6 (2004) 1475–1481.
- [49] T. Hartung, Food and thought ... on alternative methods for nanoparticle safety testing, *ALTEX* 27 (2010) 87–95.
- [50] J. Weyermann, D. Lochmann, A. Zimmer, A practical note on the use of cytotoxicity assays, *Int. J. Pharm.* 288 (2005) 369–376.
- [51] E. Fröhlich, C. Meindl, E. Roblegg, A. Griesbacher, T.R. Pieber, Cytotoxicity of nanoparticles is influenced by size, proliferation and embryonic origin of the cells used for testing, *Nanotoxicology* 6 (2012) 424–439.

- [52] H. Hosseinzadeh, F. Atyabi, R. Dinarvand, S.N. Ostad, Chitosan-Pluronic nanoparticles as oral delivery of anticancer gemcitabine: preparation and in vitro study, *Int. J. Nanomedicine* 7 (2012) 1851-1863.
- [53] A.V. Kabanov, E.V. Batrakova, V.Y. Alakhov, Pluronic block copolymers for overcoming drug resistance in cancer, *Adv. Drug Deliv. Rev.* 54 (2002) 759-779.
- [54] A. Koch, P. Tamez, J. Pezzuto, D. Soejarto, Evaluation of plants used for antimalarial treatment by the Massai of Kenya, *J. Ethnopharmacol.* 101 (2005) 95–99.
- [55] E.V. Batrakova, S. Li, A.M. Brynskikh, A.K. Sharma, Y. Li, M. Boska, N. Gong, R.L. Mosley, V.Y. Alakhov, H.E. Gendelman, A.V. Kabanov, Effects of pluronic and doxorubicin on drug uptake, cellular metabolism, apoptosis and tumor inhibition in animal models of MDR cancers, *J. Control. Release* 143 (2010) 290-301.
- [56] X. Yang, J.J. Grailer, I.J. Rowland, A. Javadi, S.A. Hurley, D.A. Steeber, S. Gong, Multifunctional SPIO/DOX-loaded wormlike polymer vesicles for cancer therapy and MR imaging, *Biomaterials* 31 (2010) 9065-9073.
- [57] C.H. Fan, C.Y. Ting, H.J. Lin, C.H. Wang, H.L. Liu, T.C. Yen, C.K. Yeh, SPIO-conjugated, doxorubicin-loaded microbubbles for concurrent MRI and focused-ultrasound enhanced brain-tumor drug delivery, *Biomaterials* 34 (2013) 3706-3715.
- [58] H-M. Yang, B.C. Oh, J.H. Kim, T. Ahn, H-S. Nam, C.W. Park, J-D. Kim, Multifunctional poly(aspartic acid) nanoparticles containing iron oxide nanocrystals and doxorubicin for simultaneous cancer diagnosis and therapy, *Colloids Surf. A Physicochem. Eng. Asp.* 391 (2011) 208–215.
- [59] F.M. Kievit, F.Y. Wang, C. Fang, H. Mok, K. Wang, J.R. Silber, R.G. Ellenbogen, M. Zhang, Doxorubicin loaded iron oxide nanoparticles overcome multidrug resistance in cancer in vitro, *J. Control. Release* 152 (2011) 76-83.
- [60] N.R. Kuznetsova, E.L. Vodovozova, Differential binding of plasma proteins by liposomes loaded with lipophilic prodrugs of methotrexate and melphalan in the bilayer, *Biochemistry* 79 (2014) 797-804.
- [61] R.M. Aparicio, M.J. García-Celma, M.P. Vinardell, M. Mitjans, In vitro studies of the hemolytic activity of microemulsions in human erythrocytes, *J. Pharm. Biomed. Anal.* 39 (2005) 1063–1067.

DISCUSSÃO

7. DISCUSSÃO GERAL

A ampla utilização da DOX como agente quimioterapêutico parte do princípio de que este antibiótico é efetivo contra inúmeros tipos de câncer, incluindo leucemias, linfomas, sarcomas e câncer de mama. Por esta razão, tornou-se um fármaco de primeira linha no tratamento do câncer. No entanto, assim como outros fármacos quimioterapêuticos, a DOX apresenta efeitos adversos graves, sendo que a cardiototoxicidade dose-dependente é o mais perigoso (BARENHOLZ, 2012). Neste contexto, pela combinação destas duas características principais (amplo uso e pouca especificidade pelo tecido tumoral), a DOX é alvo constante de pesquisas no sentido de desenvolver sistemas carreadores capazes de liberar o fármaco apenas na região específica do tumor, reduzindo, assim, a ocorrência de cardiotoxicidade, bem como dos demais efeitos adversos.

As NPs acumulam-se preferencialmente no tumor através do efeito EPR. Esta biodistribuição diferenciada permite ao fármaco encapsulado alcançar altas concentrações intratumorais e baixas concentrações em tecidos normais. NPs poliméricas têm sido extensivamente estudadas como carreadores terapêuticos e são desenvolvidas a partir de polímeros biocompatíveis e biodegradáveis sintéticos ou naturais (WANG et al., 2012).

A partir deste contexto geral, a discussão a seguir baseia-se nos três manuscritos apresentados nas seções anteriores.

O ambiente extracelular do tecido tumoral é levemente acidificado ($\text{pH}_\text{e} \sim 6,6$), assim como os compartimentos intracelulares como endossomas primários e secundários que apresentam valores de $\text{pH} \sim 6,5$ e $5,4$, respectivamente. Neste contexto, os sistemas carreadores pH-sensíveis aparecem inseridos no campo nanotecnológico como uma alternativa promissora para melhorar a entrega de fármacos especificamente na região tumoral e reduzir a toxicidade nos tecidos normais. Assim, como etapa inicial do trabalho e conforme demonstrado no **ARTIGO II**, NPs de CS incorporando o tensoativo pH-sensível 77KS foram desenvolvidas para desencadear a liberação da DOX de forma pH-dependente na região tumoral (figura 1). O tensoativo derivado de lisina, 77KS, apresenta baixa citotoxicidade e comportamento pH-sensível, que lhe confere potencial aplicabilidade na área farmacêutica (NOGUEIRA et al., 2011a, 2011b). As NPs foram preparadas pelo método de gelificação iônica, no qual foi incluído o 77KS como adjuvante bioativo (CALVO et al., 1997; NOGUEIRA et al., 2015). O método baseia-se em ligações cruzadas entre as cargas positivas do polímero CS e as cargas negativas do polianion TPP, formadas sob agitação à temperatura

ambiente. A suspensão opalescente de NPs (DOX-CS-NPs) é formada espontaneamente. Além disso, modificações nas NPs foram realizadas, tais como a inclusão dos copolímeros PEG (PEG-DOX-CS-NPs) e poloxamer (Polox-DOX-CS-NPs). Ambos possuem a propriedade de melhorar o desempenho do sistema nanoparticulado: o primeiro através do aumento do tempo de permanência das NPs na corrente sanguínea, alcançando, dessa forma, a região tumoral, e o segundo através do mecanismo de inibição da bomba de efluxo PgP, que aparece superexpressa em células MDR (TERMSARASAB et al., 2014; BATRAKOVA et al, 2010). Todas as NPs foram caracterizadas quanto ao seu tamanho, PDI, PZ, pH, EE% e teor de fármaco (tabela 1). De maneira geral, as NPs contendo DOX exibiram maior tamanho, indicando a retenção do fármaco no sistema polimérico. Além disso, a presença do 77KS não afetou de maneira significativa o tamanho das NPs. Por outro lado, NPs contendo PEG mostraram maior tamanho, justificado pela característica hidrofílica do copolímero. Valores aceitáveis de PDI foram obtidos (< 0,240), sugerindo a monodispersão dos sistemas. A respeito dos valores positivos alcançados para PZ, estes são característicos para NPs preparadas a partir da CS, devido aos grupos amino catiônicos do polímero. Além disso, a partir dos espectros de infravermelho, que podem ser vistos na figura 4, ficou evidente a formação da ligação CS/TPP, bem como a presença da DOX tanto na DOX-CS-NPs, quanto na PEG-DOX-CS-NPs.

Para as análises de teor de fármaco e cálculo de EE%, bem como para a quantificação da DOX em estudos de liberação *in vitro* e estudos de estabilidade, utilizaram-se metodologias analíticas por CLAE em fase reversa e espectrofotometria UV-Vis desenvolvidas e validadas conforme descrito no **ARTIGO I**.

É de extrema importância a quantificação adequada do fármaco encapsulado uma vez que a efetividade do sistema dependerá diretamente da concentração de ativo. Além disso, os métodos disponíveis para o produto farmacêutico não são fidedignos quando aplicados a NPs, pois estes métodos não consideram a complexa matriz que envolve polímeros, copolímeros e tensoativos. Neste sentido, desenvolveu-se e validou-se um método por CLAE em fase reversa para quantificação da DOX encapsulada. Além disso, um método por espectrofotometria UV-Vis também foi desenvolvido e validado como uma alternativa ao primeiro (ambos descritos no **ARTIGO I**). O método por CLAE empregou coluna cromatográfica C₁₈ e o comprimento de onda fixado para as análises foi 254 nm. A fase móvel constituída por acetonitrila 90% em água (v/v) e água pH 3,0 acidificada com ácido acético glacial (33:67 v/v) mostrou-se a mais adequada para a validação, proporcionando tempo de retenção curto e reproduzível de, aproximadamente, 6 minutos, assim como

resultados adequados para os parâmetros avaliados na adequabilidade do sistema. Para validação do método UV-Vis, o diluente ideal foi água pH 3,0 acidificada com ácido acético glacial. O comprimento de onda estabelecido foi 480 nm, justificado pelo fato de que a DOX apresenta coloração alaranjada e, portanto, capaz de absorver radiação na região visível. Os métodos CLAE em fase reversa e espectrofotometria UV-Vis apresentaram regressão linear significativa ($r = 0,9996$ e $r = 0,9998$, respectivamente) na faixa de concentração 1-30 µg/mL. Para avaliação dos parâmetros especificidade, precisão, exatidão e robustez, utilizaram-se como amostras as NPs desenvolvidas conforme **ARTIGO II**. Para isso, a DOX foi extraída das NPs através da mistura da suspensão de NPs com metanol (1:1 v/v), seguida de sonicação por 15 minutos. A solução resultante foi diluída em fase móvel ou água pH 3,0 até a concentração desejada. Na avaliação da especificidade, especial atenção foi dada no sentido de que as análises ocorressem sem interferência dos excipientes das NPs bem como dos modificadores PEG e poloxamer. Além da análise dos cromatogramas, para o método por CLAE, utilizou-se detector DAD para determinar a pureza do pico. Alto índice de pureza foi obtido ($> 0,9999$), demonstrando a especificidade do método. Através da análise dos espectros de absorção, ficou evidente e especificidade do método UV-Vis. Para ambos os métodos, os dados de repetibilidade e precisão intermediária apresentaram valores de DPR conforme preconizado ($< 2\%$), da mesma forma que resultados de exatidão também foram aceitáveis (98 – 102%) (ICH, 2005, tabela I). Os resultados demonstram, portanto, que os métodos são precisos e exatos. O parâmetro robustez de ambos os métodos foi avaliado através de planejamento fatorial. No que se refere ao método por CLAE, quatro fatores foram investigados em dois níveis (alto e baixo). O valor médio de teor de DOX calculado frente ao padrão injetado nas mesmas condições foi de 101,90% (tabela II). Em relação ao método por UV-Vis, três fatores foram investigados em dois níveis e o valor médio de teor obtido foi 103,14%. A partir dos valores de teor e do gráfico de Pareto (figura 2), pode-se dizer que os métodos são robustos e, portanto, capazes de quantificar o fármaco de maneira satisfatória mesmo sob pequenas variações. O método por espectrofotometria é vantajoso no sentido que não utiliza solvente orgânico, portanto com menor impacto ambiental, além da rapidez e simplicidade; porém, não substitui o método por CLAE já que este último é mais específico, sensível e capaz de analisar pequenos volumes de amostra.

Os métodos validados foram aplicados para análise de teor de seis lotes de NPs (tabela 3). Os resultados obtidos foram comparados estatisticamente através do teste t de Student e ANOVA, observando-se diferenças não-significativas ($p > 0,05$). Além disso, o método por CLAE foi utilizado para quantificação da DOX encapsulada quando as NPs foram expostas à

radiação UVC. Altos valores de índice de pureza do pico foram obtidos através de detector DAD, demonstrando que o método também pode ser utilizado em estudos de estabilidade.

Dessa forma, a partir dos métodos CLAE e espectrofotometria UV-Vis validados, realizou-se análise de teor de fármaco e EE% das NPs desenvolvidas conforme **ARTIGO II**. O método CLAE também foi utilizado para quantificação da DOX em estudos de liberação *in vitro* e estudos de estabilidade das NPs. De um modo geral, demonstraram-se as várias aplicações deste método, que contribuem para uma caracterização mais detalhada das NPs desenvolvidas.

Em relação ao teor de fármaco nas NPs e EE%, resultados satisfatórios foram obtidos: em torno de 98% e 65%, respectivamente (**ARTIGO II**). Estudos de liberação *in vitro* realizados em diferentes pHs demonstraram claramente o comportamento pH-dependente das NPs, uma vez que uma rápida liberação da DOX foi alcançada sob condições ácidas (pH 6,6 e 5,4, figura 3). Estes resultados sugerem que a liberação do fármaco é estimulada pelos pHs característicos da região do microambiente do tumor e compartimentos intracelulares, facilitando, portanto, o acúmulo da DOX nas células cancerosas. Diferenças significativas foram encontradas entre as quantidades de DOX liberadas em meio pH 7,4 *versus* pH 6,6 e 5,4. A liberação acelerada da DOX em pH 7,4 a partir da NPs contendo poloxamer pode ser explicada pela formação de estrutura porosa na NP conferida pelo copolímero (MEI et al., 2009; YAN et al., 2010).

Os perfis de liberação da DOX a partir das NPs foram submetidos à modelagem matemática (tabela 2). Os resultados mostraram que, independentemente das modificações realizadas, todas as NPs exibiram comportamento biexponencial em pH 7,4, ou seja, houve ocorrência de efeito *burst* seguido de liberação contínua da DOX. Comportamento monoexponencial foi obtido para os perfis de liberação das NPs quando submetidas aos meios pH 6,6 e 5,4, indicando que a liberação do fármaco para o meio ocorre em uma única etapa.

Os mecanismos de liberação de fármaco a partir de NPs descritos são dessorção, difusão e degradação da matriz polimérica (GAN; WANG, 2007). Além disso, a liberação pode ser facilitada por estímulos físicos, químicos ou biológicos, tais como térmicos, pH e enzimáticos (AYDIN; PULAT, 2012; LIU et al., 2014). O modelo de Korsmeyer-Peppas foi utilizado para avaliar o mecanismo de liberação da DOX a partir das NPs expostas a diferentes valores de pH. Para isto, a concentração acumulada de fármaco liberado para o meio foi plotada *versus* tempo. Para sistemas de liberação de fármacos esféricos, o expoente de liberação (n) $\leq 0,43$ indica difusão Fickiana, enquanto $0,43 \leq n \leq 0,85$ referem-se à difusão não-Fickiana ou transporte anômalo e valores de $n \geq 0,85$ indicam transporte caso II

(PEPPAS, 1985). A partir disto, difusão Fickiana e não-Fickiana foram observadas como possíveis mecanismos de liberação, sendo que os resultados obtidos variaram de acordo tanto com a composição da NP, quanto com o pH do meio de liberação. Em resumo, pode-se ressaltar que a liberação da DOX em pH 7,4 (independente das modificações nas NPs) ocorre por difusão não-Fickiana, ou seja, mecanismo de liberação dependente de difusão e relaxamento das cadeias poliméricas, podendo ser a razão para a lenta liberação do fármaco em condições fisiológicas. Para as NPs em pH 6,6 e 5,4, verificou-se que a liberação da DOX ocorre por difusão Fickiana.

Com intuito de melhorar a estabilidade das NPs, estas foram liofilizadas (L-NPs) após otimização inicial do processo conforme descrito no **ARTIGO II**. As L-NPs foram caracterizadas e os resultados são exibidos na tabela 1. Os resultados alcançados foram satisfatórios, mas sugerem que o processo necessita de estudos futuros nos quais diferentes crioprotetores e tempos de congelação e/ou secagem podem ser deliberados e analisados com maior profundidade.

Durante o estudo de estabilidade a baixa temperatura, verificou-se agregação do sistema, com aumento de tamanho e PDI tanto das suspensões de NPs, quanto das NPs liofilizadas, sugerindo, assim, que mais estudos são necessários no sentido de melhorar o comportamento do sistema quanto à manutenção de suas características físico-químicas por um período de tempo mais prolongado. Por outro lado, tanto as suspensões de NPs, como as L-NPs, apresentaram teor próximo ao inicial mesmo após dois meses de armazenamento. Além disso, as L-NPs apresentaram resultados positivos quanto à sua capacidade de proteger a DOX da radiação UVA, com aumento de $t_{1/2}$ em até 15 vezes, quando comparadas com as respectivas suspensões. Portanto, pode-se dizer que a liofilização das NPs aumenta a fotoestabilidade da DOX.

Estudos de hemólise e citotoxicidade *in vitro* foram conduzidos com o objetivo de aprofundar o conhecimento acerca do potencial terapêutico/tóxico das NPs incorporando o tensoativo 77KS, contendo ou não os modificadores PEG e poloxamer (**ARTIGO III**). As NPs objeto destes estudos foram preparadas conforme descrito no **ARTIGO II**. Como parte adicional da caracterização físico-química, mediu-se o diâmetro médio de partícula e PZ das NPs quando em contato com o meio de cultivo (DMEM 5% FBS), simulando as condições do ensaio de citotoxicidade *in vitro* (figura 2). Essas medições são importantes para a compreensão das respostas obtidas nos estudos toxicológicos. Os resultados obtidos mostram claramente o papel do meio na estabilidade das NPs, uma vez que uma tendência à agregação foi observada neste caso. O fato pode ser explicado pela presença de proteínas no meio, que

se ligariam à superfície das NPs através de interações de cargas, aumentando assim seu tamanho hidrodinâmico. Além disso, os valores de PZ que se aproximam do neutro acabam favorecendo a agregação. No entanto, após 24 h de incubação no meio, a 37°C, pode-se observar uma redução no tamanho hidrodinâmico. A reduzida protonação da CS quando em pH ~ 7,4 supõe uma redução na interação deste polímero com o TPP e o 77KS. Este processo teria um equilíbrio lento, que poderia justificar a redução no diâmetro médio de partícula observada apenas ao final do tempo de incubação (24 h). Considerando o comportamento das NPs em meio de cultivo, destaca-se que NPs secundárias são também captadas pelas células via endocitose (HORIE, 2012), o que mantém, portanto, a atividade farmacológica do fármaco encapsulado.

Ao longo do **ARTIGO III**, através dos estudos de hemólise, conduzidos com o eritrócito como modelo de membrana endossomal, verificou-se a capacidade lítica de membrana pH-sensível das NPs (figura 3 e 4). Comparando-se os resultados obtidos para as NPs com e sem 77KS, é possível comprovar que as NPs incorporando o tensoativo são capazes de romper membranas biológicas de forma sensível ao pH. Dessa forma, pode-se predizer uma maior liberação do fármaco encapsulado no ambiente intracelular. Além disso, os modificadores PEG e poloxamer não interferiram na capacidade lítica das NPs. Ainda, destaca-se que a atividade lítica de membrana das NPs foi dependente do tempo de incubação e da concentração da formulação. A partir destes dados, pode-se inferir que o comportamento pH-sensível das NPs é, claramente, conferido pelo 77KS. Tais dados são justificados pela presença de grupo carboxílico na molécula do tensoativo. Estes grupos tendem a protonar em pH ácido, o que torna a molécula não-iônica e, portanto, hidrofóbica. Assim, a NP é capaz de interagir com as membranas celulares solubilizando-as ou alterando sua permeabilidade.

Como uma etapa indispensável durante o desenvolvimento de novas nanotecnologias, realizou-se um estudo da atividade antitumoral *in vitro* das NPs. Os estudos *in vitro* são importantes especialmente nas fases iniciais de desenvolvimento de uma nova formulação como etapa prévia ao uso de animais, por questões éticas, legais e econômicas. Os tratamentos (DOX livre e encapsulada) foram aplicados em duas linhagens celulares tumorais (HeLa e MCF-7) e uma não-tumoral (fibroblastos 3T3), utilizada como controle da atividade inespecífica das NPs. Os resultados demonstraram que a DOX nanoencapsulada foi mais eficiente em inibir a proliferação das células tumorais em comparação com o fármaco livre (figura 5c-h). A acentuada atividade citotóxica desses nanossistemas pode estar relacionada ao seu reduzido diâmetro médio de partícula, além da carga superficial positiva das NPs de CS, que facilita a internalização celular através de ligação com cargas negativas da membrana

plasmática (PARK et al., 2006). Cabe ressaltar que as NPs exibiram efeitos tóxicos muito baixos contra linhagem celular não-tumoral na faixa de concentração testada (figura 5b), assim como as NPs sem DOX permitiram elevada viabilidade para os três tipos celulares (figura 5a). Além disso, em experimentos realizados em pH simulando o microambiente tumoral ($pH_e \sim 6,6$), verificou-se uma atividade citotóxica pH-dependente, pois uma menor viabilidade celular foi detectada (figura 6) após 24 h de incubação com as NPs. Nesse caso, somando-se aos resultados obtidos nos estudos de liberação *in vitro* (**ARTIGO II**), pode-se dizer que a liberação da DOX é facilitada à medida que se diminui o pH do meio, indicando maior especificidade destas NPs para desencadear a liberação do fármaco encapsulado a nível do tecido tumoral extracelular e/ou endossomal, assim como menor liberação inespecífica em pH fisiológico.

Com intuito de verificar a compatibilidade das suspensões de NPs desenvolvidas neste trabalho com os componentes sanguíneos, estudou-se sua hemocompatibilidade utilizando ensaio de hemólise (figura 7). As NPs mostraram-se levemente hemolíticas em 1 h de incubação nas menores concentrações testadas (10 e 20 $\mu\text{g/mL}$), apresentando taxas de hemólise inferiores a 10%. No entanto, com o mesmo tempo de incubação, a concentração mais alta (40 $\mu\text{g/mL}$) exibiu hemólise considerável ($> 15\%$). Os resultados sugerem, então, que as suspensões de NPs são hemocompatíveis até a concentração de 20 $\mu\text{g/mL}$. Nesse caso, cabe ressaltar que esta concentração é superior àquelas que demonstraram atividade citotóxica contra as linhagens celulares tumorais.

CONCLUSÕES

8. CONCLUSÕES

- Desenvolveram-se NPs de CS pH-sensíveis incorporando o tensoativo 77KS, como sistema carreador do fármaco antitumoral DOX, visando ao direcionamento deste especificamente ao microambiente do tumor e/ou ao interior da célula cancerosa;
- O método de gelificação iônica mostrou-se adequado para a preparação das NPs, as quais apresentaram tamanho médio nanométrico de partículas, baixo índice de polidispersão e valores positivos de potencial zeta. A eficiência de encapsulação manteve-se em torno de 65%, assim como o teor de fármaco mostrou-se próximo ao teórico;
- A incorporação dos copolímeros PEG e poloxamer formou NPs com tamanhos adequados, dentro da faixa nanométrica, e sem promover alterações significativas na atividade citotóxica das NPs, representando, assim, um esforço no sentido de melhorar a eficiência do sistema em alcançar o alvo desejado;
- O método por cromatografia a líquido de alta eficiência desenvolvido foi validado e mostrou-se específico, linear, preciso, exato e robusto para identificação e quantificação de doxorrubicina em NPs de CS. O método foi adequado para a determinação de eficiência de encapsulação, análise de teor, estudos de estabilidade e liberação *in vitro*;
- O método por espectrofotometria no UV-Vis foi desenvolvido para identificação e quantificação de doxorrubicina em NPs de CS e foi e validado cumprindo parâmetros de especificidade, linearidade, precisão, exatidão e robustez. A aplicabilidade do método foi demonstrada para análise de teor de DOX nas NPs;
- As NPs desenvolvidas exibiram perfil de liberação pH-dependente, sendo que a liberação ocorreu de forma mais lenta em pH simulando condições fisiológicas, enquanto que em pH simulando o microambiente do tumor e os compartimentos endossomais alcançou-se 100% de liberação da DOX em um menor tempo de teste;
- As suspensões de NPs mostraram-se estáveis quanto às suas características físico-químicas durante o período de duas semanas em baixas temperaturas. Por outro lado, as NPs não foram capazes de melhorar a fotoestabilidade da DOX em comparação com o fármaco livre em solução. No entanto, as formulações liofilizadas mostraram-se apropriadas para este fim;

- Em estudo de hemólise, utilizando o eritrócito como modelo de membrana endossomal, as NPs incorporando o tensoativo 77KS apresentaram capacidade significativa de romper as membranas celulares de modo pH-dependente. Por outro lado, as NPs sem 77KS não demonstraram atividade lítica de membrana em condições ácidas, comprovando o papel deste adjuvante para a obtenção das NPs pH-sensíveis;
- Os sistemas nanoparticulados desenvolvidos provaram ser hemocompatíveis, confirmado sua segurança para administração intravenosa, com ressalva para a maior concentração testada em 1 h de contato com as células sanguíneas;
- Através dos estudos de citotoxicidade *in vitro* comprovou-se que as NPs pH-sensíveis contendo DOX são mais eficazes em inibir o crescimento das células tumorais em comparação ao fármaco livre. A atividade antitumoral das NPs foi especialmente pronunciada quando em pH simulando condições levemente acidificadas do microambiente tumoral ($pH_e \sim 6,6$). Além disso, baixo potencial citotóxico foi observado em linhagem celular não-tumoral (3T3) submetida ao mesmo tratamento, indicando um certo índice de seletividade das NPs pelas células tumorais;
- Portanto, o conjunto de resultados obtidos na presente dissertação demonstrou a viabilidade da preparação de NPs poliméricas pH-sensíveis como potenciais carreadores para melhorar a eficácia do tratamento antitumoral com o fármaco DOX. Destaca-se que a incorporação do tensoativo pH-sensível 77KS às NPs tem potencial para possibilitar a redução dos efeitos adversos associados ao tratamento com DOX, especialmente devido ao direcionamento deste fármaco à região tumoral e/ou ao interior das células cancerosas.

REFERÊNCIAS BIBLIOGRÁFICAS

9. REFERÊNCIAS BIBLIOGRÁFICAS

ABDEL-FATTAH, W. I.; JIANG, T.; EL-BASSYOUNI, G. E.; LAURENCIN, C. T. Synthesis, characterization of chitosan and fabrication of sintered chitosan microsphere matrices for bone tissue engineering. **Acta Biomaterialia**, v. 3, p. 503 – 514, 2007.

AGNIHOTRI, S. A.; MALLIKARJUNA, N. N.; AMINABHAVI, T. M. Recent advances on chitosan-based micro- and nanoparticles in drug delivery. **Journal of Controlled Release**, v. 100, p. 5 – 28, 2004.

AKAGI T., KIM H., AKASHI M. pH-dependent disruption of erythrocyte membrane by amphiphilic poly(amino acid) nanoparticles. **Journal of Biomaterials Science Polymer Edition**, v. 2, p. 315-328, 2010.

AKIMOTO, J.; NAKAYAMA, M.; OKANO, T. Temperature-responsive polymeric micelles for optimizing drug targeting to solid tumors. **Journal of Controlled Release**, v. 193, p. 2 – 8, 2014.

ALHARETH, K.; VAUTHIER, C.; GUEUTIN, C.; PONCHEL, G.; MOUSSA, F. HPLC quantification of doxorubicin in plasma and tissues of rats treated with doxorubicin loaded poly(alkylcyanoacrylate) nanoparticles. **Journal of Chromatography B**, v. 887, p. 128– 132, 2012.

ALLARD-VANNIER, E.; COHEN-JONATHAN, S.; GAUTIER, J.; HERVÉ-AUBERT, K.; MUNNIER, E.; SOUCÉ, M.; LEGRAS, P.; PASSIRANI, C.; CHOURPA, I. Pegylated magnetic nanocarriers for doxorubicin delivery: A quantitative determination of stealthiness *in vitro* and *in vivo*. **European Journal of Biopharmaceutics**, v. 81, p. 498 – 505, 2012

ANDERSON, G. R.; STOLER, D. L.; BRENNER, B.M. Cancer: the evolved consequence of a destabilized genome. **BioEssays**, v. 23, p. 1037 – 1046, 2001.

ARCAMONE, F.; FRANCESCHI, G.; PENCO, S. Adiamycin (14-hydroxydaunomycin), a novel antitumor antibiotic. **Tetrahedron Letter**, v. 13, p. 1007 – 1010, 1969.

ARNOLD, R.D.; SLACK, J.E.; STRAUBINGER, R.M. Quantification of Doxorubicin and metabolites in rat plasma and small volume tissue samples by liquid chromatography/electrospray tandem mass spectroscopy. **Journal of Chromatography B**, v. 808, p. 141–152, 2004.

AUBEL-SADRON, G.; LONDOS-GAGLIARDI, D. Daunorubicin and doxorubicin, anthracycline antibiotics, a physicochemical and biological review. **Biochimie**, v. 66, p. 333-352, 1984.

AYDIN, R.S.T.; PULAT, M. 5-Fluorouracil encapsulated chitosan nanoparticles for pH-stimulated drug delivery: evaluation of controlled release kinetics. **Journal of Nanomaterials**, v. 2012, p. 1-10, 2012.

BAE, Y.; NISHIYAMA, N.; FUKUSHIMA, S.; KOYAMA, H.; YASUHIRO, M.; KATAOKA, K. Preparation and biological characterization of polymeric micelle drug carriers with intracellular pH-triggered drug release property: tumor permeability, controlled subcellular drug distribution, and enhanced in vivo antitumor efficacy. **Bioconjugate Chemical**, v. 16, p. 122 – 130, 2005.

BARENHOLZ, Y. Doxil®- The first FDA-approved nano-drug: lessons learned. **Journal of Controlled Release**, v. 160, p. 117 – 134, 2012.

BATRAKOVA, E.V.; KABANOV, A.V. Pluronic block copolymers: Evolution of drug delivery concept from inert nanocarriers to biological response modifiers. **Journal of Controlled Release**, v. 130, p. 98–106, 2008.

BATRAKOVA, E.V.; LI, S.; BRYNSKIKH, A.M.; SHARMA, A.K.; LI, Y.; BOSKA, M.; GONG, N.; MOSLEY, R.L.; YU, V.; ALAKHOV, V.Y.; GENDELMAN, H.E.; KABANOV, A.V. Effects of pluronic and doxorubicin on drug uptake, cellular metabolism, apoptosis and tumor inhibition in animal models of MDR cancers. **Journal of Controlled Release**, v. 143, p. 290–301, 2010.

BETANCOURT, T.; BROWN, B.; BRANNON-PEPPAS, L. Doxorubicin-loaded PLGA nanoparticles by nanoprecipitation: preparation, characterization and *in vitro* evaluation. **Future Medicine**, v.2, p. 219 – 232, 2007.

BRITISH PHARMACOPOEIA. Doxorubicin Hydrochloride, v. I, p. 743, London, 2007.

CALVO, P.; REMUÑAN-LÓPEZ, C.; VILA-JATO, J.L.; ALONSO, M. J. Chitosan and chitosan/ethylene oxide-propylene oxide block copolymer nanoparticles as novel carriers for proteins and vaccines. **Pharmaceutical Research**, v.14, p. 1431 - 1436, 1997.

CARUTHERS, S. D.; WICKLINE, S. A.; LANZA, G. M. Nanotechnological applications in medicine. **Current Opinion in Biotechnology**, v. 18, p. 26 – 30, 2007.

CHEN, Z.P.; ZHANG, Y.; XU, K.; XU, R.Z.; LIU, J.W.; GU, N. Stability of hydrophilic magnetic nanoparticles under biologically relevant conditions. **Journal of Nanoscience and Nanotechnology**, v. 8, p. 6260–6265, 2008.

CHO, H.J.; YOON, H.Y.; KOO, H.; KO, S.; SHIM, J.; LEE, J.; KIM, K.; KWON, I.C.; KIM, D. Self-assembled nanoparticles based on hyaluronic acid-ceramide (HA-CE) and Pluronic for tumor-targeted delivery of docetaxel. **Biomaterials**, v. 32, p. 7181-7190, 2011.

COUVREUR, P.; BARRATT, G.; FATTAL, E.; LEGRAND, P.; VAUTHIER, C. Nanocapsule Technology: a review. **Critical Reviews in Therapeutic Drug Carrier Systems**, v. 19, p. 99 – 134, 2002.

DADSETAN, M.; TAYLOR, K.E.; YONG, C.; BAJZER, Z.; LU, L.; YASZEMSKI, M.J. Controlled release of doxorubicin from pH-responsive microgels. **Acta Biomaterialia**, v. 9, p. 5438–5446, 2013.

DASH, M.; CHIELLINI, F.; OTTENBRITE, R.M.; CHIELLINI, E. Chitosan - A versatile semi-synthetic polymer in biomedical applications. **Progress in Polymer Science**, v. 36 p. 981–1014, 2011.

DU, C.; DENG, D.; SHAN, L.; WAN, S.; CAO, J.; TIAN, J. ACHILEFU, S.; GU, Y. A pH-sensitive doxorubicin prodrug based on folate-conjugated BSA for tumor-targeted drug delivery. **Biomaterials**, v. 34, p. 3087 – 3097, 2013.

DU, J.; DU, X.; MAO, C.; WANG, J. Tailor-made dual pH-sensitive polymer-doxorubicin nanoparticles for efficient anticancer drug delivery. **Journal of the American Chemical Society**, v. 113, p. 17560 – 17563, 2011.

EUROPEAN PHARMACOPOEIA 7.0. Doxorubicin Hydrochloride, p. 1879, 01/2008:0714, 2008.

DUTTA, D.; SUNDARAM, S.K.; TEEGUARDEN, J.G.; RILEY, B.J.; FIFIELD, L.S.; JACOBS, J.M.; ADDLEMAN S.R.; KAYSEN, G.A.; MOUDGIL, B.M.; WEBER, T.J. Adsorbed proteins influence the biological activity and molecular targeting of nanomaterials. **Toxicological Sciences**, v. 100, p. 303–315, 2007.

FDA, Food and Drug Administration. FDA news release. Disponível em: <<http://www.fda.gov/newsevents/newsroom/pressannouncements/ucm337872.htm>>. Acesso em 20 abr 2014.

GABIZON, A.; SHMEEDEA, H.; GRENADE, T. Pharmacological basis of pegylated liposomal doxorubicin: Impact on cancer therapy. **European Journal of Pharmaceutical Sciences**, v. 45, p. 388–398, 2012.

GAN, Q.; WANG, T. Chitosan nanoparticle as protein delivery carrier – Systematic examination of fabrication conditions for efficient loading and release. **Colloids and Surfaces B: Biointerfaces**, v. 59, p. 24–34, 2007.

GAUTIER, J.; MUNNIER, E.; PAILLARD, A.; HERVÉ, K.; DOUZIECH-EYROLLES, L.; SOUCÉ, M.; DUBOIS, P.; CHOURPA, I. A pharmaceutical study of doxorubicin-loaded PEGylated nanoparticles for magnetic drug targeting. **International Journal of Pharmaceutics**, v. 423, p. 16– 25, 2012.

GAVENDA, A.; SEVCIK, J.; PSOTOVA, J.; BEDNAR, P.; BARTAK, P.; ADAMOVSKY, P.; SIMANEK, V. Determination of anthracycline antibiotics doxorubicin and daunorubicin by capillary electrophoresis with UV absorption detection. **Electrophoresis**, v. 22, p. 2782 – 2785, 2001.

GEORGE, M.; ABRAHAM, T. E. Polyionic hydrocolloids for the intestinal delivery of protein drugs: alginate and chitosan – a review. **Journal of Controlled Release**, v. 114, p. 1 – 14, 2006.

GEWIRTZ, D. A. A critical evaluation of the mechanisms of action proposed for the antitumor effects of the anthracycline antibiotics Adriamycin and daunorubicin. **Biochemical Pharmacology**, v. 57, p. 727 – 741, 1999.

HAN, H.S.; LEE, J.; KIM, H.R.; CHAE, S.Y.; KIM, M.; SARAVANAKUMAR, G.; YOON, H.Y.; YOU, D.G.; KO, H.; KIM, K.; KWON, I.C.; PARK, J.C.; PARK, J.H. Robust PEGylated hyaluronic acid nanoparticles as the carrier of doxorubicin: Mineralization and its effect on tumor targetability in vivo. **Journal of Controlled Release**, v. 168, p. 105–114, 2013.

HANS, M. L.; LOWMAN, A. M. Biodegradable nanoparticles for drug delivery and targeting. **Current Opinion in Solid State & Material Science**, v. 6, p. 319 – 327, 2002.

HARTUNG, T. Food and thought....on alternative methods for nanoparticle safety testing. **ALTEX**, v. 27, p. 87 - 95, 2010.

HORIE, M.; KATO, H.; FUJITA, K.; ENDOH, S.; IWASHI, H. In vitro evaluation of cellular response Induced by manufactured nanoparticles, **Chemical Research in Toxicology**, v. 25, p. 605–619, 2012.

HOSSEINZADEH, H.; ATYABI, F.; DINARVAND, R.; OSTAD, R.N. Chitosan–Pluronic nanoparticles as oral delivery of anticancer gemcitabine: preparation and in vitro study. **International Journal of Nanomedicine**, v. 7, p. 1851 – 1863, 2012.

HU, T.; LE, Q.; WU, Z.; WU, W. Determination of doxorubicin in rabbit ocular tissues and pharmacokinetics after intravitreal injection of a single dose of doxorubicin-loaded poly- β -hydroxybutyrate microspheres. **Journal of Pharmaceutical and Biomedical Analysis**, v. 43, p. 263-269, 2007.

HUANG, Y. W.; WU, C. H.; ARONSTAM, R. S. Toxicity of transition metal oxide nanoparticles: recent insights from *in vitro* studies. **Materials**, v. 3, p. 4842 - 4859, 2010. International Conference on Harmonisation (ICH) of Technical Requirements for Registration of Pharmaceuticals for Human Use **Q2 R1: Guideline on Validation of Analytical Procedure – Methodology**, 2005.

JAIN, A.; JAIN, S.K. *In vitro* and cell uptake studies for targeting of ligand anchored nanoparticles for colon tumors. **European Journal of Pharmaceutical Sciences**, v. 35, p. 404 – 416, 2008.

JAIN, D. Cardiotoxicity of doxorubicin and other anthracycline derivatives. **Journal of Nuclear Cardiology**, v. 7, p. 53 – 62, 2000.

JANES, K. A.; FRESNEAU, M. P.; MARAZUELA, A.; FABRA A.; ALONSO, M. J. Chitosan nanoparticles as delivery systems for doxorubicin. **Journal of Controlled Release**, v. 73, p. 255 – 267, 2001.

JIN, Y.; HU, H.; QIAO, M.; ZHU, J.; QI, J.; HU, C.; ZHANG, Q.; CHEN, D. pH-sensitive chitosan-derived nanoparticles as doxorubicin carriers for effective anti-tumor activity: preparation and in vitro evaluation. **Colloids and Surfaces B: Biointerfaces**, v. 94, p. 184 – 191, 2012.

KABANOV, A.V.; BATRAKOVA, E.V.; ALAKHOV, V.Y. Pluronic® block copolymers for overcoming drug resistance in Cancer. **Advanced Drug Delivery Reviews**, v. 54, p. 759–779, 2002.

KANG, S.I.; NA, K.; BAE, Y.H. Physicochemical characteristics and doxorubicin-release behaviors of pH/temperature-sensitive polymeric nanoparticles. **Colloids and Surfaces A: Physicochem. Eng. Aspects**, v. 231, p. 103–112, 2003.

KIEVIT, F.M.; WANG, F.Y.; FANG, C.; MOK, H.; WANG, K.; SILBER, J.R.; ELLENBOGEN, R.G.; ZHANG, M. Doxorubicin loaded iron oxide nanoparticles overcome

multidrug resistance in cancer in vitro. **Journal of Controlled Release**, v. 152, p. 76–83, 2011.

KIM, S.S.; LEE, Y.M.; CHO, C.S. Synthesis and properties of semi-interpenetrating polymer networks composed of B-chitin and poly (ethylene glycol) macromere. **Polymer**, v. 36, p. 4497 – 4501, 1995.

KRIZMAN, D. B.; WAGNER, L.; LASH, A.; STRAUSBERG, R. L.; EMMERT-BUCK, M. R. The cancer genome anatomy project: EST sequencing and the genetics of cancer progression. **Neoplasia**, v. 1, n. 2, p. 101 – 106, 1999.

KUMAR, M. N. V. R. A review of chitin and chitosan applications. *Reactive & Functional Polymers*, v. 46, p. 1 – 27, 2000.

KUMARI, A.; YADAV, S.K.; YADAV, S.C. Biodegradable polymeric nanoparticles based drug delivery systems. **Colloids and Surfaces B: Biointerfaces**, v. 75, p. 1–18, 2010.

LANZ-LANDÁZURI, A.; ILARDOYA, A.M.; GARCÍA-ALVAREZ, M.; MUÑOZ-GUERRA, S. Poly(b,L-malic acid)/Doxorubicin ionic complex: A pH-dependent delivery system. **Reactive & Functional Polymers**, v. 81, p. 45–53, 2014.

LEE, E. S.; OH, K. T.; KIM, D.; YOUN, Y. S.; BAE, Y. H. Tumor pH-responsive flower-like micelles of poly (L-lactic acid)-b-poly (ethylene glycol)-b-poly(L-histidine). **Journal of Controlled Release**, v. 123, p. 19 - 26, 2007.

LEE, E.S.; GAO, Z.; BAE, Y.H. Recent progress in tumor pH targeting nanotechnology. **Journal of Controlled Release**, v. 132, p. 164–170, 2008.

LI, Y.; WANG, J.; WIENTJES, M.G.; AU, J.L-S. Delivery of nanomedicines to extracellular and intracellular compartments of a solid tumor. **Advanced Drug Delivery Reviews**, v. 64, p. 29–39, 2012.

LIU, J.; HUANG, Y.; KUMAR, A.; TAN, A.; JIN, S.; MOZHI, A.; LIANG, X. pH-Sensitive nano-systems for drug delivery in cancer therapy. **Biotechnology Advances**, v. 32, p. 693–710, 2014.

LIU, Q.; LI, R.; ZHU, Z.; QIAN, X.; GUAN, W.; YU, L.; YANG, M.; JIANG, X.; LIU, B. Enhanced antitumor efficacy, biodistribution and penetration of docetaxel-loaded biodegradable nanoparticles. **International Journal of Pharmaceutics**, v. 430, p. 350 – 358, 2012.

LU, H.; YUAN, G.; HE, Q.; CHEN, H. Rapid analysis of anthracycline antibiotics doxorubicin and daunorubicin by microchip capillary electrophoresis. **Microchemical Journal**, v. 92, p. 170 – 173, 2009.

LV, S.; TANG, Z.; LI, M.; LIN, J.; SONG, W.; LIU, H.; HUANG, Y.; ZHANG, T.; CHEN, X. Co-delivery of doxorubicin and paclitaxel by PEG-polypeptide nanovehicle for the treatment of non-small cell lung cancer. **Biomaterials**, v. 35, p. 6118-6129, 2014.

MEI, L.; ZHANG, Y.; ZHENG, Y.; TIAN, G.; SONG, C.; YANG, D.; CHEN, H.; SUN, H.; TIAN, Y.; LIU, K.; LI, Z.; HUANG, L. A novel docetaxel-loaded poly (ε-caprolactone)/pluronic f68 nanoparticle overcoming multidrug resistance for breast cancer treatment. **Nanoscale Research Letter**, v. 4, p. 1530-1539, 2009.

MINOTTI, G.; MENNA, P.; SALVATORELLI, E.; CAIRO, G.; GIANNI, L. Anthracyclines: Molecular advances and pharmacologic developments in antitumor activity and cardiotoxicity. **Pharmacological Reviews**, v. 56, n. 2, p.185 – 229, 2004.

MITRA, S.; GAUR, U.; GHOSH, P. C.; MAITRA, A. N. Tumour targeted delivery of encapsulated dextran-doxorubicin conjugate using chitosan nanoparticles as carrier. **Journal of Controlled Release**, v. 74, p. 317 – 323, 2001.

MOHANRAJ, V. J.; CHEN, Y. Nanoparticles – a review. **Tropical Journal of Pharmaceutical Research**, v. 5 (1), p. 561 – 573, 2006.

MOLOUGHNEY, J.G.; WEISLEDER, N. Poloxamer 188 (P188) as a Membrane Resealing Reagent in Biomedical Applications. **Recent Pat Biotechnologie**, v. 6, p. 200 - 211, 2013.

NAJAFABADI, A.H.; ABDOUSS, M.; FAGHIHI, S. Synthesis and evaluation of PEG-O-chitosan nanoparticles for delivery of poor water soluble drugs: Ibuprofen. **Materials Science and Engineering C**, v. 41, p. 91–99, 2014.

NGAH, W. S. W.; GHANI, S. A.; KAMARI, A. Adsorption behavior of Fe(II) and Fe(III) ions in aqueous solution on chitosan and cross-linked chitosan beads. **Bioresource Technology**, v. 96, p. 443 – 450, 2005.

NOGUEIRA, D. R.; MITJANS, M.; INFANTE, M.R.; VINARDELL, M.P. The role of counterions in the membrane-disruptive properties of pH-sensitive lysine-based surfactants. **Acta Biomaterialia**, v. 7, p. 2846-2856, 2011a.

NOGUEIRA, D.R.; MITJANS, M.; INFANTE M.R.; VINARDELL M.P. Comparative sensitivity of tumor and non-tumor cell lines as a reliable approach for in vitro cytotoxicity screening of lysine-based surfactants with potential pharmaceutical applications. **International Journal of Pharmaceutics**, v. 420, p. 51– 58, 2011b.

NOGUEIRA, D.R.; MITJANS, M.; ROLIM, C.M.B.; VINARDELL M.P. Mechanisms Underlying Cytotoxicity Induced by Engineered Nanomaterials: A Review of *In Vitro* Studies. **Nanomaterials**, v. 4, p. 454 – 484, 2014.

NOGUEIRA, D.R.; SCHEEREN, L.E.; VINARDELL, M.P.; MITJANS, M.; INFANTE, M.R.; ROLIM, C.M.B. Nanoparticles incorporating pH-responsive surfactants as a viable approach to improve the intracellular drug delivery. **Material Science and Engineering C**, v. 57, p. 100-106, 2015.

NOGUEIRA, D. R.; TAVANO, L.; MITJANS, M.; PEREZ, L.; INFANTE, M. R.; VINARDELL, M. P. *In vitro* antitumor activity of methotrexate via pH-sensitive chitosan nanoparticles. **Biomaterials**, v. 34, p. 2758 - 2772, 2013.

OCTAVIA, Y.; TOCCHETTI, C. G.; GABRIELSON, K. L.; JANSSENS, S.; CRIJNS, H. J.; MOENS, A. L. Doxorubicin-induced cardiomyopathy: from molecular mechanisms to therapeutic strategies. **Journal of Molecular and Cellular Cardiology**, v. 52, p. 1213 – 1225, 2012.

PANDEY, S.K.; GHOSH, S.; MAITI, P.; HALDAR, C. Therapeutic efficacy and toxicity of tamoxifen loaded PLA nanoparticles for breast cancer. **International Journal of Biological Macromolecules**, v. 72, p. 309 – 319, 2015.

PARK, J.S.; HAN, T.H.; LEE, K.Y.; HAN, S.S., HWANG, J.J.; MOON, D.H.; KIM, S.Y.; CHO, Y.W. N-acetyl histidine-conjugated glycol chitosan self-assembled nanoparticles for intracytoplasmic delivery of drugs: endocytosis, exocytosis and drug release, **Journal of Controlled Release**, v. 115, p. 37-45, 2006.

PARK, J.; FONG, P. M.; LU, J.; RUSSELL, K. S.; BOOTH, C. J.; SALTZMAN, W. M.; FAHMY, T. M. PEGylated PLGA nanoparticles for the improved delivery of doxorubicin. **Nanomedicine**, v. 5, p. 410 – 418, 2009.

PEPPAS, L. B.; BLANCHETTE, J. O. Nanoparticle and targeted systems for cancer therapy. **Advanced Drug Delivery Reviews**, v. 64, p. 206 – 212, 2012.

PEPPAS, N.A. Analysis of Fickian and non-Fickian drug release from polymers. **Pharmaceutica Acta Helvetiae**, v. 60, p. 110-111, 1985.

PRABAHARAN, M. Chitosan-based nanoparticles for tumor-targeted drug delivery. **International Journal of Biological Macromolecules**, v. 72, p. 1313–1322, 2015.

QIU, L.; LI, Z.; QIAO, M.; LONG, M.; WANG, M.; ZHANG, X.; TIAN, C.; CHEN, D. Self-assembled pH-responsive hyaluronic acid-g-poly(L-histidine) copolymer micelles for targeted intracellular delivery of doxorubicin. **Acta Biomaterialia**, v. 10, p. 2024–2035, 2014.

RAMAKRISHNAN, R.; GABRILOVICH, D. L. Novel mechanism of synergistic effects of conventional chemotherapy and immune therapy of cancer. **Cancer Immunol Immunother**, v. 62, p. 405 – 410, 2013.

RAMASAMY, T.; TRAN, T. H.; CHO, H. J.; KIM, J. H.; KIM, Y. I.; JEON, J. Y.; CHOI, H.; YONG, C. S.; KIM, J. O. Chitosan –based polyelectrolyte complexes as potential nanoparticulate carriers: physicochemical and biological characterization. **Pharmaceutical Research**, v. 31, p. 1302 – 1314, 2013.

RAMPINO, A.; BORGOGNA, M.; BLASI, P.; BELLICH, B.; CESARO, A. Chitosan nanoparticles: preparation, size evolution and stability. **International Journal of Pharmaceutics**, v. 455, p. 219 – 228, 2013.

RANSON M. R.; CHEESEMAN, S.; WHITE, S.; MARGISON, J. Caleyx (stealth liposomal doxorubicin) in the treatment of advanced breast cancer. **Critical Review in Oncology/Hematology**, v. 37, p. 115 – 120, 2001.

RINAUDO, M. Chitin and chitosan: properties and applications. **Progress in Polymer Science**, v. 31, p. 603 – 632, 2006.

RINAUDO, M.; PAVLOV, G.; DESBRIERES, J. Influence of acetic acid concentration on the solubilization of chitosan. **Polymer**, v. 40, p. 7029 – 7032, 1999.

RODRIGUES, A. S.; LOPES, A. R.; LEÃO, A.; COUCEIRO, A.; RIBEIRO, A. B. S.; RAMOS, F.; SILVEIRA, M. I. N.; OLIVEIRA, C. R. Development of a analytical methodology for simultaneous determination of vincristine and doxorubicin in pharmaceutical preparations for oncology by HPLC-UV. **Journal of Chromatographic Science**, v. 47, p. 387 – 391, 2009.

SANCHEZ, L.; MITJANS, M.; INFANTE, M.R.; GARCÍA, M.T.; MANRESA, M.A.; VINARDELL, M.P. The biological properties of lysine-derived surfactants. **Amino Acids**, v. 32, p. 133-136, 2007.

SAWYER, D. B.; PENG, X.; CHEN, B.; PENTASSUGLIA, L.; LIM, C. C. Mechanisms of anthracycline cardiac injury: can we identify strategies for cardioprotection? **Progress in Cardiovascular Diseases**, v. 53, p. 105 – 113, 2010.

SCHAFFAZICK, S. R.; GUTERRES, S. S.; FREITAS, L. L; POHLMANN, A. R. Caracterização e estabilidade físico-química de sistemas poliméricos nanoestruturados para administração de fármacos. **Química Nova**, v. 26, n. 5, p. 726 – 737, 2003.

SINGAL, P. K.; ILISKOVIC, N.; LI, T.; KUMAR, D. Adriamycin cardiomyopathy: pathophysiology and prevention. **The FASEB Journal**, v. 11, p. 931 – 936, 1997.

SOHAEBUDDIN, S. K.; THEVENOT, P. T.; BAKER, D.; EATON, J. W.; TANG, L. Nanomaterial cytotoxicity is composition, size, and cell type dependent. **Particle and Fibre Toxicology**, v. 7, p. 22-39, 2010.

SON, Y. J.; JANG, J.; CHO, Y. W.; CHUNG, H.; PARK, R.; KWON, I. C.; KIM, I.; PARK, J. Y.; SEO, S. B.; PARK, C. R.; JEONG, S. Y. Biodistribution and anti-tumor efficacy of doxorubicin loaded glycol-chitosan nanoaggregates by EPR effect. **Journal of Controlled Release**, v. 91, p. 135 – 145, 2003.

TAKEMURA, G.; FUJIWARA, H. Doxorubicin-induced cardiomyopathy from the cardiotoxic mechanisms to management. **Progress in Cardiovascular Diseases**, v. 49, p. 330-352, 2007.

TAN, M. L.; CHOONG, P. F. M.; DASS, C. R. Review: doxorubicin delivery systems based on chitin for cancer therapy. **Journal of Pharmacy and Pharmacology**, v. 61, p. 131 – 142, 2009.

TAVANO, L.; AIELLO, R.; IOELE, G.; PICCI, N.; MUZZALUPO, R. Niosomes from glucuronic acid-based surfactante as new carriers for câncer therapy: preparations, characterization and biological properties. **Colloids and Surfaces B: Biointerfaces**, v. 118, p. 7 – 13, 2014.

TAVANO, L.; MUZZALUPO, R.; MAURO, L.; PELLEGRINO, M.; ANDÒ, S.; PICCI, N. Transferrin-conjugated Pluronicniosomes as a new drug delivery system for anticancer therapy. **Langmuir**, v. 29, p. 12638 – 12646, 2013.

TERMSARASAB, U.; CHO, H.; KIM, D. H.; CHONG, S.; CHUNG, S.; SHIM, C.; MOON, H. T.; KIM, D. Chitosan oligosaccharide-arachidic acid-based nanoparticles for anti-cancer drug delivery. **International Journal of Pharmaceutics**, v. 441, p. 373 – 380, 2013.

TERMSARASAB, U.; YOON, I.; PARK, J.; MOON, H. T.; CHO, H.; KIM, D. Polyethylene glycol-modified arachidyl chitosan-based nanoparticles for prolonged blood circulation of doxorubicin. **International Journal of Pharmaceutics**, v. 464, p. 127 – 134, 2014.

TIAN, L.; BAE, Y.H. Cancer nanomedicines targeting tumor extracellular pH. **Colloids and Surfaces B: Biointerfaces**, v. 99, p. 116– 126, 2012.

TIYABOONCHAI, W. Chitosan nanoparticles: a promising system for drug delivery. **Naresuan University Journal**, v. 11, p. 51 – 66, 2003.

UNSOY, G.; KHODADUST, R.; YALCIN, S.; MUTLU, P.; GUNDUZ, U. Synthesis of doxorubicin loaded magnetic chitosan nanoparticles for pH responsive targeted drug delivery. **European Journal of Pharmaceutical Sciences**, v. 62, p. 243–250, 2014.

U.S. PHARMACOPEIA 37 – NATIONAL FORMULARY 32. Doxorubicin Hydrochloride Injection, p. 2715, 2014.

URVA, S. R.; SHIN, B. S.; YANG, V. C.; BALTHASAR, J. P. Sensitive high performance liquid chromatographic assay assessment of doxorubicin pharmacokinetics in mouse plasma and tissues. **Journal of Chromatography B**. v. 877, p. 837 – 841, 2009.

VEJPONGSA, P.; YEH, E.T.H. Prevention of anthracycline-induced cardiotoxicity. **Journal of the American College of Cardiology**, v. 64, p. 938-945, 2014.

VIVES, M.A.; INFANTE, M.R.; GARCIA, E.; SELVE, C.; MAUGRAS, M.; VINARDELL, M.P. Erythrocyte hemolysis and shape changes induced by new lysine-derivate surfactants. **Chemico-Biological Interactions**, v. 118, p. 1–18, 1999.

WANG, A.Z.; LANGER, R.; FAROKHZAD, O.C. Nanoparticle Delivery of Cancer Drugs. **Annual Review of Medicine**, v. 63, p. 185 – 198, 2012.

WANG, L.; REN, K.; WANG, H.; WANG, Y.; JI, J. pH-sensitive controlled release of doxorubicin from polyelectrolytemultilayers. **Colloids and Surfaces B: Biointerfaces**, v. 125 p. 127–133, 2015.

WILCZEWSKA, A. Z.; NIEMIROWICZ, K.; MARKIEWICZ, K. H.; CAR, H. Nanoparticles as drug delivery systems. **Pharmacological Reports**, v. 64, p. 1020 – 1037, 2012.

World Health Organization (WHO). Cancer. Fevereiro 2014. Disponível em <<http://www.who.int/mediacentre/factsheets/fs297/en/>>. Acesso em 09 abr. 2014.

YAN, F.; ZHANG, C.; ZHENG, Y.; MEI, L.; TANG, L.; SONG, C.; SUN, H.; HUANG, L. The effect of poloxamer 188 on nanoparticle morphology, size, cancer cell uptake, and cytotoxicity. **Nanomedicine: Nanotechnology, Biology and Medicine**, v. 6, p. 170-178, 2010.

YE, H.; KARIMA, A.A.; LOHA, X.J. Current treatment options and drug delivery systems as potential therapeutic agents for ovarian cancer: A review. **Materials Science and Engineering C**, v. 45, p. 609–619, 2014.

ZAGOTTO, G.; GATTO, B.; MORO, S.; SISSI, C.; PALUMBO, M. Anthracyclines: recente developments in their separation and quantitation. **Journal of Chromatography B**, v. 764, p. 161 – 171, 2001.

ZHANG, J.; CHEN, X. G.; LI, Y. Y.; LIU, C. S. Self-assembled nanoparticles based on hydrophobically modified chitosan as carrier for doxorubicin. **Nanomedicine**, v. 3, p. 258 – 265, 2007.

ZHAO, P.; DASH, A.K. A simple HPLC method using a microbore column for the analysis of doxorubicin. **Journal of Pharmaceutical and Biomedical Analysis**, v. 20, p. 543–548, 1999.

ZHAO, Y.; SUN, C.; LU, C.; DAI, D.; LV, H.; WUB, Y.; WANA, C.; CHEN, L.; LIN, M.; LI, X. Characterization and anti-tumor activity of chemical conjugation of doxorubicin in polymeric micelles (DOX-P) *in vitro*. **Cancer Letters**, v. 311, p. 187–194, 2011.

ZHOU, Q.; CHOWBAY, B. Determination of doxorubicin and its metabolites in rat serum and bile by LC: application to preclinical pharmacokinetic studies. **Journal of Pharmaceutical and Biomedical Analysis**, v. 30, p. 1063 – 1074, 2002.